International Journal of Thermofluids 21 (2024) 100568

Contents lists available at ScienceDirect

International Journal of Thermofluids

journal homepage: www.sciencedirect.com/journal/international-journal-of-thermofluids

Unveiling the Dynamics of Entropy Generation in Enclosures: A Systematic Review

Goutam Saha [a,b], Ahmed A.Y. Al-Waaly [c], Maruf Md Ikram [d], Raghav Bihani [d], Suvash C. Saha [a,*]

[a] School of Mechanical and Mechatronic Engineering, University of Technology Sydney, Sydney, NSW 2006, Australia
[b] Department of Mathematics, University of Dhaka, Dhaka 1000, Bangladesh
[c] Department of Mechanical Engineering, Wasit University, Kut 52001, Wasit, Iraq
[d] Department of Mechanical Engineering, Michigan State University, MI 48824-1226, USA

ARTICLE INFO

Keywords:
Entropy generation
Systematic review
cavities
Natural convection
Mixed convection
Nanofluids
Hybrid nanofluids

ABSTRACT

This extensive review aims to provide a thorough understanding of entropy generation (Egen) in confined conduits, or enclosures, by examining a vast array of peer-reviewed research. The review covers various studies on Egen in enclosures with different geometric configurations and highlights the significant effects of thermophysical dynamics, such as temperature gradient, viscous dissipation, frictional drag, and magnetic field strength, on Egen characterization. The review covers a broad range of studies that investigate Egen in enclosures with diverse geometric configurations and different types of fluids, including air, water, and various types of nanofluids. Furthermore, the review also includes different enclosure structures, such as I, L, C, U, semicircular, triangular, square, rectangular, rhombic, trapezoidal, polygonal, and channel types, as well as wavy wall configurations. Notably, the review also encompasses both 2D and 3D cases to present a complete comprehension of Egen in confined conduits. In addition, the review carefully evaluates the validity methods utilized in numerical investigations, incorporating a diverse array of mesh types and sizes utilized in research. A thorough examination of the vast literature demonstrates that enclosures with obstacles, such as single or multiple rotating cylinders, exhibit a noticeable increase in Egen. Also, the review highlights that the use of nanofluids significantly increases Egen. These findings have important practical implications in the analysis of thermofluid systems, including but not limited to heat exchangers, chip cooling, food storage, solar ponds, and nuclear reactor systems. Based on the comprehensive review conducted in this study, several future research directions have been proposed for the emerging field of Egen in enclosures. This study explores the intricate mechanisms of Egen in enclosures and highlights potential avenues for further investigation in this area. These insights will contribute to the advancement of the knowledge base and practical applications of thermofluid systems, including heat exchangers, chip cooling, food storage, solar ponds, and nuclear reactor systems.

1. Introduction

A comprehensive study explored the entropy generation (Egen) inside enclosed cavities of different geometries. The present work reviewed the importance and applications of cavities in different fields, such as cooling systems, storage units, and industrial thermomechanical optimization, etc. By exploring a multitude of enclosure shapes, this study provides a comprehensive analysis of the flow and thermal behavior within these enclosures under different thermophysical boundary conditions. The study considers various thermal boundary conditions, such as temperature, heat flux, adiabatic, isothermal, and mixed boundary conditions. These conditions significantly influence the flow patterns, temperature distribution, and Egen within the enclosures. Hussein et al. [1] did an analysis of natural convection in enclosures and showed that heat transfer and temperature distribution under isothermal conditions had a significant impact on the rate and distribution of Egen. Cho et al. [2] studied natural convection and Egen in a nanofluid-filled U-shaped enclosure. There was a constant heat flux on one wall, a constant low temperature on the other, and adiabatic conditions on the upper and lower walls. These factors affected Egen. This review paper examines how different thermal conditions affect heat transfer and system performance. It provides valuable insights for researchers to optimize heat transfer and reduce Egen.

* Corresponding author.
E-mail addresses: gsahamath@du.ac.bd (G. Saha), aalwaaly@uowasit.edu.iq (A.A.Y. Al-Waaly), ikrammar@msu.edu (M.M. Ikram), bihanira@msu.edu (R. Bihani), Suvash.Saha@uts.edu.au (S.C. Saha).

https://doi.org/10.1016/j.ijft.2024.100568

Available online 9 January 2024

Nomenclature

A	Aspect ratio
AB	Adams-Bashforth method
ADI	Alternate Direct Implicit scheme
ALE	Arbitrary-Lagrangian–Eulerian approach
Am	Amplitude
ANN	Artificial Neural Network
Be	Bejan number
Br	Buoyancy ratio parameter
BiCGStab	Biconjugate gradient stabilized method
Bn	Bingham number
C	Concentration
CDS	Central differencing schemes
Ca	Carreau number
CVM	Control volume method
CVFDM	Control volume Finite difference method
CVFEM	Control volume Finite element method
d	Center of opening
d_c	Diameter of a cylinder
D	Diffusion coefficient
Da	Darcy number
Du	Dufour number
d_p	Nanoparticles diameter
E_{tot}	Total energy per unit mass
E	Elasticity modulus
Ec	Eckert number
Egen	Entropy generation
f	Fluid
FC	Free convection
FoC	Forced Convection
Fc	Forchheimer parameter
FDM	Finite difference method
FDLBM	Finite difference Lattice Boltzmann method
FEM	Finite element method
FVM	Finite volume method
FSI	Fluid–structure interaction
Ge	Gebhart number
Gr	Grashof number
h	Opening ratio
Ha	Hartmann number
Ir	Irreversibility ratio
K	Vortex viscosity parameter
K_T	Thermal conductivity ratio
Kr	Chemical reaction parameter
K_n	Knudsen number
LBM	lattice Boltzmann method
Le	Lewis number
LRBF	Local Radial Basis Function
m	nanoparticle shape factor
M	Magnetic parameter
Ma	Marangoni number
MC	Mixed convection
ML	Machine Learning
MRT	Multiple-Relaxation-Time
MSQM	Multivariate Spectral Quasilinearisation Method
MWCNT	Multi wall carbon nanotubes
n	Flow behavior index for a power-law fluid
nf	Nanofluid
N	Buoyancy ratio
NC	Natural Convection
N_b	Brownian motion
N_t	Thermophoresis parameter
NN	Neural Network
Pe	Peclet number
PCM	Phase change material
Pr	Prandtl number
Q	is the heat source or sink
q	Heat generation or absorption
QUICK	Quadratic upstream interpolation for convective kinematics
R	Opening ratio
RBF-FD	Radial-basis-function-based finite difference
Rq	Heat flux ratio
Ra	Rayleigh number
Ra_I	Internal Rayleigh number
Ra_E	External Rayleigh number
RBSOR	Red and black SOR method
Rc	Thermal conductivity ratio
Rd	Radiation parameter
Re	Reynolds number
Ri	Richardson number
RSM	Response surface methodology
s, np	Solid or nanoparticles
Sc	Schemidt number
Sh	Sherwood number
SIMPLE	Semi-implicit method for pressure-linked equations
SOR	Successive over relaxation
SUR	Successive under relaxation
Sr	Soret number
Ste	Stefan number
S_{ff}	Entropy generation due to fluid friction
S_{HT}	Entropy generation due to heat transfer
S_{MT}	Entropy generation due to mass transfer
S_{TOT}	Total entropy generation
t	Time
T	Temperature
TDMA	Tri-diagonal matrix algorithm
x, y, z	are the Cartesian coordinate systems
ρ	Density
μ	Dynamic viscosity
$\vec{v} = (u, v, w)$	Velocity vector
φ	Inclination angle
χ	Nanoparticles concentration
ω	Angular velocity
γ	Magnetic field
τ	Stress tensor
ρg	Gravitational force

In addition to thermal boundary conditions, different hydraulic boundary conditions also influence Egen within enclosures. Fixed, movable, and elastic boundaries, velocities, pressure distributions, no-slip conditions, and flow regimes have an impact on the fluid flow behavior and overall energy transport within the enclosure. In laminar flow, the interaction of flow instabilities and shear layers can lead to vortices and affect Egen. During fully turbulent flow, near-wall coherent structures can strongly influence eddies convection and thus increase entropy [3]. Ellahi et al. [4] studied the effects of constant pressure on Egen in the magnetohydrodynamic (MHD) flow of nanofluid through porous media. The constant pressure boundary condition influenced the rate of Egen. The selection of appropriate hydraulic boundary conditions is therefore crucial to minimizing Egen and optimizing enclosure efficiency.

The enclosure's geometry, including its size and shape, has an impact on the system's flow patterns, heat transfer properties, and ultimately the generation of entropy. Enclosures with sharp corners exhibit higher Egen compared to smoother geometries. Sharp edges lead to increased fluid disturbances and enhanced fluid mixing [5]. The presence of obstacles inside the enclosure influenced Egen as well [6]. Selimefendigil et al. [7] placed circular, square, and diamond obstacles inside a square enclosure and observed that average heat transfer decreased and Egen increased. The aspect ratio of the enclosure, which is the ratio of its length to width or height, also played a role in determining the flow patterns and heat transfer distribution, thereby affecting Egen [8]. Similarly, the inclination angle of the enclosure, which is the angle between the enclosure's walls and the horizontal plane, also played a significant role in Egen [4].

The study explored a wide range of fluid types, including pure water, air, nanofluids, phase-change materials, porous media, and non-Newtonian fluids. The study of various fluids provided insights into their respective characteristics and how they affect Egen. For example, nanofluids improve thermal conductivity, which leads to lower Egen. But it also increased the viscosity of the base fluid, which resulted in higher Egen [9,10]. Several factors affect nanofluids' role in Egen in enclosures, including the type of nanoparticles, their volume fraction, the base fluid, and the geometry of the enclosure. Ahlawat and Sharma [11] investigated the impact of nanoparticle volume concentration and an external magnetic field on heat transport and Egen in a vented, heated complex enclosure filled with MgO/Ag-H_2O hybrid nanofluid. They found that Egen increased with χ and Ra. Alipanah et al. [12] compared Egen of natural convection heat transfer in a square enclosure using Al_2O_3-H_2O nanofluid and pure water. They found that the addition of nanoparticles to the pure fluid had a significant effect on Egen. This analysis of different fluids helps identify suitable fluids for specific purposes, resulting in better energy efficiency and lower irreversibility.

The effect of porous media in enclosures is also extensively studied in this research. Porous media in enclosures generally increase Egen (more surface area for heat transfer between fluids) [13], but it depends on several variables such as porosity [4], permeability [14], the shape of the enclosure, flow characteristics [15], and boundary conditions [16]. They alter the flow patterns within the enclosure, leading to changes in heat transfer and fluid flow characteristics [17]. Several factors reduced total Egen in enclosures filled with porous media, including the Da, Ha, χ, and magnetic field strength [18].

Entropy generation in enclosures is critically influenced by the interplay of fluid friction, magnetic field effects, and heat transfer mechanisms. Understanding these mechanisms and their dependencies on various factors such as fluid properties, enclosure geometry, and boundary conditions is crucial for optimizing system performance and energy efficiency while minimizing Egen. The interaction between the fluid and the enclosure wall leads to viscous dissipation. This frictional force converts some of the fluid's mechanical energy into heat, leading to an increase in entropy. The magnitude of Egen due to fluid friction depends on the properties of the fluid, the geometry of the enclosure, and the velocity distribution within the flow. Makinde [19] analyzed Egen in variable-viscosity hydromagnetic boundary layer flow and found that fluid friction was a significant factor contributing to Egen. Çiçek et al. [14] studied Egen in the mixed convection of a nanofluid-filled annulus and highlighted the influence of fluid friction on Egen. Generally, higher fluid velocities and viscosities led to increased fluid friction and higher Egen.

Like fluid friction, thermal strata within the enclosures are closely linked to Egen. The transfer of heat from regions of higher temperature to regions of lower temperature leads to a dissipation of energy and an increase in entropy. Conduction, convection, and radiation are the primary modes of heat transfer within enclosures. Conduction occurs through the solid walls of the enclosure and generates entropy due to thermal gradients [20]. Convection, on the other hand, involves the transfer of heat through fluid motion, leading to additional Egen due to fluid friction [21]. Radiation is an irreversible process that contributes to Egen. As electromagnetic waves emitted by the surfaces of the enclosure carry energy away, the system becomes more disordered, resulting in an increase in entropy [22].

Similar to thermal strata, the magnetic field also contributed to Egen as it induced magnetoconvection that altered flow patterns and increased convective heat transfer [23]. It led to reduced temperature gradients and Egen. The presence of magnetic fields also impacts the electrical conductivity of the fluid, leading to an increase in resistive heating and the consequent generation of entropy [24]. The orientation and strength of magnetic fields also affect Egen [25]. Hussain et al. [26] investigated the influence of an inclined magnetic field on the mixed convection in a partially heated square double lid-driven enclosure filled with Al_2O_3-H_2O nanofluid. The inclination angle of the magnetic field influenced the structure of the flow inside the enclosure. Mahmud and Fraser [27] studied Egen in a porous enclosure and concluded that Egen increased with an increase in magnetic field. Sivaraj and Sheremet [28], in their study with ferrofluid in a square enclosure with a non-uniformly heated plate, found that a magnetic field suppressed convective flow, heat transfer, and Egen.

Many different parts, including electronics, solar collectors, heat exchangers, automotive systems, and reactors, incorporate enclosures. Electronic components often had enclosures to help with airflow and cooling [29]. Smartphones have enclosures that keep the system's components from overheating. They also had an impact on the functionality and structural quality of electronic components [30]. Solar collectors employ enclosures to increase energy capture and efficiency [31]. Enclosures in nuclear reactors are linked to swelling evolution and structural material degradation, which have an impact on the deterioration of material properties and the creation of radiation-tolerant materials [32]. Additionally, improving heat transmission and lowering flow resistance in heat exchangers depends greatly on the form and geometry of enclosures [33]. Microwave enclosure perturbation research and better exhaust gas after-treatment systems utilize the enclosures in automotive catalytic devices [34]. Enclosures are utilized in additive manufacturing procedures to incorporate piezoelectric materials or sensors in vehicle parts [35]. Such multifaceted applications will be facilitated through thermofluid system optimization from the perspective of Egen and its control. Thus, its study is critical to optimizing thermal management and increasing energy efficiency.

The current research endeavors to establish a solid groundwork by conducting an extensive examination of recent studies related to Egen within enclosures. This comprehensive overview serves as the base for the study, aiming to delve into critical insights that hold significant importance for the sectors mentioned earlier. The foundational platform laid by this research enhances the depth and relevance of the study, enabling a more enlightened investigation into the subject matter. The future scope of work in Egen in enclosures is very promising. Current methods for calculating Egen are often computationally expensive and can be inaccurate. The development of more accurate and efficient methods would allow engineers to design more efficient systems. Entropy generation can have a significant impact on the stability of flow patterns. The study of these effects could lead to the development of new methods for controlling flow patterns and preventing instabilities. Also, further research needs to be done on novel enclosure geometries, alternative working fluids, and multi-objective optimization to minimize Egen.

2. Methodology

We carried out a systematic review following the PRISMA guidelines to thoroughly explore the subject of Egen in enclosures, as shown in Fig. 1. The review aimed to identify and analyze articles published between January 2014 and March 2023 from a range of reputable online databases, including ScienceDirect, Wiley and Sons, MDPI, Taylor and Francis, and Springer. The search strategy employed a combination of

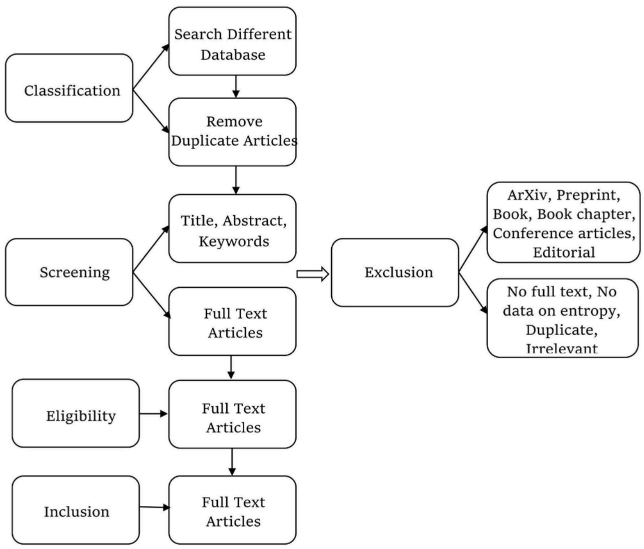

Fig. 1. Flow chart of Systematic Review Process [36]

keywords related to Egen and cavity types to ensure that a comprehensive range of relevant articles were identified. The selection criteria for the articles included in the review were based on their relevance to the research question as well as their quality and reliability. To ensure a comprehensive and thorough search, a variety of search terms were employed, including 'Entropy generation', 'Cavity and entropy generation', and a range of specific cavity types. The specific cavity types that were included in the search terms were square, rectangular, triangular, trapezoidal, wavy-shaped, C-shaped, I-shaped, L-shaped, U-shaped, semi-circular, three-dimensional, lid-driven, modified, hexagonal, octagonal, and other types of cavities. Additionally, the search terms also included variations on the theme of nanofluids and hybrid nanofluids, as these have been identified as important factors affecting Egen within cavities. As such, search terms such as 'Cavity and entropy generation and nanofluid' and 'Cavity and entropy generation and hybrid nanofluid' were also included. In the data extraction process, we ensured that our research was of high quality and reliable. Firstly, we focused only on articles written in English and checked the references to each article to identify related articles. Two researchers, named GS and AA, performed the data extraction process independently to reduce possible biases. To select the articles, the researchers checked the title, year, and abstract of each article and made independent decisions. In cases where there was disagreement, a third researcher, named SS, supervised the process and resolved the conflicts. The selected articles were stored in the following format: 'Name of the first author and year'. We excluded duplicate articles, review articles, book chapters, letters to editors, books, articles that were not accessible, and articles that were not related to our research. We assumed that the selected databases maintained all the criteria during the peer-review process, thereby ensuring quality. Overall, our rigorous data extraction process ensured that the articles we selected were of high quality and relevant to our research.

3. Mathematical Model

Numerous publications have delved into the study of Egen in enclosures of various shapes over the years. These investigations have covered a range of enclosure geometries, including squares, rectangles, triangles, hexagons, octagons, trapezoids, T-shapes, U-shapes, L-shapes, M-shapes, V-shapes, H-shapes, I-shapes, C-shapes, arc shapes, and other modified configurations. In addition, these inquiries have explored the impact of several factors on Egen resulting from heat transfer and fluid friction, such as the enclosure shape, working fluid, boundary conditions, and the presence of inserted objects like fins, cylinders, blocks, and rotating blades, which may either enhance or impair heat transfer.

The modeling of various fluid flow phenomena in engineering and physics relies on the application of the Navier-Stokes equations, which describe the motion of a fluid. These equations consist of three fundamental parts: the continuity equation, which ensures the conservation of mass within the fluid system; the momentum equation, which accounts for the forces acting on the fluid; and the energy equation, which characterizes the transfer of thermal energy. The Navier-Stokes equations find wide application across a broad range of fluid types and flow conditions, encompassing incompressible and compressible flows, steady and unsteady flows, Newtonian and non-Newtonian fluids, laminar and turbulent flows, and fluids with varying properties such as air, water, and nanofluids. Furthermore, the system under consideration can possess different geometries, including two-dimensional or three-dimensional configurations. Solving these equations presents a formidable challenge, compounded by the inclusion of body forces commonly encountered in fluid systems, such as gravity and electromagnetic forces. Additionally, other types of body forces may significantly influence the system's behavior and necessitate their incorporation into the modeling process. These forces encompass phenomena such as buoyancy forces, Brownian motion of particles, thermophoresis effects, heat generation or absorption, radiation effects, and the porous medium effect, which can be described using the Foechheimer-Brinkman model. Properly accounting for these forces is vital when studying and modeling fluid systems, as they can have a pronounced impact on the overall behavior and dynamics of the system. A similar statement is true for the energy equation and the mass transfer equation as well, since there can be several external sources of heat and mass transfer. The general form of the mass, momentum, energy, and mass transfer equations is given below in vector form. Since there can be several external sources involved in the respective property transport, these other sources are incorporated into the respective governing equations through the term "other terms." Therefore, the term "other terms" refers to the force, the rate of energy transfer, and the rate of mass transfer in the momentum equation, energy equation, and mass transfer equation respectively, which can be seen below.

Continuity equation:

$$\frac{\partial \rho}{\partial t} + \nabla.(\rho \vec{v}) = 0 \tag{1}$$

Momentum equation:

$$\frac{\partial(\rho \vec{v})}{\partial t} + \nabla.(\rho \vec{v}\vec{v}) = -\nabla \mathrm{p} + \nabla.\tau + \rho \mathrm{g} + \text{other terms} \tag{2}$$

Energy equation:

$$\frac{\partial(\rho E)}{\partial t} + \nabla.(\rho \vec{v} E) = -\nabla.(\rho \vec{v}) + \nabla.(\kappa \nabla \mathrm{E}) + \mathrm{Q} + \text{other terms} \tag{3}$$

Mass transfer equation:

$$\frac{\partial(\rho C)}{\partial t} + \nabla.(\rho \vec{v} C) = \nabla.(D\ \nabla \mathrm{C}) + \text{other terms} \tag{4}$$

Entropy generation due to fluid friction:

$$S_{ff} = \mu(\nabla \vec{v})^2$$

Entropy generation due to heat transfer:

$$S_{HT} = q/T$$

Entropy generation due to mass transfer:

$$S_{MT} = -\left(\frac{\rho D}{C}\right) \nabla.\mathrm{C}$$

Bejan number:

$$Be = \frac{S_{HT}}{S_{TOT}}$$

Details of some non-dimensional parameters are presented in Appendix.

Thoroughly documenting the validation procedure within a study is crucial to guaranteeing the precision of numerical findings and offering a valuable reference for subsequent investigations. Regrettably, there is a dearth of such information in previous literature review studies. As such, we would like to provide some validation information here. Saha et al. [36] present the details regarding the validation of heat transfer analysis. However, as our current research is focused on Egen analysis, this section will specifically present validation results related to entropy. The following are the most frequently utilized results that we generated and presented here for validating Egen as shown in Fig. 2 [6,11,37–79]. Fig. 2 presents the variation of local thermal Egen, local frictional Egen and local Egen as well as local Be for a square cavity with Ra = 10^5. The thermal Egen achieved its highest point, reaching approximately 59.61, whereas the frictional Egen peaks at around 567.48. This significant contrast in their respective maximum values underscores the considerable influence and dominance of frictional effects in comparison to thermal effects within the studied system. The dominance of local frictional Egen is notably pronounced, as indicated by the local Egen map. This prevailing influence is also discernible from the local Bejan map.

4. Quantitative Data Analysis

The visual representation in Fig. 3 provides a comprehensive view of the most commonly used words found in the abstracts of the selected articles. A detailed analysis indicates that the primary subjects explored in these articles include entropy, total entropy, Egen, natural convection, mixed convection, steady and unsteady flow, as well as Newtonian and non-Newtonian fluids. Another significant area of focus is nanofluids and hybrid nanofluids, which are increasingly becoming popular in the field of fluid dynamics. In addition, these articles showcase a strong emphasis on employing numerical methods such as Finite Element Method (FEM), Finite Volume Method (FVM), Finite Difference Method (FDM), and lattice Boltzmann method (LBM) for conducting numerical experiments.

According to the data presented in Fig. 4, it is clear that among the various types of cavities, square enclosures are the most extensively researched, accounting for almost half (46.6%) of the total number of articles. The second most studied type of enclosure is three-dimensional enclosures, which make up 8.5% of the articles. However, other shapes of enclosures have also been studied in significant numbers. Trapezoidal, triangular, wavy-shaped, rectangular, L-shaped, rhombic, semi-circular, and U-shaped enclosures are all represented in the literature. These different enclosure shapes represent 5.4%, 4.9%, 4.5%, 3.6%, 3.1%, 2.7%, 2.2%, and 1.3% of the total number of articles, respectively. Moreover, it is worth noting that there are some less common enclosure shapes that have still received a fair amount of attention in the literature. For example, the channel flow enclosure, I-shaped, modified, and concave/convex side enclosures have each been studied in 1.8% of the articles. This indicates that researchers are exploring a wide range of enclosure shapes and configurations and that there is a growing interest in understanding the behavior and properties of different types of enclosures.

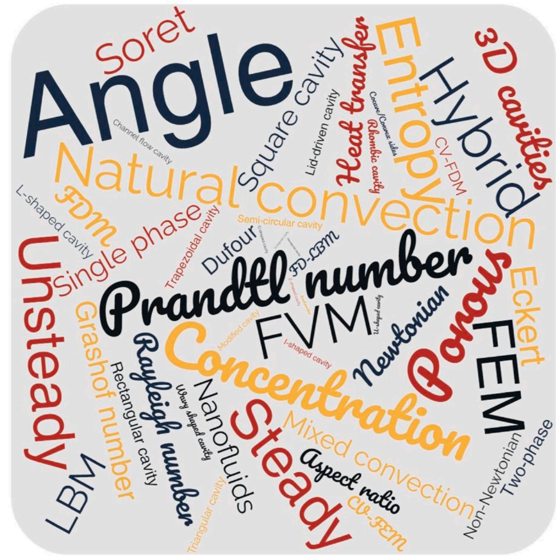

Fig. 3. Word-Cloud Map

The data presented in Fig. 5 reveals some interesting insights about the focus of research in the field of fluid dynamics. The majority of articles, 93%, concentrated on Newtonian fluids, while only a small proportion, 7%, considered non-Newtonian fluids. Among the types of fluids investigated, nanofluids and hybrid nanofluids were the most commonly studied, with 65% of articles focusing on these topics. The remaining 35% of articles explored conventional fluids such as air and water. In terms of the mode of heat transfer, natural convection garnered the most attention, with 76% of articles focusing on this area. In contrast, mixed and forced convection were the topics of study in only 24% of articles. The temporal nature of the fluids being analyzed was also considered, with 74% of articles focusing on steady-state flow conditions and 26% on unsteady-state flow conditions. Another noteworthy finding was that the majority of articles, 91%, used a two-dimensional model to study fluid dynamics. Additionally, the single-phase model was the most common, with 96% of articles using this approach. However, this also highlights the need for further research in the area of two-phase models, which received less attention. Overall, these findings provide a glimpse into the trends and gaps in research in the field of fluid dynamics and highlight areas that may require further attention in the future.

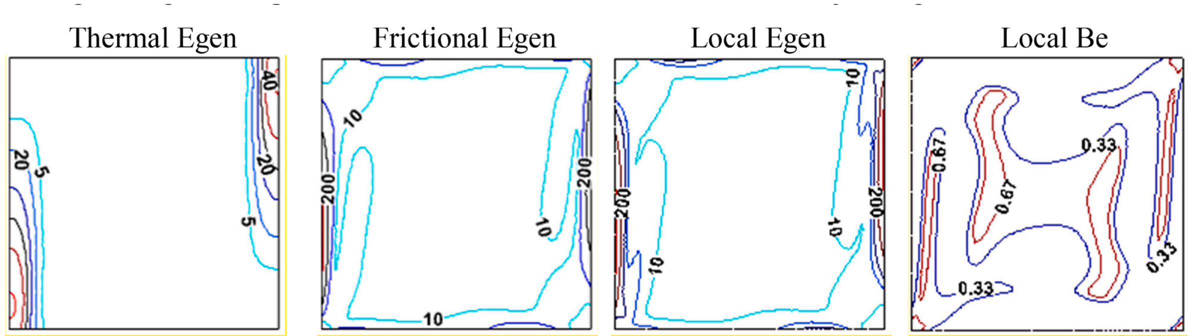

Fig. 2. Variation of thermal, frictional, local Egen, and local Be for Pr = 0.71, Ra = 10^5

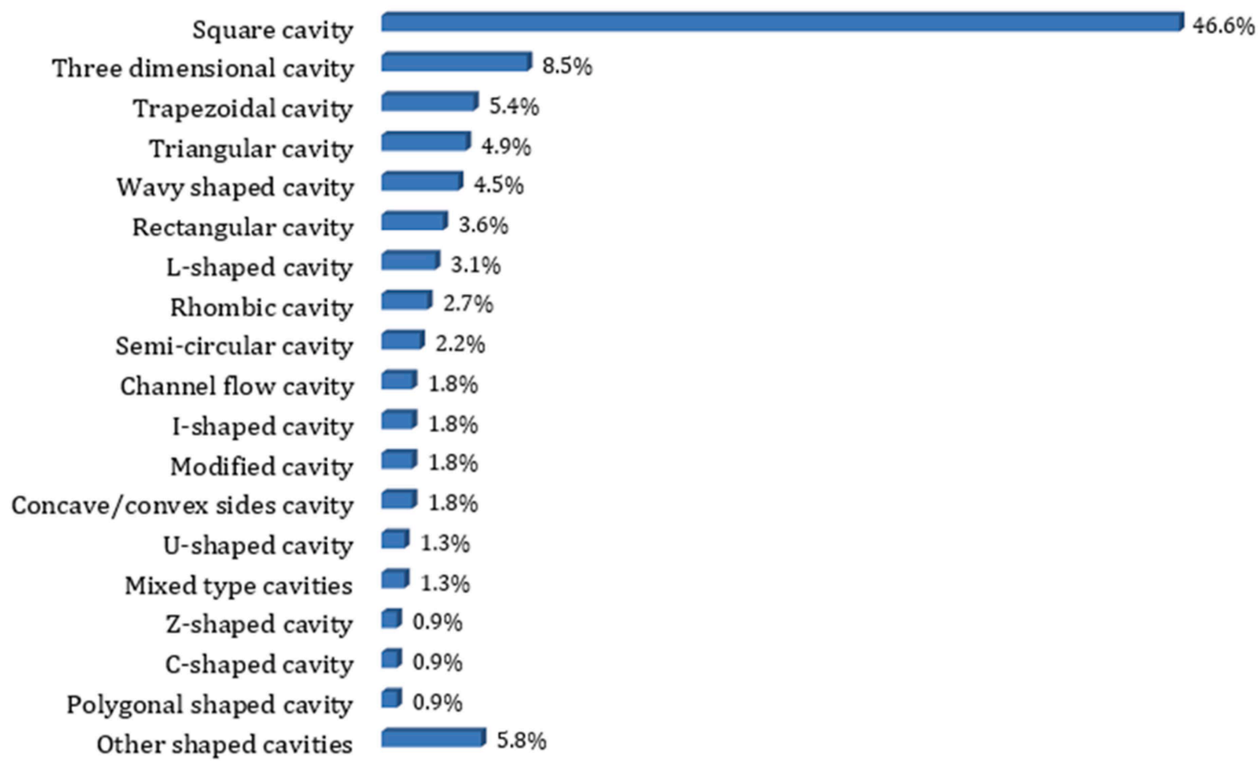

Fig. 4. Number (%) of physical domains

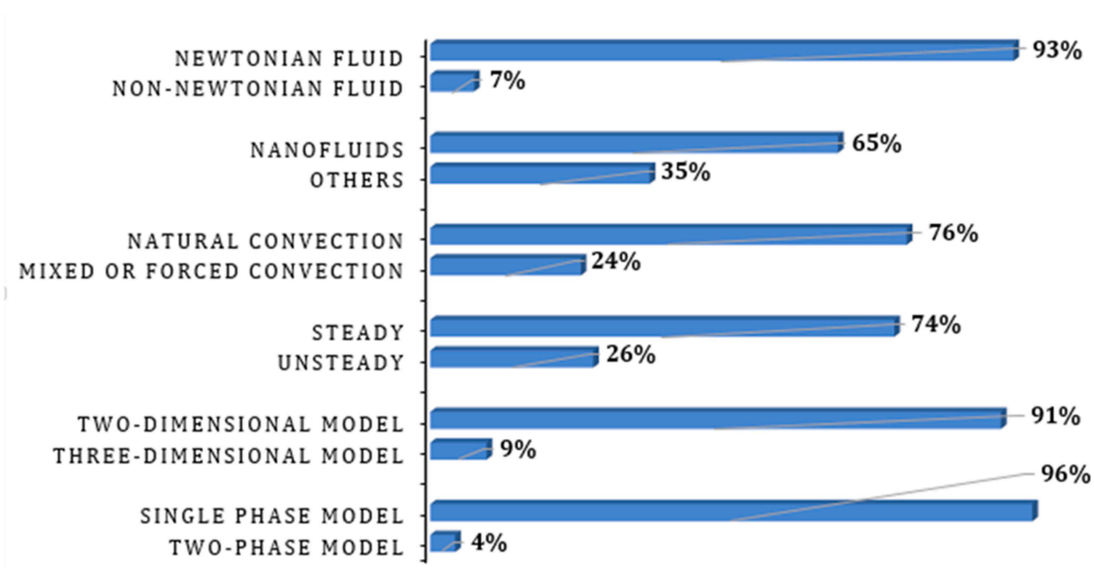

Fig. 5. Number (%) of different categories

The researcher's analysis, depicted in Fig. 6, reveals the varied numerical approaches employed in their investigations. A significant 36% of the research employs the finite element method (FEM), indicating its widespread acceptance as a reliable approach. The finite or control volume method (FVM or CVM) ranks second, with 28% of the research utilizing this numerical approach. The finite difference method (FDM) is used in 11% of the research, establishing it as the third most commonly used approach. Interestingly, the lattice Boltzmann method (LBM) is used in 9% of the research, suggesting its increasing popularity as a reliable numerical technique. Furthermore, the literature reports the existence of various hybrid methods, such as FD-LBM (6%), CV-FEM (4%), and CV-FVM (4%). Additionally, 2% of the research employed other techniques not explicitly mentioned above.

5. Entropy Generation Analysis

Tables 1 to 24 display the findings of research conducted on Egen analysis by the flow of natural or mixed or forced convection in different shapes of enclosures. In addition, this section will provide a brief overview of some relevant references that were selected for discussion. The study included in Tables 1 to 24 examined various aspects of natural or mixed convection flow in enclosures, such as the effect of different geometries and boundary conditions on flow patterns and Egen. Additionally, some investigations focused on the impact of nanoparticles on

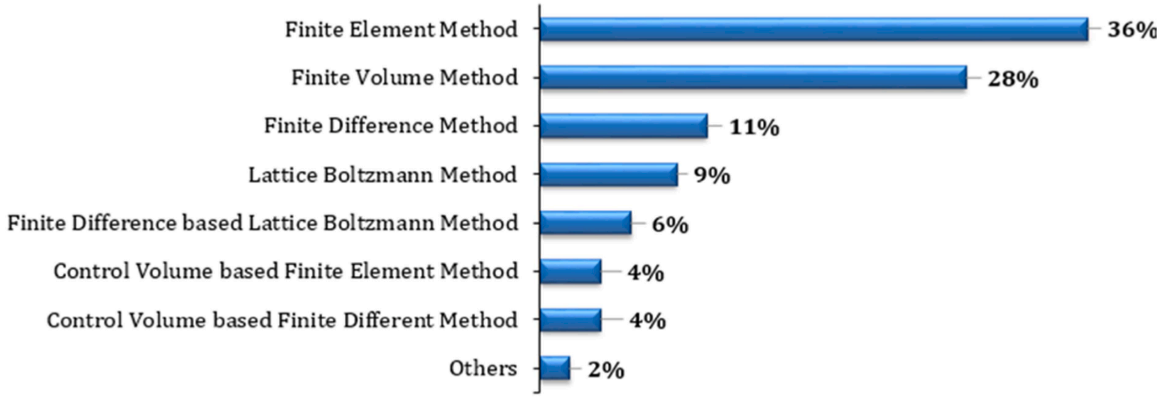

Fig. 6. Number (%) of numerical methods used by research

the thermal and fluid behavior of the flow.

Table 1 presents various research works on natural convection in a square enclosure. Some of the selected articles are described below:

Al-Kouz et al. [91] studied Egen analysis in a square enclosure with two hot fins fixed on the left wall. Their observations showed that an increase in nanofluid concentration resulted in an increase in Egen for both low Ra cases and as both heat and Ra increased. Conversely, Egen decreased when Ra was high and the nanofluid concentration increased. Baghsaz et al. [92] investigated how the sedimentation of nanoparticles affected natural convection within a square enclosure. Their findings indicated that increased porosity (ε), Ra, and Da led to a higher level of irreversibility. When permeability was low, the total Egen had lower values. Zhou et al. [93] used numerical simulations to examine Egen within a square enclosure. The left boundary was established as having a hot temperature while the left wall remained cold. Their findings revealed that Egen increased as the Gr rose, and the contour lines were concentrated near the hot wall. Additionally, CNT-Ga produced the highest Egen while Cu-Ga had the lowest value. Şahin [73] analyzed Egen in a square enclosure with linear heating. The heating center was positioned on the left wall, while the right wall had a uniform temperature, and the other boundaries were insulated. The findings revealed that the total Egen had the lowest value at H_L=1, where the highest heat transfer occurred, regardless of the value of Ra. Additionally, the maximum Egen resulting from heat transfer happened at H_L=0.25, while the maximum Egen due to fluid friction depends on the heating centerr's location. Later, Şahin [74] conducted a study that examined entropy generation within a square enclosure. The study found that as Ra increased, Egen increased for all types of particles. At low Ra=10^4, heat transfer caused most of the Egen, with boron-H_2O nanoparticles leading to an increase in Egen compared to other nanofluids. Ahlawat and Sharma [11] investigated Egen in a square enclosure. It is seen that increasing the thickness of the porous media resulted in an increase in Be and a decrease in Egen. Additionally, an increase in Ko (dimensionless vortex viscosity parameter) and χ led to an increase in heat transfer irreversibility over frictional irreversibility. Gokulavani et al. [94] studied Egen in a square enclosure with a hot baffle placed at the center of the enclosure. It is observed that entropy due to heat transfer was the predominant factor, with higher values observed in the suction case.

Table 2 displays a compilation of different research studies focusing on MHD natural convection within a square enclosure. A summary of a few chosen articles is provided below:

Ahrar et al. [106] conducted a numerical simulation aimed at examining how an external magnetic field affects Egen in a square enclosure containing a hot elliptical object. The study revealed that as the Ha increased, the total Egen decreased, but it increased with Ra. Al-Rashed [107] conducted a numerical investigation on a square enclosure exposed to a constant magnetic field. Their findings indicated that as Ra increased and Ha decreased, the total Egen increased. Alnaqi et al. [108] studied the impact of a magnetic field and radiation on Egen in an inclined square enclosure. They observed that at high Ra, the total Egen increased with higher χ and Rd but decreased with lower Ra values. Alsabery et al. [129] investigated Egen within a square enclosure with a hot trapezoidal object affixed to the bottom wall, exposed to an inclined magnetic field. The upper boundary was insulated, while the vertical boundaries were cold. The study revealed that Egen from viscous dissipation decreased. Additionally, increasing χ and the length of the trapezoidal object resulted in decreased global Egen. Arun and Satheesh [44] examined Egen in a square enclosure with an adiabatic rectangular block positioned at the center. Their findings indicated that for Ra values between 10^3 and 10^4, the non-dimensional Egen increased by 65.5% due to heat transfer, 99.2% due to fluid friction, and 66.2% due to fluid concentration. Additionally, the total Egen decreased as Ha increased for all Ra values.

Goqo et al. [110] explored the flow characteristics of a porous medium containing nanoparticles within a square enclosure. They found that considering the Brownian motion of the particles, Egen increaseswith Ra. Moreover, an increase in Rd resulted in a rise in the total Egen for all values of Ha. Hajatzadeh Pordanjani et al. [130] conducted a study on Egen in a square enclosure. The left boundary had a variable temperature distribution, with four cases: sinusoidal, fixed, first-order, and second-order profiles, while the right boundary remained cold and the other boundaries were insulated. As Ra increased, the maximum and minimum Nu increased by 9.1% and 7.6% for cases a and d, respectively, resulting in a corresponding maximum and minimum increase in Egen of 42.9 and 19.2 times for these cases. Additionally, increasing Ha led to a maximum entropy reduction of 64% and a minimum reduction of 60% for the case with a parabolic temperature profile. Finally, adding a 6% volume fraction of nanoparticles resulted in a 12% increase in Egen. Al Kalbani et al. [112] analyzed Egen within a square enclosure. Four different boundary conditions were considered: (a) cold top boundary and hot bottom boundary; (b) hot left boundary and cold right boundary; (c) hot top boundary and cold bottom boundary; and (d) cold left boundary and hot right boundary, with the other boundaries being adiabatic. They found that the total Egen due to friction was dominant for the top heated boundary. Additionally, the minimum Egen was higher for case (a) and lower for case (c). Li et al. [113] conducted a study on Egen in a square enclosure and separated by a diagonal partition. The partition divided the enclosure into left and lower sections at a high temperature and an upper right section in contact with a cold boundary. The study revealed that increasing Ra from 10^3 to 10^5 resulted in a 90% increase in Egen. Additionally, increasing Ha from 0 to 40 decreased Egen by 46%. The study also found that increasing Rd up to 3 resulted in a 6.6% intensification of Egen. Furthermore, when the hot length intensity increased from 0.1 to 0.9, Egen increased by 2.8 times. Li et al. [33] studied to investigate the Egen inside an inclined square enclosure, focusing on the effect of Rd and

Table 1
Research work on natural convection in a square enclosure

References	Tools	Domain	Flow details	Constants
Basak et al. [80]	FEM	Inclined square enclosure	2D, steady, NC	$10^3 \le$ Ra$\le 10^5$, Pr = 0.025, 998, $0 \le \varphi \le 60$
El-Maghlany et al. [81]	FVM, TDMA	Square enclosure	2D, laminar, NC, steady, Newtonian, incompressible	Pr = 0.7, $10^3 \le$ Ra$\le 10^5$, $0\le$ q$\le$ 10
Lam and Arul Prakash [70]	FEM	Square porous enclosure with multiple blocks	2D, laminar, NC, unsteady, Newtonian, incompressible	$10^3 \le$ Ra$\le 10^6$, $10^{-5}\le$ Da$\le 10^{-2}$
Singh et al. [77]	FEM	Tilted square enclosure	2D, NC, steady	Pr = 0.025, 998.24, $10^3\le$ Ra$\le 10^5$, $0\le \varphi \le 75$
Alipanah et al. [12]	FVM, SIMPLE	Square enclosure	2D, steady, NC, Al_2O_3-H_2O nanofluid	$10^4\le$ Ra$\le 10^7$, $0\le \chi \le$ 0.05, Pr = 6.2, dp = 40, 1 nm
Singh et al. [76]	FEM	Tilted porous square enclosure	2D, NC, steady	Pr = 0.015, 1000, $10^{-5}\le$ Da$\le 10^{-2}$, $10^3\le$ Ra$\le 10^6$, $0\le \varphi \le$ 90
Biswal et al. [48]	FEM	Porous square inclined enclosure	2D, steady, NC, laminar. Newtonian, incompressible	$0\le \varphi \le 90$, $10^{-5}\le$ Da$\le 10^{-2}$, Pr = 0.025, 998.24, Ra=10^6
Ismael et al. [82]	FDM	Square porous enclosure with triangular solid	2D, steady, NC, CuO-H_2O nanofluid	$0\le \chi \le 0.05$, $10\le$ Ra$\le 10^3$
Sheremet et al. [6]	FVM, SIMPLE	Square enclosure with block	2D, steady, NC, Cu-H_2O nanofluid	$10^3\le$ Ra$\le 10^6$, $0\le \chi \le$ 0.05
Ashorynejad and Hoseinpour [83]	LBM	Porous square enclosure	2D, steady, NC, H_2O based Al_2O_3, Cu, TiO_2 nanofluids, laminar, incompressible	$0\le \chi \le 0.06$, Pr=6.2, Ra=10^5, Da=10^{-2}
Bouchoucha et al. [84]	CVM, SIMPLER	Square enclosure	2D, steady, FC, laminar, Al_2O_3-H_2O nanofluid, Newtonian, incompressible	$10^4\le$ Ra$\le 10^6$, $0\le \chi \le$ 0.1
Ghasemi and Siavashi [55]	LBM	Porous square enclosure	2D, steady, NC, Cu-H_2O nanofluid, laminar, Newtonian, incompressible	$10^3\le$ Ra$\le 10^6$, $0\le \chi \le$ 6%, $10^{-3}\le$ Da$\le 10^{-1}$
Rahimi et al. [10]	LBM	Square enclosure with blocks	2D, steady, NC, laminar, DWCNTs-H_2O nanofluid, Newtonian, incompressible	$10^3\le$ Ra$\le 10^6$, $0\le \chi \le$ 0.5%
Siavashi et al. [85]	FVM, SIMPLE, TDMA	Porous inclined square enclosure with blocks	2D, steady, NC, two-phase model	Pr=0.71, N= - 0.8, $0\le \varphi \le$ 90, $10^{-6}\le$ Da$\le 10^{-1}$, $10^4\le$ Ra$\le 10^6$, $0.1\le$ Le$\le$ 10
Sheremet et al. [86]	FDM	Square enclosure	2D, unsteady, NC	$10^3\le$ Ra$\le 10^5$, Pr = 7, Le = 1000, N = N_b = N_t = 0.1
Alsabery et al. [87]	FDM	Square enclosure with solid block	2D, steady, NC, laminar, Al_2O_3-H_2O nanofluid	$10^3\le$ Ra$\le 10^6$, $0\le \chi \le$ 0.09, $0.44\le$ $K_T\le$ 23.8
Kashyap and Dass [88]	LBM	Porous square enclosure	2D, two-phase, laminar, Cu-H_2O nanofluid, NC. steady, Newtonian, incompressible	$10^3\le$ Ra$\le 10^5$, $10^{-6}\le$ Da$\le 10^{-1}$, $0\le \chi \le 0.05$
Kefayati et al. [64]	FD-LBM	Inclined square enclosure	2D, unsteady, NC, Bingham fluid, laminar, incompressible	$10^3\le$ Ra$\le 10^5$, $2\le$ Le$\le$ 10, $0\le$ Du, Sr$\le$ 5, $0\le$ Ec$\le$ 0.1, -1$\le$ N$\le$ 1, $0\le \varphi \le 120$, Pr = 1, $0.1\le$ Bn$\le$ 12
Kefayati and Tang [69]	FD-LBM	Open square enclosure	2D, unsteady, NC, Bingham fluid, incompressible	$10^3\le$ Ra$\le 10^5$, $2.5\le$ Le$\le$ 10, $0\le$ Du, Sr$\le$ 5, Ec = 0.001, 0.01, -1$\le$ N$\le$ 1, $0.1\le$ Bn$\le$ 12
Rahimi et al. [89]	LBM	Sqare enclosure with multiple blocks	2D, unsteady, NC, DWCNTs–H_2O nanofluid	0.01%$\le \chi \le$ 0.4%, $10^3\le$ Ra$\le 10^6$
Siavashi et al. [90]	FVM, SIMPLE	Square enclosure with porous fins	2D, steady, Cu-H_2O nanofluid, NC, two-phase mixture model, laminar, Newtonian	$10^4\le$ Ra$\le 10^6$, $10^{-4}\le$ Da$\le 10^{-1}$, $0\le \chi \le 0.04$
Al-Kouz et al. [91]	FVM, SIMPLE	Square enclosure with fins	2D, laminar, FC, Al_2O_3-Air nanofluid, steady	$10^3\le$ Ra$\le 10^6$, $0\le \chi \le$ 0.02, $0\le$ $K_n\le$ 0.1
Baghsaz et al. [92]	FVM, PIMPLE	Porous square enclosure	2D, unsteady, NC, two phase mixture model, laminar, Al_2O_3-H_2O nanofluid, incompressible	$10^4\le$ Ra$\le 10^7$, $10^{-5}\le$ Da$\le 10^{-2}$
Zhou et al. [93]	FVM, QUICK, SIMPLE	Square enclosure	2D,laminar, NC, steady, Cu-Ga, Diam-Ga, CNT-Ga nanofluids, two-phase mixture model, Newtonian, incompressible	$10^4\le$ Gr$\le 10^6$, $0.01\le \chi \le 0.15$, dp = 20 nm
Sahin [73]	FVM	Square enclosure	2D, NC, steady	$10^3\le$ Ra$\le 10^6$, Pr = 0.71
Şahin [74]	FVM, SIMPLE	Square enclosure	2D, steady, NC, laminar, boron-H_2O nanofluid	$10^4\le$ Ra$\le 10^6$, $0\le \chi \le$ 0.04
Ahlawat and Sharma [11]	FDM, SOR, SUR	Square porous enclosure with block	2D, Cu-Al_2O_3-H_2O hybrid nanofluid, steady, laminar, incompressible	$10^{-5}\le$ Da$\le 10^{-3}$, $10^3\le$ Ra$\le 10^5$, $0\le \chi \le 0.1$, $2\le$ K$\le$ 7
Gokulavani et al. [94]	FDM, TDMA	Porous open square enclosure with baffle	2D, Cu-TiO_2-H_2O hybrid nanofluid, unsteady, laminar, incompressible	$0\le \chi \le 0.04$, $10^4\le$ Ra$\le 10^6$, $10^{-4}\le$ Da$\le 10^{-2}$, $100\le$ Re$\le$ 500

Table 2
Research work on MHD natural convection in a square enclosure

References	Tools	Domain	Flow details	Constants
Mahmoudi et al. [95]	LBM	Square enclosure	2D, MHD, NC, steady, Al_2O_3-H_2O nanofluid, Newtonian, laminar, incompressible	$10^3 \leq$ Ra$\leq 10^6$, $0\leq$ Ha≤ 60, $0\leq \chi \leq 0.06$
Mejri et al. [96]	LBM	Square enclosure	2D, laminar, NC, MHD, Al_2O_3-H_2O nanofluid, Newtonian, steady, incompressible	$10^3\leq$ Ra$\leq 5\times 10^4$, $0\leq$ Ha≤ 50, $0\leq \varphi \leq 180$, $0\leq \chi \leq 0.06$
Selimefendigil and Öztop [7]	FEM	Square enclosure with obstacles	2D, unsteady, NC, MHD	$10^4\leq Ra_I$, $Ra_E\leq 10^6$, $0\leq \chi \leq 0.05$, $0\leq$ Ha≤ 50
Mamourian et al. [97]	RSM, FVM, SIMPLE	Square enclosure	2D, MHD, Al_2O_3-H_2O nanofluid, NC, laminar, incompressible, Newtonian, steady	$10^3\leq$ Ra$\leq 10^6$, $0\leq$ Ha≤ 50, $0\leq \varphi \leq 90$, Pr $= 6.2$, $0\leq \chi \leq 0.05$
Ahrar and Djavareshkian [98]	Hybrid FD-LBM	Square enclosure	2D, MHD, NC, unsteady	$10^3\leq$ Ra$\leq 10^8$, $0\leq$ Ha≤ 100
Gibanov et al. [99]	FDM	Partially porous square open enclosure	2D, MHD, FC, unsteady, Fe_3O_4-H_2O nanofluid	Ra$=10^5$, Da$=10^{-5}$, Pr $= 6.26$, $0\leq$ Ha≤ 100, $0\leq \varphi \leq 180$, $0\leq \chi \leq 0.05$
Ghasemi and Siavashi [100]	LBM	Porous square enclosure	2D, MHD, FC, Cu-H_2O nanofluid, steady, incompressible	$10^3\leq$ Ra$\leq 10^6$, $0\leq$ Ha≤ 20, $0\leq \chi \leq 0.12$, $0\leq K_T\leq 70$
Malik and Nayak [101]	FVM, QUICK, SIMPLE	Porous square enclosure	2D, MHD, unsteady, laminar, Newtonian, incompressible	$10^4\leq$ Gr$\leq 10^6$, $1\leq$ Ha≤ 50, $0.001\leq$ Da≤ 1, Pr$=6.2$, $0\leq \chi \leq 0.2$
Mohammadpourfard et al. [102]	CVM, SIMPLEC	Square enclosure	2D, steady, MHD, FC, two-phase mixture, Fe_3O_4-H_2O nanofluid	$\chi=0.04$, dp $= 10$ nm, $10^5\leq$ Ra$\leq 10^6$
Gibanov et al. [103]	FDM	Open square enclosure with porous blocks	2D, MHD, FC, unsteady, Fe_3O_4-H_2O nanofluid	Pr$=6.82$, Ra$=10^4$, Da$=10^{-3}$, 10^{-7}, $0\leq$ Ha≤ 100, $0\leq \chi \leq 0.05$
Mansour et al. [104]	FDM, SUR	Porous square enclosure	2D, MHD, FC, steady, Cu-Al_2O_3-H_2O hybrid nanofluid, laminar, incompressible	$0\leq$ Ha≤ 100, $0.03\leq \chi \leq 0.1$, $10^{-6}\leq$ Da$\leq 10^{-2}$, Ra$=10^4$
Mehryan et al. [71]	FEM	Square enclosure	2D, MHD, FC, steady, Fe_3O_4-H_2O nanofluid, Newtonian	$10^3\leq$ Ra$\leq 10^6$, $0\leq$ Ha≤ 50, $0\leq \chi \leq 0.08$
Rashad et al. [105]	FDM, SUR	Inclined square porous enclosure	2D, steady, MHD, NC, Cu-H_2O nanofluid, laminar, incompressible	Ra$=10^5$, $0\leq \chi \leq 0.05$, $0\leq$ Ha≤ 25, $0\leq \varphi \leq 360$
Sivaraj and Sheremet [28]	FVM, SIMPLE, QUICK, TDMA	Square enclosure with plate	2D, MHD, NC, laminar, Newtonian, unsteady, Fe_3O_4-H_2O nanofluid	$0\leq \varphi \leq 90$, $0\leq$ Ha≤ 100, $0\leq \chi \leq 0.04$
Zhang et al. [79]	LBM	Porous square enclosure	2D, MHD, steady, incompressible	$0\leq \varphi \leq 60$, $10^5\leq$ Ra$\leq 6\times 10^6$, $10^{-5}\leq$ Da$\leq 10^{-1}$
Ahrar et al. [106]	FD-LBM, SIMPLE	Square enclosure	2D, MHD, FC, unsteady, Al_2O_3-H_2O nanofluid, laminar	$0\leq$ Ha≤ 90, $0\leq \chi \leq 0.04$, $1\leq$ Le$\leq 10^5$, $0\leq \varphi \leq 90$, $10^5\leq$ Ra$\leq 10^6$
Al-Rashed [107]	CVM, SIMPLE	Square enclosure with blades	2D, MHD, FC, steady, Al_2O_3-H_2O nanofluid, incompressible	$10^3\leq$ Ra$\leq 10^6$, $-45\leq \varphi \leq 45$, $0\leq$ Ha≤ 40, $0\leq \chi \leq 0.06$
Alnaqi et al. [108]	FVM, SIMPLE	Inclined square enclosure with fin	2D, MHD, steady, laminar, Newtonian, incompressible, Al_2O_3-H_2O nanofluid	$10^3\leq$ Ra$\leq 10^6$, $0\leq$ Ha≤ 40, $0\leq \chi \leq 0.06$, $0\leq Rd \leq 3$
Alsabery et al. [109]	FEM	Square enclosure with trapezoidal body	2D, MHD, Al_2O_3-H_2O non-homogeneous nanofluid, steady, laminar, Newtonian	$10^3\leq$ Ra$\leq 10^6$,$0\leq$ Ha≤ 50, $0\leq \chi \leq 0.04$
Arun and Satheesh [44]	LBM	Square enclosure with block	2D, MHD, FC, steady, incompressible	$10^3\leq$ Ra$\leq 10^5$, $0\leq$ Ha≤ 50, $2\leq$ Le≤ 10, $-2\leq$ N≤ 2, Pr $= 0.054$
Goqo et al. [110]	MSQM	Porous square enclosure	2D,MHD, steady, FC, laminar, incompressible	$0\leq$ Ra$\leq 10^5$, $0.1\leq N_b\leq 0.5$, $0.1\leq N_t\leq 0.5$, $0.2\leq$ Le≤ 4, $0\leq$ Ha≤ 20
Hajatzadeh Pordanjani et al. [111]	FVM, SIMPLE	Inclined square enclosure	2D, MHD, Al_2O_3-H_2O nanofluid, laminar, Newtonian, steady, incompressible	$10^3\leq$ Ra$\leq 10^6$, $0\leq$ Ha≤ 60, $0\leq \varphi \leq 90$, $0\leq \chi \leq 0.06$
Al Kalbani et al. [112]	FEM	Titled square enclosure	2D, unsteady, MHD, Cu-H_2O nanofluid, FC, laminar	$0.001\leq \chi \leq 0.1$, $10^3\leq$ Ra$\leq 10^6$, $0\leq$ Ha≤ 60
Li et al. [113]	CV-FDM, SIMPLE	Inclined square enclosure with conductive partition	2D, MHD, NC, steady, Al_2O_3-H_2O nanofluid, laminar, Newtonian, incompressible	$10^3\leq$ Ra$\leq 10^5$, $0\leq$ Ha≤ 40, $0\leq \chi \leq 0.05$, $0\leq$ Rd≤ 3, $0\leq \varphi \leq 90$
Li et al. [114]	CV-FDM, SIMPLE	Inclined square enclosure with baffle	2D, MHD, FC, steady, Al_2O_3-H_2O nanofluid, laminar, Newtonian, incompressible	$10^3\leq$ Ra$\leq 10^6$, $0\leq$ Ha≤ 40, $0\leq \varphi \leq 90$, $0\leq \chi \leq 0.06$, $0\leq$ Rd≤ 3
Rabbi et al. [115]	ANN, FEM	Square enclosure	2D, MHD, Cu-H_2O nanofluid, steady	$10^3\leq$ Ra$\leq 10^7$, $0\leq$ Ha≤ 100, $0\leq \chi \leq 0.05$
Selimefendigil and Öztop [116]	FEM	Inclined square enclosure with conductive region	2D, MHD, NC, laminar, Newtonian, steady	$10^4\leq$ Ra$\leq 10^6$, $0\leq \varphi \leq 180$, $0\leq$ Ha≤ 50, $0\leq \chi \leq 0.03$
Seyyedi et al. [117]	CV-FEM	Inclined square enclosure	2D, steady, MHD, NC, laminar	Pr $= 0.733$, $0\leq$ Ha≤ 100, $10^4\leq$ Ra$\leq 10^5$, $0\leq \varphi \leq 60$
Tayebi and Chamkha [118]	FVM, SIMPLE	Square enclosure with hollow cylinder	2D, steady, MHD, FC, laminar, Cu-Al_2O_3-H_2O hybrid nanofluid, Newtonain, incompressible	$0\leq \chi \leq 0.09$, Pr $= 6.2$, $0\leq$ Ha≤ 50, $10^3\leq$ Ra$\leq 10^6$
Khetib et al. [119]	FVM, SIMPLE	Square enclosure with fins	2D, MHD, NC, steady, Al_2O_3-H_2O nanofluid	$0\leq \varphi \leq 90$, $0\leq$ Ha≤ 40, Ra$=10^5$, $\chi=0.03$
Reddy and Sreedevi [120]	FDM	Square enclosure	2D, MHD, steady, laminar, FC, Ag-Cu-EG hybrid nanofluid, incompressible	$0.01\leq$ Rd, $\chi \leq 0.1$, $5.2\leq$ Pr≤ 8.2, $10^4\leq$ Ra$\leq 10^5$, $0.1\leq$ M≤ 1
Tian et al. [121]	CV-FDM, SIMPLE	Oblique square enclosure with block	2D, steady, laminar, Al_2O_3-H_2O nanofluid, incompressible	$0\leq \chi \leq 0.06$, $0\leq \varphi \leq 90$, $0\leq$ Ha≤ 90
Ahmed et al. [39]	FVM	Porous square enclosure	2D, MHD, NC, steady, Cu-Al_2O_3-H_2O hybrid nanofluid	$-2\leq$ q≤ 2, $0\leq$ Rd≤ 1, $0\leq$ K≤ 2, $0\leq$ Ha≤ 100, $0\leq \chi \leq 0.05$, $0\leq \varphi \leq 180$
Reddy and Sreedevi [122]	FDM	Square enclosure	2D, MHD, FC, steady, Ag-SWCNT-H_2O hybrid nanofluid, laminar, incompressible	$0.01\leq$ Rd, $\chi \leq 0.1$, $5.2\leq$ Pr≤ 8.2, $0.1\leq$ M≤ 0.7, $10^3\leq$ Ra$\leq 10^4$
Reddy et al. [123]	FDM, SUR	Porous square enclosure	2D, MHD, NC, Cu-H_2O nanofluid, laminar, Newtonian, steady, incompressible	$0\leq \chi \leq 0.1$, $0\leq \varphi \leq 360$, $0\leq$ Ha≤ 50, $10^{-7}\leq$ Da$\leq 10^{-2}$, $10^2\leq$ Ra$\leq 10^6$
Reddy et al. [124]	FDM	Square enclosure	2D, steady, MHD, MWCNT-H_2O nanofluid, laminar, incompressible	$0.01\leq$ Rd, $\chi \leq 0.1$, $10^3\leq$ Ra$\leq 10^4$, $5.2\leq$ Pr≤ 8.2, $0.1\leq$ M≤ 0.7
Shah et al. [125]	NN, ML, LBM	Square enclosure with multiple fins	2D, MHD, NC, steady, Al_2O_3-H_2O nanofluid	$0\leq \varphi \leq 90$, $10^2\leq$ Ra$\leq 10^6$, $0\leq \chi \leq 0.04$

(*continued on next page*)

Table 2 (*continued*)

References	Tools	Domain	Flow details	Constants
Akhter et al. [126]	FEM, SIMPLER	Square porous enclosure with obstacle	2D, MHD, NC, Cu-Al_2O_3-H_2O hybrid nanofluid, steady	$0\leq$ Ha$\leq$ 100,$10^4\leq$ Ra$\leq$ 10^7, $0\leq \chi \leq$ 0.05,$10^{-5}\leq$ Da$\leq$ 10^{-2}
Bilal et al. [127]	FEM	Inclined square enclosure	2D, MHD, Cu-H_2O nanofluid, natural convection, unsteady	$0\leq$ Ha$\leq$ 100, $0\leq \varphi \leq 90$, $10^3\leq$ Ra$\leq$ 10^6, $0\leq \chi \leq 0.8$
Kumar et al. [128]	FEM	Porous square enclosure	2D, MHD, FC, laminar, incompressible, steady	$10\leq$ Ra$\leq$ 500,0.5$\leq$ Le$\leq$ 10, 0.1$\leq$ Sr$\leq$ 1, $0\leq$ Ge$\leq$ 10, $0\leq$ Du$\leq$ 1

Egen. The study revealed that increasing the heat transfer rate and aspect ratio resulted in a magnification of Egen. Furthermore, increasing Ha led to a 35% reduction in Egen. The maximum Egen occurred when the inclination was 0^o, and an increase in nanoparticles led to an increase in Egen.

Selimefendigil and Öztop [116] studied the impact of two crossed elliptic geometries within a square enclosure of varying inclinations. They discovered that an increase in Ha led to a reduction in total Egen. The angle of 135^o had the least effect on Egen in the enclosure. Additionally, Egen increased when the vertical elliptical radius was greater than the horizontal elliptical radius. The presence of nanoparticles had a minor impact on Egen, and there was hardly any difference in the effect between pure water and nanofluid. Seyyedi et al. [117] examined MHD natural convection occurring within an inclined square enclosure. It is found that, for each Ha, the maximum Egen was associated with the inclination angle, and that Egen decreased as Ha increased. Additionally, increasing the Ra value resulted in greater Egen as a result of the magnetic field's influence. Tayebi and Chamkha [118] examined Egen within a square enclosure. Their findings indicated that an increase in buoyancy forces led to an increase in both heat transfer Egen and total Egen. However, an increase in Ha caused a reduction in heat transfer and Egen. Additionally, an increase in the amount of hybrid nanoparticles had a negligible effect on total Egen. Khetib et al. [119] investigated Egen within an inclined square enclosure. They attached two hot fins to the right wall, which were positioned at different inclination angles: straight, angular, and curved. Their findings revealed that the curved fins generated the highest amount of entropy compared to the other two types of fins, while the straight fins had the lowest Egen values. Moreover, increasing the angle of the fins (in the case of angular fins) led to an increase in Egen, and Egen increased further as the curvature of the fins (in the case of curved fins) increased. Reddy and Sreedevi [120] studied the Egen phenomenon in a square enclosure. They observed that an increase in the magnetic field resulted in a reduction of Egen. Conversely, an increase in Rd led to an increase in the total Egen.

Tian et al. [121] investigated Egen in a square enclosure. A square heater was situated at the enclosure's center. They found that Egen rises with Ra and that the lowest Egen occurs at a low magnetic field. Additionally, increasing the enclosure's inclination results in a decrease in Egen. Furthermore, a 21% increase in Egen occurs when the magnetic field is increased. Ahmed et al. [39] examined Egen in a square enclosure filled with a hybrid nanofluid. They observed that the total Egen was improved by Rd. Shah et al. [125] sought to examine the behavior of Al_2O_3-H_2O nanofluid within a square enclosure at varying inclinations. The right side of the enclosure was cool while the left side was hot, with two fins attached to the left boundary in straight and triangular shapes. Their findings revealed that the inclusion of radiation led to a decrease in Egen by 4.2% and 2.6% for rectangular and triangular fins, respectively. Additionally, the rectangular fin demonstrated the highest Egen across various inclination angles of the enclosure. An increase in χ by 4% resulted in a 5.4% increase in Egen for both fins. Akhter et al. [126] used numerical analysis to examine Egen inside a square enclosure. It is seen that an increase in Ra, Da, and χ led to an increase in Egen, while Ha led to a decrease in Egen. Furthermore, they found that at low Ra, Egen due to heat transfer was dominant, while at high Ra, fluid friction Egen was higher. Bilal et al. [127] investigated Egen within a square. The top wall of the enclosure was hot, while the other walls were cold. Their findings revealed that magnetic Egen was zero when Ha was zero but increased for Ha values less than 40 and decreased for Ha values greater than 40. Kumar et al. [128] studied the phenomenon of Egen within a square enclosure. The findings revealed that the Egen was predominantly concentrated in the regions adjacent to the vertical wall, specifically at the top right and bottom left corners. Interestingly, as the viscous dissipation increased, Egen was found to amplify. The study also observed that an elevated buoyancy ratio resulted in augmented upthrust forces, subsequently leading to increased Egen. Furthermore, as the ratio of thermal diffusivity to molecular diffusivity increased, the overall entropy within the system decreased.

Table 3 presents a collection of diverse research investigations concentrating on mixed convection within a square enclosure. Here are brief summaries of selected articles included in the table:

Selimefendigil and Oztop [131] carried out a study on Egen in a square enclosure that included inlet and outlet ports, with each port being 0.25 of the length of the wall. A cold flow was introduced into the enclosure from the inlet port with a uniform velocity, while all boundaries were considered to be hot. The findings revealed that total Egen increased for Ha between 0 and 50 but decreased beyond this range. They also noted that there was only a slight change in Egen with variations in the angle of the magnetic field. Alsabery et al. [132] studied

Table 3
Research work on mixed convection in a square enclosure

References	Tools	Domain	Flow details	Constants
Alsabery et al. [129]	FEM, ALE	Square enclosure with FSI & cylinder	2D, unsteady, MC, laminar, Newtonian, incompressible	$10^4\leq$ Ra$\leq$ 10^7, $-1\leq \omega \leq$ 1, Pr = 4.623, $10^{12}\leq$ E$\leq$ 10^{15}
Selimefendigil and Oztop [131]	FEM	Vented square enclosure	2D, steady, MHD, MC, CuO-H_2O nanofluid, Newtonian, incompressible	$100\leq$ Re$\leq$ 500, $0\leq$ Ha$\leq$ 50, $0\leq \chi \leq$ 0.04, Pr = 6.9, Ra=10^5, φ=45
Alsabery et al. [132]	FEM	Square enclosure with cylinder	2D, steady, MC, laminar, two-phase, Newtonian, Al_2O_3-H_2O nanofluid	$10^4\leq$ Ra$\leq$ 10^7, $0\leq \omega \leq$ 600, $0\leq \chi \leq$ 0.04, Pr = 4.623, Le = 3.5×10^5, Sc = 3.55×10^4
Hamzah et al. [57]	FVM, SIMPLE	Vented square enclosure with multiple cylinders	2D, steady, MC, Newtonian, incompressible	$0\leq \omega \leq 15$, $100\leq$ Re$\leq$ 500, $10^3\leq$ Gr$\leq$ 10^6
Kashyap et al. [133]	MRT-LBM	Lid-driven square enclosure with block	2D, steady, laminar, Newtonian, incompressible, NC & MC	$10^4\leq$ Gr$\leq$ 10^6, Pr = 0.025, 5.83, 151, 0.01$\leq$ Ri$\leq$ 100
Çiçek and Baytaş [134]	FVM, SIMPLE	Vented square enclosure	2D, laminar, MC, SiO_2-H_2O nanofluid, Newtonian, incompressible, unsteady	0.1$\leq$ Ri$\leq$ 20, $50\leq$ Re$\leq$ 500, Pr = 0.71, 0.01$\leq$ dp (μ)$\leq$ 5

Egen in a square enclosure. They discovered that Egen increased with the rotational speed of the cylinder for all Ra values, with the highest value observed at Ra=10^7. However, the increase in Egen was minimal for low and medium Ra values. Additionally, a significant increase in global Egen occurred after Ra>10^5, while the change was negligible before Ra < 10^5. Hamzah et al. [57] used numerical simulation to investigate the thermal and hydraulic behavior, as well as Egen, resulting from the rotation of two reversely rotating cylinders around a heated cylinder inside a square enclosure. Their findings indicated that the average Egen increased with Gr for all rotational speeds of the cylinders. Additionally, the local Egen reached its highest value when the rotating cylinders were positioned before the heated cylinder. Kashyap et al. [133] studied Egen within a square enclosure containing fluids with different Pr. They placed a square hot block at the enclosure's center and treated the left boundary as insulated while considering the other three boundaries as cold. The study revealed that for the prescribed Gr, the increase in Pr augmented Egen due to viscous effects was more significant in natural convection than mixed convection. Çiçek and Baytaş [134] investigated the elimination of solid particles ranging from 5 μm to 0.01 μm, as well as Egen within a vented square enclosure under mixed convection. The enclosure featured an inlet port on the bottom left boundary for incoming fluid at a temperature of 273K and an exit port at the top of the right boundary. The findings indicated that the lowest Egen was observed at Ri = 5 for a given Re = 50. Additionally, an increase in Re led to greater local and overall Egen in the presence of solid particles, with larger particle diameters resulting in even higher Egen.

Table 4 showcases a compilation of various research studies that examine the flow of non-Newtonian fluids within a square enclosure. Below are concise summaries of the selected articles featured in the table:

In a study by Kefayati and Tang [137], a square enclosure containing two inner cold circular objects was examined for Egen. It is found that an increase in Ra resulted in higher Egen due to fluid friction, and an increase in buoyancy ratio led to enhanced Egen. Additionally, an increase in Ha led to a higher total Egen. In a separate study by Kefayati and Tang [138], Egen within a square enclosure containing an inner cold cylinder at varying positions was investigated. Results indicated that an increase in Ra led to higher Egen due to friction, while an increase in buoyancy ratio enhanced Egen due to heat transfer. An increase in Le resulted in higher mass transfer and Egen but decreased Egen due to fluid friction and heat transfer. The study also found that the minimum Egen occurred when the cold cylinder was close to the bottom wall, while the highest total Egen occurred when the cylinder was at the center of the enclosure and had a larger size. Vahabzadeh Bozorg and Siavashi [139] conducted a study on Egen inside a square enclosure. Two cylinders were placed in the middle of the enclosure, with one at a hot temperature of 315K and the other at a cold temperature of 305K. Four different rotation cases were considered: both cylinders rotating anticlockwise, both rotating clockwise, cold rotating anticlockwise and hot rotating clockwise, and cold rotating clockwise and hot rotating anticlockwise. The study found that thermal irreversibility was the primary cause of Egen. The maximum Egen rates were caused by shear-thinning nanofluids, and their values were higher for Ri equal to 0.01 or 100. Iftikhar et al. [140] investigated Egen in a square enclosure. They found that the lowest Egen occurred when the bi-viscosity parameter was β = 0.002. They also observed that an increase in Ha resulted in a higher level of Egen due to flow friction. In addition, the maximum and minimum Egen occurred when Ri was equal to 1 and 10^3, respectively.

Table 5 presents a collection of diverse research investigations focusing on square cavities with one wavy side wall. Here are brief summaries of the selected articles included in the table:

Parveen and Mahapatra [9] conducted a study on Egen in a square enclosure with a wavy top wall. It is seen that the overall Egen increased as Ra increased but decreased with an increase in Ha, buoyancy ratio, and undulation number. Egen in a wavy-walled inclined square

Table 4
Research work on square enclosure with non-Newtonian fluid

References	Tools	Domain	Flow details	Constants
Kefayati [66]	FD-LBM	Square enclosure	2D, laminar, NC, steady, non-Newtonian, incompressible	$10^4 \leq$ Ra$\leq 10^5$, $0.6 \leq$ n≤ 1.4, $2.5 \leq$ Le≤ 5, $0 \leq$ Sr, Du≤ 1, $-1 \leq$ N≤ 1, Pr = 5
Kefayati [67]	FD-LBM	Square enclosure	2D, unsteady, Cu-H_2O nanofluid, NC, non-Newtonian	$10^4 \leq$ Ra$\leq 10^5$, $0.6 \leq$ n≤ 1, $0 \leq$ Ha≤ 90, $0 \leq \chi \leq 0.06$
Kefayati [68]	FD-LBM	Square enclosure	2D, laminar, NC, unsteady, non-Newtonian, incompressible, MHD	$10^4 \leq$ Ra$\leq 10^5$, $0.6 \leq$ n≤ 1, $0 \leq$ Ha≤ 90, $0 \leq \chi \leq 0.06$
Kefayati [62]	FD-LBM	Porous square enclosure	2D, laminar, NC, Cu-H_2O nanofluid, unsteady, non-Newtonian	$10^4 \leq$ Ra$\leq 10^5$, $10^{-3} \leq$ Da$\leq 10^{-1}$, $0.6 \leq$ n≤ 1, $0 \leq \chi \leq 0.04$
Selimefendigil and Öztop [135]	FEM	Square enclosure with cylinder	2D, unsteady, MHD MC, non-Newtonian	$0.01 \leq$ Ri≤ 100, $0 \leq$ Ha≤ 50, $-50 \leq \omega \leq 50$, $0 \leq \varphi \leq 90$, $0.6 \leq$ n≤ 1.4
Kefayati [63]	FD-LBM	Porous square enclosure	2D, unsteady, NC, laminar, non-Newtonian, incompressible	$10^4 \leq$ Ra$\leq 10^5$, $10^{-4} \leq$ Da$\leq 10^{-2}$, $0.1 \leq$ Pr≤ 10, $0.1 \leq$ N≤ 4, $0.4 \leq$ n≤ 1, $1 \leq$ Le≤ 10, $0.1 \leq$ Nt≤ 1, $0.1 \leq$ Nb≤ 5, Pr = 0.1
Kefayati and Tang [65]	FD-LBM	Square enclosure	2D, MHD, NC, unsteady, non-Newtonian, laminar, incompressible	$10^4 \leq$ Ra$\leq 10^5$, $0 \leq$ Ha≤ 30, $0.1 \leq$ N≤ 4, $0.4 \leq$ n≤ 1, $1 \leq$ Le≤ 10, $0.1 \leq$ Nt≤ 1, $0.1 \leq$ Nb≤ 5, Pr = 1
Wang et al. [136]	LRBF	Square enclosure with cylinder	2D, MHD, MC, unsteady, non-Newtonian	Pr = 0.71, $1 \leq$ Re≤ 50, $0.1 \leq$ Ri≤ 20
Kefayati and Tang [137]	LBM	Square enclosure with multiple cylinders	2D, MHD, NC, Carreau fluid, non-Newtonian, incompressible, laminar, unsteady	$10^4 \leq$ Ra$\leq 10^5$, $-1 \leq$ N≤ 1, $0 \leq$ Ha≤ 90, $0.2 \leq$ n≤ 1.8
Kefayati and Tang [138]	FD-LBM	Square enclosure with cylinder	2D, laminar, unsteady, FC, Carreau fluid, non-Newtonian, incompressible	$10^4 \leq$ Ra$\leq 10^5$, $1 \leq$ Ca≤ 20, $2.5 \leq$ Le≤ 10, $0 \leq$ Du, Sr≤ 5, $1 \leq$ Ec≤ 10, $-1 \leq$ N≤ 1, $0.2 \leq$ n≤ 1.8
Vahabzadeh Bozorg and Siavashi [139]	FVM, SIMPLE, QUICK	Square enclosure with cylinders	2D, steady, MC, Cu-H_2O nanofluid, Two-phase mixture, laminar, non-Newtonian, incompressible	$0.01 \leq$ Ri≤ 100, $10^4 \leq$ Ra$\leq 10^6$, $0 \leq \chi \leq 0.04$, $0.5 \leq$ n≤ 1.5
Iftikhar et al. [140]	FEM	Square enclosure	2D, steady, MHD MC, non-	Pr = 6.2, 10, $0.1 \leq$ Ri$\leq$

(continued on next page)

Table 4 (*continued*)

References	Tools	Domain	Flow details	Constants
			Newtonian, laminar, bi-viscosity fluid	10^3, 0≤ Ha≤ 10^2, Gr=10^5, 10≤ Re≤ 60

enclosure and exposed to a uniform magnetic field was investigated by Shahriari et al. [75]. The study concluded that as Ha decreased and Ra increased, there was an increase in Egen. Additionally, in the presence of a magnetic field at Ra=10^5, the increase in χ resulted in more Egen. Alsabery et al. [144] investigated Egen in a square enclosure, divided into three parts. The first part was located at the top, while the second part consisted of a porous medium. The third part was the bottom wall, which had a wavy surface and was kept at a high temperature, while the vertical walls were cold and the top wall was adiabatic. They observed a significant decrease in Egen at a porosity level of 0.2. Furthermore, as Da increased from 10^{-3} to 10^{-2}, Egen increased by an order of magnitude, and the presence of nanoparticles in the system resulted in a reduction in total Egen. Geridonmez and Oztop [145] studied the behavior of Egen within a square enclosure that had a wavy wall. It is seen that increasing Ha from 10 to 100 resulted in a 71.58% reduction in total Egen. Additionally, an increase in the ratio of solid thermal conductivity to fluid conductivity led to an increase in Egen. The total Egen was found to increase as the angle of the magnetic field increased from 0^o to 45^o, but then decreased for angles between 45^o and 90^o.

Table 6 displays a compilation of various research studies that investigate cavities with wavy side walls. Below are concise summaries of the selected articles featured in the table:

Alsabery et al. [40] conducted a study on hydraulic and thermal behavior as well as Egen inside a square enclosure. Two fins, each with a length of 0.25 of the enclosure's side length, were attached to the top wall. They concluded that an increase in Ra and heater height led to an enhancement in global Egen, but this effect decreased as χ decreased. Alsabery et al. [42] examined the impact of mixed convection on Egen in a wavy square enclosure. The enclosure features a cold left wall and a partially heated center on the right wall, as well as a conductive rotating cylinder at the center. The study findings indicate that when Ra is low, the rotational direction of the cylinder does not affect Egen, which is solely driven by heat transfer. In cases where conduction dominates, Egen near the wavy walls is caused by heat transfer, whereas in cases where fluid friction prevails, entropy is generated due to fluid friction. Chattopadhyay et al. [148] studied Egen inside a double lid-driven wavy square enclosure. They found that Egen decreased linearly with increasing Ri and that the highest total Egen occurred when the walls were moving in the opposite directions. Afsana et al. [149] investigated Egen inside a square, wavy enclosure. According to their investigation, they discovered that as the value of χ increased, the effect of fluid friction and heat transfer on Egen decreased in the absence of a magnetic field. Additionally, an increase in the power-law index resulted in a 54% reduction in total Egen with the magnetic field and an 80% reduction without the magnetic field. Boulahia [49] examined the behavior of Egen in a square enclosure. The enclosure had corrugated and thermally insulated upper and lower bottom surfaces, while the vertical walls were cold, and a hot square object was located at the center of the enclosure. The study found that increasing χ and decreasing Ha improved Egen due to heat transfer. Meanwhile, Egen due to fluid friction decreased with χ and Ha but increased with the number of undulations. Abderrahmane et al. [150] investigated Egen in a square enclosure with wavy vertical walls. It is found that Ha, degree of undulation, power-law index, and maximum and minimum values of the rotational angle of the elliptical cylinder all contributed to an increase in Egen.

Table 7 presents a variety of research studies focusing on cavities with a Z-shaped configuration. The following are brief summaries of the selected articles included in the table:

Hussain et al. [151] studied the double diffusive behavior of a MHD laminar flow and Egen in a Z-staggered enclosure. It is found that as Le increased from 0.1 to 10, Egen decreased, and also Egen decreased with an increase in Ha. Rasool et al. [152] investigated Egen within a Cleveland Z-staggered enclosure under the influence of a magnetic field. Their findings revealed that as Re increased, Be decreased, indicating a rise in Egen due to friction.

Table 8 showcases a compilation of diverse research investigations centered around cavities with a triangular configuration. Some of the selected articles are described below:

Liu et al. [159] investigated Egen in an inclined enclosure, which was divided into two triangular cavities. The study found that increasing Ra from 10^3 to 10^5 resulted in a 13% increase in Egen. Furthermore, when Ha was changed from 0 to 40, there was an 8% reduction in Egen. Increasing the inclination angle resulted in a greater reduction in Egen. Selimefendigil et al. [160] studied the impact of nanofluid on Egen in a triangular enclosure. They placed a rotating cylinder in the enclosure's center and had a flexible inclined cold wall, a partially heated left wall, and an insulated base wall. Their findings indicated that the total Egen rose as the elastic modulus, rotational speed, and χ increased. Afrand et al. [161] examined Egen in an inclined triangular enclosure. Their findings revealed that the total Egen increased by 2.32% as Ra increased. Additionally, the increase in Egen decreased with an increase in the enclosure angle, with the highest value observed at an angle of 60^o. Li et al. [162] conducted research on Egen within a slanted triangular container. In case (a), the top wall, which formed the hypotenuse, was chilly, while the left wall was partially heated. In case (b), the right wall was partially heated, while the left wall remained insulated. Their findings indicated that as Ra increased, thermal Egen increased by 80% in case (a) and 88% in case (b) for the Newtonian fluid, while for the non-Newtonian fluid, the increase was 210% in case (a) and 175% in case (b).

Table 5
Research work on Square enclosure with one wavy side

References	Tools	Domain	Flow details	Constants
Shirvan et al. [141]	FVM, SIMPLE, RSM	Wavy square enclosure	2D, steady, NC, Cu-H_2O nanofluid, Newtonian, laminar, incompressible	10^3≤ Ra≤ 10^5, 0≤ χ ≤ 4%
Chamkha and Selimefendigil [142]	FEM	Porous square enclosure with triangular wavy side	2D, steady, MHD, FC, Cu-H_2O nanofluid	10^4≤ Gr≤ 10^6, 0≤ Ha≤ 50, 10^{-4}≤ Da≤ 10^{-1}, 0≤ χ ≤ 5%
Pal et al. [143]	FVM, SIMPLE, QUICK	Lid-driven square enclosure with wavy wall	2D, unsteady, MC, Cu-H_2O nanofluid, Newtonian, incompressible	0≤ Ri≤ 5, 10^3≤ Gr≤ 5×10^4, 0≤ χ ≤ 9%, 100≤ Re≤ 500
Parveen and Mahapatra [9]	FDM, Bi-CGStab, TDMA	Wavy square enclosure	2D, MHD, NC, steady, Al_2O_3-H_2O nanofluid, laminar, incompressible	10^3≤ Ra≤ 10^5, 0≤ Ha≤ 60, 0≤ χ ≤ 0.2, Pr = 6.2, Le = 2, -2≤ N≤ 2
Shahriari et al. [75]	LBM	Inclined wavy square enclosure	2D, MHD, CuO-H_2O nanofluid, NC	Pr = 6.2, 10^3≤ Ra≤ 10^5, 0≤ χ ≤ 0.04, 0≤ Ha≤ 90, 0≤ φ ≤ 60
Alsabery et al. [144]	FEM	Wavy square enclosure with partially porous	2D, laminar, steady, incompressible, NC, Al_2O_3-H_2O nanofluid, Newtonian	0≤ χ ≤ 0.04, 10^{-6}≤ Da≤ 10^{-2}, Ra = 10^6, Pr = 4.623, A = 1.0
Geridonmez and Oztop [145]	RBF-FDM	Square enclosure with wavy conducting solid block	2D, MHD, steady, FC, TiO_2-Cu-H_2O hybrid nanofluid, laminar, Newtonian, incompressible	Pr = 6.2, 10≤ Ha≤ 100, 10^3≤ Ra≤ 10^5, 0.01≤ A≤ 0.1, 0≤ φ ≤ 90, 0≤ χ ≤ 2%, 1≤ K_T≤ 10

Table 6
Research work on wavy sides enclosure

References	Tools	Domain	Flow details	Constants
Hussain [58]	CVM	Sinusoidal porous enclosure	2D, MHD, NC, laminar, incompressible, steady	Pr = 0.024, 0≤ φ ≤ 90, 10^3≤ Ra≤ 10^6, 0≤ Ha≤ 100, 10^{-6}≤ Da≤ 10^{-2}, 1≤ Le≤ 10, 0≤ N≤ 10
Alsabery et al. [146]	FEM	Wavy porous enclosure with cylinder	2D, steady	10^5≤ Ra≤ 10^6, -1000≤ ω ≤ 1000, 10^{-6}≤ Da≤ 10^{-2}
Alsabery et al. [41]	FEM	Wavy enclosure with cylinder	2D, laminar, MC, steady, Al_2O_3-H_2O nanofluid, Newtonian	10^3≤ Ra≤ 10^6, 0≤ χ ≤ 0.04, 0≤ ω ≤ 750
Cho [147]	FVM, SIMPLE, TDMA	Lid-driven wavy enclosure	2D,steady, MC, Cu-H_2O nanofluid, laminar, Newtonian, incompressible	10^{-2}≤ Ri≤ 10^2, 0≤ χ ≤ 0.04, Pr = 6.2, 1≤ Re≤ 200
Alsabery et al. [40]	FEM	Wavy enclosure with blocks	2D, NC, laminar, Cu-H_2O, Al_2O_3-H_2O nanofluids, steady, Cu-Al_2O_3-H_2O hybrid nanofluid, Newtonian	10^3≤ Ra≤ 10^6, 0≤ χ ≤ 0.04, Pr = 4.623
Alsabery et al. [42]	FEM	Wavy enclosure with cylinder	2D, laminar, MC, steady, Newtonian	10^3≤ Ra≤ 10^5, 0≤ χ ≤ 0.04, -1000≤ ω ≤ 1000, Pr = 4.623
Chattopadhyay et al. [148]	FDM, hybrid BiCGStab	Double lid-driven wavy enclosure	2D, steady, laminar, MC, incompressible	0.01≤ Ri≤ 100, Gr=10^4, 0≤ φ ≤ 90, Pr = 0.71
Afsana et al. [149]	FVM, CDS, SIMPLER, Bi-CGSTAB	Rectangular wavy enclosure	2D, MHD, NC, Fe_3O_4-H_2O nanofluid, non-Newtonian	10^3≤ Ra≤ 10^5, 0≤ Ha≤ 20, 0.6≤ n≤ 1.4, 0≤ χ ≤ 0.01, Pr = 6.8377
Boulahia [49]	FVM, SIMPLE, TDMA	Wavy enclosure with hot object	2D, unsteady, MHD, free convection, Cu-H_2O nanofluid, Newtonian	10^3≤ Ra≤ 10^6, 0≤ Ha≤ 45, 0≤ χ ≤ 0.05
Abderrahmane et al. [150]	FEM	Wavy porous enclosure with elliptical obstacle	2D, non-Newtonian, FC, steady, MHD, Al_2O_3-CMC nanofluid, laminar, incompressible	0.8≤ n≤ 1.4, 10^3≤ Ra≤ 10^6, 10^{-5}≤ Da≤ 10^{-2}, 0≤ Ha≤ 100, 0≤ φ ≤ 90

Table 7
Research work on Z-shaped enclosure

References	Tools	Domain	Flow details	Constants
Hussain et al. [151]	FEM	Z-staggered enclosure	2D, MHD, NC Casson fluid, steady, laminar, incompressible	10^4≤ Ra≤ 10^7, 0≤ φ ≤ 90, 0.1≤ Le≤ 10, Pr=6.8, Ha = 25
Rasool et al. [152]	FEM	Z-staggered enclosure	2D, MWCNT-H_2O nanofluid, laminar, steady, incompressible	0≤ Ha≤ 30, 10^{-5}≤ Da≤ 10^{-2}, 1≤ Re≤ 1000

Table 8
Research work on triangular enclosure

References	Tools	Domain	Flow details	Constants
Bhardwaj et al. [45]	FDM	Porous right-angled triangular enclosure	2D,unsteady, NC, laminar, incompressible	10^3≤ Ra≤ 10^6, 10^{-4}≤ Da≤ 10^{-2}
Rathnam et al. [153]	FEM	Porous triangular cavities	2D, steady, NC	Pr=0.015, 7.2, 10^{-5}≤ Da≤ 10^{-2}, Ra=10^6
Selimefendigil et al. [154]	FEM	Lid-driven triangular enclosure	2D, steady, MHD MC, CuO-H_2O nanofluid	0≤ Ri≤ 100, 0≤ Ha≤ 50, 0≤ φ ≤ 90, 0≤ χ ≤ 0.05
Bondareva et al. [155]	FDM	Open triangular enclosure	2D, steady, laminar, Newtonian, NC, Cu-H_2O nanofluid	10^4≤ Ra≤ 10^6, Pr = 7, 0≤ χ ≤ 0.05
Roy et al. [156]	FEM	Lid-driven triangular cavities	2D, steady, MC, laminar, Newtonian	10^3≤ Gr≤ 10^5, 1≤ Re≤ 100, Pr = 0.026, 7.2
Roy et al. [157]	FEM	Lid-driven porous triangular cavities	2D, steady, MC, laminar	Gr= 10^5, 10≤ Re≤ 100, Pr = 0.026, 7.2, 10^{-4}≤ Da≤ 10^{-2}
Chamkha et al. [158]	FEM	Lid-driven triangular enclosure	2D, MHD, MC, steady, Al_2O_3-H_2O nanofluid	0.01≤ Ri≤ 100,0≤ Ha≤ 40, Pr=6.9, 0≤ χ ≤ 0.03
Liu et al. [159]	FV-FEM	Triangular enclosures	2D, steady, MHD NC, Al_2O_3-H_2O nanofluid, laminar, Newtonian, incompressible	10^3≤ Ra≤ 10^5, 0≤ Ha≤ 40, 0≤ φ ≤ 90, 0≤ χ ≤ 0.06
Selimefendigil et al. [160]	FEM, ALE	Triangular enclosure with cylinder	2D, steady, MC, Newtonian, laminar	1≤ Ri≤ 100, 10^4≤ Ra≤ 10^6, -3000≤ ω ≤ 3000, 0≤ χ ≤ 0.05
Afrand et al. [161]	FDM, SIMPLE	Inclined triangular enclosure	2D, FC, MHD, Al_2O_3-H_2O nanofluid, laminar, steady, Newtonian, incompressible	10^3≤ Ra≤ 10^6, 0≤ Ha≤ 40, 0≤ φ ≤ 90, 0≤ Rd≤ 2, 0≤ χ ≤ 0.03
Li et al. [162]	FD-LBM	Inclined triangualr enclosure	2D, MHD, laminar, incompressible, non- Newtonian, steady	0.6≤ n≤ 1.4,10^3≤ Ra≤ 10^5, 0≤ Ha≤ 60, 0≤ φ ≤ 90

Table 9 displays a collection of research studies examining cavities with a trapezoidal shape. The following are brief summaries of the selected articles included in the table:

Mahapatra et al. [169] studied Egen within a trapezoidal enclosure. In case 1, the right boundary was linearly heated, while in case 2, it was kept cold. The study also explored different aspect ratios at angles of 45°, 60°, and 90°. They found that in case 1, the maximum values of Egen due to heat transfer and fluid friction decreased as Ha increased, assuming other parameters remained constant. Additionally, the highest value of Egen due to heat transfer occurred near the top of both side boundaries in case 1, while the maximum values were observed at the right bottom

Table 9
Research work on trapezoidal enclosure

References	Tools	Domain	Flow details	Constants
Ramakrishna et al. [72]	FEM	Porous trapezoidal enclosure	2D, steady, NC, Newtonian, laminar, incompressible	$10^{-5} \leq$ Da $\leq 10^{-3}$, $0.015 \leq$ Pr $\leq 10^{3}$, Ra$=10^{6}$, $0 \leq \varphi \leq 90$
Aghaei et al. [163]	FVM, SIMPLER	Trapezoidal enclosure	2D, steady, MHD, MC, Cu-H_2O nanofluid	$15 \leq \varphi \leq 60$, Gr$=10^{4}$, $30 \leq$ Re $\leq 10^{3}$, $25 \leq$ Ha ≤ 100, $0 \leq \chi \leq 0.04$
Selimefendigil et al. [164]	FEM	Trapezoidal cavities	2D, unsteady, NC, laminar, CuO-H_2O, Al_2O_3-H_2O nanofluids	$10^{3} \leq$ Ra $\leq 10^{6}$, $0 \leq$ Ha ≤ 50, $0 \leq \chi \leq 0.04$
Astanina et al. [165]	FDM	Trapezoidal porous enclosure	2D, MHD, NC, unsteady, Fe_3O_4-H_2O nanofluid	Pr=6.82, Ra$=10^{5}$, Da$=10^{-3}$, $0 \leq$ Ha ≤ 100, $0 \leq \varphi \leq 180$, $0 \leq \chi \leq 0.05$
Ishak et al. [60]	FEM	Lid-driven trapezoidal enclosure with cylinder	2D, steady, MC, Al_2O_3-H_2O nanofluid, incompressible	$0.01 \leq$ Ri ≤ 10, $5 \leq$ Re ≤ 500, $0 \leq \chi \leq 0.04$
Mebarek-Oudina et al. [166]	FEM	Trapezoidal enclosure with cylinder	2D, steady, laminar, Cu-Al_2O_3-H_2O hybrid nanofluid, Newtonian	$0 \leq$ Ha ≤ 100, $-4000 \leq \omega \leq 4000$, $0 \leq \varphi \leq 90$, $10^{3} \leq$ Ra $\leq 10^{5}$, $0 \leq \chi \leq 0.08$
Mondal and Mahapatra [167]	FDM, BiCGStab	Trapezoidal enclosure	2D, MHD, MC, steady, Al_2O_3-H_2O nanofluid, laminar	$0.5 \leq$ A ≤ 2, $0.01 \leq$ Ri ≤ 100, $10^{2} \leq$ Ra $\leq 10^{3}$, $45 \leq \varphi \leq 90$, $20 \leq$ Ha ≤ 40, $0 \leq \chi \leq 0.05$, $1 \leq$ Le ≤ 2
Mondal et al. [168]	FDM	Trapezoidal enclosure	2D, steady, MHD, MC, laminar, Al_2O_3-H_2O nanofluid	$0.2 \leq$ A ≤ 0.4, Pr=6.2, Re=100, $20 \leq$ Ha ≤ 60, $0 \leq \chi \leq 0.1$
Mahapatra et al. [169]	FDM, BiCGStab	Trapezoidal enclosure	2D, steady, MHD, NC, laminar, incompressible	$0.5 \leq$ A ≤ 1.5, Pr $=$ 0.015, 0.7, $10^{3} \leq$ Ra $\leq 10^{5}$, $20 \leq$ Ha ≤ 40, $45 \leq \varphi \leq 90$
Shuvo et al. [170]	FEM	Lid-driven trapezoidal enclosure	2D, steady, MC, laminar, incompressible, Al_2O_3-H_2O nanofluid	$0 \leq \varphi \leq 45$, $0 \leq$ Re $\leq 10^{3}$, $10^{-2} \leq$ Gr $\leq 10^{6}$, $0.1 \leq$ Ri ≤ 10, $0 \leq \chi \leq 0.01$
Zidan et al. [171]	FEM	Porous trapezoidal enclosure with baffles	2D, MHD, NC, Al_2O_3-H_2O nanofluid	$10^{4} \leq$ Ra $\leq 10^{6}$, $0 \leq$ Ha ≤ 40, $10^{-3} \leq$ Da $\leq 10^{-1}$, $0 \leq \chi \leq 0.02$
Aljaloud et al. [172]	LBM	Trapezoidal enclosure with obstacle	2D, MHD, MC, steady, Ag-MgO-H_2O hybrid nanofluid, laminar	$0 \leq$ Ha ≤ 60, $0.25 \leq$ Ri ≤ 4, $-5 \leq$ Q ≤ 5, $0 \leq \chi \leq 0.04$

corners. Shuvo et al. [170] studied Egen within two tilted isosceles trapezoidal cavities with lid-driven motion. The angle of inclination for the hot bottom boundary was set at 0°, 30°, and 45°. They observed that both cases exhibited similar behavior in terms of Egen, where the contribution from heat transfer was more dominant than that from fluid friction. Zidan et al. [171] employed numerical simulation to investigate the entropy convection occurring within a trapezoidal-shaped enclosure. The enclosure was subjected to cold top and bottom walls and adiabatic side walls. Additionally, three hot baffles of varying sizes were affixed at the middle positions of both side walls. The top baffle was the largest, with the size gradually decreasing to the third baffle. Three different scenarios were analyzed: case A, where all baffles were present; case B, where the top baffles were removed; and case C, where the middle baffles were removed. The research findings revealed that the total Egen increased with higher Da and decreased with Ha. However, for higher Ra values, the situation was reversed in case A. Aljaloud [172] conducted a study that focused on examining MHD mixed convection and Egen within a trapezoidal enclosure. To investigate the impact of temperature variation, a rectangular object with an aspect ratio of 0.25 was introduced into the enclosure. The findings of the study indicated that a decrease in Ri resulted in an increase in Egen. Specifically, a reduction of 14% in Egen was observed when the rectangular block's temperature transitioned from hot to cold.

Table 10 presents a compilation of research studies investigating square cavities with one or more moving walls. Some of the selected articles are described below:

Taghizadeh and Asaditaheri [78] delved into the exploration of mixed convection and Egen within an inclined square enclosure. A porous circular object with a diameter of 0.2 times the length of the wall was present, with a porosity of 0.8. The findings revealed several noteworthy observations. Firstly, for low Ri (Ri $=$ 0.01), the primary contributor to the total Egen was fluid friction induced by the movement of the top wall. In the case of MC with Ri $=$ 1, heat transfer emerged as the main source of Egen. Furthermore, the study demonstrated that reducing the permeability of the porous cylinder resulted in enhanced Egen for Ri $=$ 0.01, whereas the angle of enclosure inclination had no effect. However, for Ri $=$ 5 and 10, the angle of enclosure inclination exhibited a considerable impact on Egen compared to the effect of Da. Additionally, both the angle of inclination and permeability were found to have a significant influence on Egen for Ri $=$ 0.01. Barnoon et al. [179] studied the effect of Egen in an inclined square enclosure. Inside the enclosure, two cylinders with identical radii were placed equidistant from the walls. One of the cylinders rotated at a constant speed towards the right, while the other walls remained stationary. They observed that an increase in Ha led to a decrease in Egen at a specific Ri. Furthermore, when Ha was held constant, a decrease in Ri resulted in a reduction in Egen. It was also noted that the contribution of viscous Egen increased with higher Ri compared to that of heat transfer. Kashyap and Dass [180] examined Egen inside a square enclosure under different boundary conditions. Three cases were investigated, each involving specific movements and heating/cooling arrangements of the boundaries. The findings revealed that heat transfer played a significant role in Egen. Additionally, in Case 1, the left boundary was heated and moved upward, while the right boundary was cooled and moved downward. The remaining boundaries were stationary and insulated. Case 1 resulted in the highest Egen, and increasing χ led to an increase in Egen. Alshare et al. [181] examined the phenomenon of Egen in a square lid-driven enclosure. The findings of their research indicated that as Ri increased, the total Egen also increased. Interestingly, the highest Egen was observed within the range of Ri $=$ 50 to 100. At higher Ri values, the dominant contributor to Egen was friction. Additionally, an increase in Ha led to an augmentation of Egen due to the magnetic field, but a reduction in Egen was caused by heat transfer.

Table 11 showcases various research studies focusing on rectangular cavities. Some of the selected articles are described below:

El-Maghlany and Minea [184] examined the Egen of various ionic

Table 10
Research work on lid-driven square enclosure

References	Tools	Domain	Flow details	Constants
Roy et al. [173]	FEM	Lid-driven square enclosure	2D, steady, MC, laminar, incompressible	Pr = 0.026, 7.2, 10≤ Re≤ 100, 10^3≤ Gr≤ 10^5
Roy et al. [174]	FEM	Lid-driven porous square enclosure	2D, steady, MC, laminar	10^{-5}≤ Da≤ 10^{-2}, 10^3≤ Gr≤ 10^5, Pr = 0.026, 7.2, 10≤ Re≤ 100
Roy et al. [175]	FEM	Lid-driven square enclosure	2D, steady, MC, laminar, incompressible	10^3≤ Gr≤ 10^5, Pr = 0.015, 7.2, 10≤ Re≤ 100
Bouabda et al. [176]	CV-FEM	Lid-driven porous square enclosure	2D, unsteady, MHD, MC, Newtonian, incompressible	10^{-3}≤ Da≤ 1, 0≤ Ha≤ 100, Pr = 7.0, 10^4≤ Ra≤ 10^5, 10≤ Re≤ 50, 0.25≤ Fc≤ 0.87
Hussain et al. [26]	FEM	Double lid-driven enclosure	2D, unsteady, MHD, MC, Al_2O_3-H_2O nanofluid	1≤ Re≤ 100, 1≤ Ri≤ 50, 1≤ Ha≤ 100, 0≤ χ ≤ 0.2, 0≤ φ ≤ 90, Pr = 6.2
Roy et al. [177]	FEM	Lid-driven porous square enclosure	2D, steady, MC, laminar, incompressible	Gr = 10^5, Pr = 0.015, 7.2, 10≤ Re≤ 100, 10^{-4}≤ Da≤ 10^{-2}
Gibanov et al. [103]	FDM	Lid-driven square enclosure	2D, unsteady, MC, laminar, Al_2O_3-H_2O nanofluid	0.01≤ Ri≤ 10, 0≤ χ ≤ 0.05, 1.0≤ K_T≤ 20.0, dp = 47 nm
Hussain et al. [178]	FEM	Lid-driven porous square enclosure	2D, Newtonian, steady, Al_2O_3-H_2O nanofluid, MC, incompressible	10^{-5}≤ Da≤ 10^{-2}, 0.01≤ Ri≤ 5, 0.1≤ Le≤ 7, 0≤ χ ≤ 4%, 0≤ Kr≤ 4%, -0.4≤ q≤ 0.4, -2≤ Br≤ 2
Taghizadeha and Asaditaheri [78]	FVM, SIMPLE	Lid-driven square enclosure with porous cylinder	2D, laminar, MC, steady	0.01≤ Ri≤ 10, 10^{-5}≤ Da≤ 10^{-2}, 0≤ φ ≤ 90, Re = 100, Pr = 0.7
Barnoon et al. [179]	FVM, SIMPLE	Lid-driven square enclosure with rotating cylinders	2D, steady, MHD, MC, laminar, two phase, Newtonian, Al_2O_3-H_2O nanofluid	1≤ Ri≤ 100, 0≤ Ha≤ 30, 0≤ φ ≤ 90, -3≤ ω ≤ -1, 1≤ χ ≤ 3%, dp=30 nm
Kashyap and Dass [180]	LBM	Double lid-driven square enclosure	2D, two phase, MC, Cu-Al_2O_3-H_2O hybrid nanofluid	0≤ χ ≤ 3%, 0.1≤ Ri≤ 10, Gr = 10^4, Pr = 6.2
Alshare et al. [181]	FEM	Lid-driven square enclosure with elliptical cylinder	2D, steady, MHD MC, Al_2O_3-H_2O nanofluid	0≤ φ ≤ 90, 1≤ Ri≤ 100, 0≤ χ ≤ 8%

liquids within a rectangular enclosure. The outcomes of their research revealed that the inclusion of nanoparticles led to an increase in Egen. Hu and Mei [185] studied the influence of Sr and Du effects on thermosolutal behavior and Egen within an inclined rectangular enclosure. They observed that the buoyancy ratio and Da played a significant role in enhancing Egen, resulting from heat transfer, fluid friction, and moisture-based heat transfer. Specifically, raising the buoyancy ratio and Da increased Egen by 90%. Furthermore, when the wall thickness increased, all forms of Egen decreased by 30%. Regarding the horizontal position of the enclosure, Egen approached a minimum and maintained a constant value. Additionally, variations in Sr from 0 to 1.5 led to a 22% increase in Egen due to heat transfer and a 110% increase in Egen due to fluid friction. On the other hand, an increase in Du from 0 to 1.5 resulted in a 50% decrease in Egen due to heat transfer and a 7% decrease in Egen due to moisture transfer. Finally, the total Egen experienced a 16% increase due to the Sr effect and a 40% increase due to the Du effect. Alqaed et al. [186] studied the phenomenon of Egen within a rectangular enclosure. They deduced that an increase in Ra correlated with a rise in Egen. Similarly, an increase in Ha resulted in higher Egen. Additionally, the maximum value of Egen was observed when the inclination angle of the closure was set at 30 degrees, whereas the minimum Egen occurred when the enclosure was positioned vertically or horizontally. In their study, Kumar and Gangawane [187] examined the phenomenon of Egen within a rectangular enclosure. They introduced a heated rectangular object, occupying a width that is 0.2 times the width of the enclosure, at the center of the enclosure. They observed that the density of Egen caused by fluid friction increased as Ra increased. When Ra changed from 10^4 to 10^5, Egen due to heat transfer and species transport (SC) increased by 56% and 47%, respectively.

Table 12 showcases various research studies focusing on C-shaped cavities. Some of the selected articles are described below:

Chamkha et al. [8] explored Egen occurring in a C-shaped enclosure. Additionally, all other boundaries of the enclosure were thermally insulated. The findings of the study confirmed that an increase in χ led to a corresponding increase in Egen. Furthermore, this effect was observed to intensify as Ra increased. Additionally, the application of a magnetic field was found to enhance Egen within the system. Mansour et al. [188] studied numerically to understand Egen in a C-shaped enclosure. The research revealed that as χ, Egen within the system also increased. This effect was observed across all values of the magnetic field.

Table 13 showcases various research studies focusing on channel flow type cavities. Some of the selected articles are described below:

Hussain et al. [191,192] conducted two separate studies regarding mixed convection, entropy generation, and the influence of various parameters on these processes. In their first study [191], they investigated Egen within a horizontal channel containing an open enclosure. An adiabatic square obstacle of square shape was introduced, with the bottom wall being hot. The other walls of the enclosure and the channel were insulated, while the left end of the channel was cold. Three different vertical positions of the obstacle were considered. They concluded that an increase in Ha resulted in an elevation of Egen due to fluid friction and the magnetic force. Conversely, there was a decrease in Egen due to heat transfer and the total Egen. Additionally, the study revealed that Egen increased with higher values of Ri, Re, and χ. In their second study [192], they examined Egen within an inclined open channel enclosure. The left wall of the enclosure was hot, while the fluid entering the channel had a cold temperature. The remaining boundaries were maintained under constant conditions. They found that for an inclination angle of 135°, Egen due to fluid friction, heat transfer, and the total Egen all increased. Furthermore, an increase in the porosity parameter led to enhanced Egen due to heat transfer and fluid friction.

Table 14 showcases various research studies focusing on I-shaped cavities. Some of the selected articles are described below:

Armaghani et al. [193] examined Egen in an inclined porous I-shaped enclosure. They observed that the maximum Egen was observed when Da was equal to 10^{-1}, regardless of the enclosure's inclination angle. Additionally, they observed that for a range of positions (D) of the bottom heat source between 0.5 and 0.7, Egen decreased as Ha increased. However, when D was set to 0.3 and 0.4, there was a slight increase in Egen with increasing Ha. Asadi et al. [194] studied Egen in a double lid-driven I-shaped enclosure that was filled with a porous medium containing nanoparticle at a concentration of 4%. The top wall of the enclosure moved with a velocity of 10 m/s to the right, while the bottom wall moved at the same speed to the left. The temperature of the

Table 11
Research work on rectangular enclosure

References	Tools	Domain	Flow details	Constants
Salari et al. [182]	FVM	Rectangular enclosure with circular corners	2D, steady, NC, incompressible	$10^3 \leq$ Ra$\leq 10^5$, 1$\leq$ A$\leq$ 4, $10^{-5} \leq$ Ir$\leq 10^{-2}$
Fersadou et al. [183]	FVM, SIMPLE	Rectangular open cavities	2D, MHD, MC, Cu-H_2O nanofluid, laminar, steady, Newtonian	0$\leq$ Ha$\leq$ 50, 0$\leq$ Ri$\leq$ 10, 0$\leq$ R$\leq$ 8, 0$\leq$ Rq$\leq$ 1, 0.01$\leq \chi \leq$ 0.1
Hajatzadeh Pordanjani et al. [130]	FVM, SIMPLE	Rectangular enclosure	2D, MHD, FC, laminar, Newtonian, steady, incompressible, Al_2O_3-H_2O nanofluid	$10^3 \leq$ Ra$\leq 10^5$, 0$\leq$ Ha$\leq$ 40, 0$\leq \varphi \leq$ 90, 0$\leq$ Rd$\leq$ 3, 0$\leq \chi \leq$ 0.06
El-Maghlany and Minea [184]	FVM	Rectangular enclosure	2D, steady, NC, Al_2O_3-H_2O nanofluid	$10^3 \leq$ Ra$\leq 10^5$, 0$\leq \chi \leq$ 0.1
Hu and Mei [185]	FVM, QUICK, SOR	Inclined rectangular enclosure	2D, Moisture air, steady, laminar, incompressible, Newtonian	$10^{-9} \leq$ Da$\leq 10^{-1}$, 0$\leq \varphi \leq$ 90, 0$\leq$ Sr$\leq$ 1.5,0$\leq$ Du$\leq$ 1.5, -10$\leq$ N$\leq$ 10
Alqaed et al. [186]	CVM, SIMPLE	Rectangular enclosure with blades	2D, steady MHD, NC, Al_2O_3-H_2O nanofluid, Newtonian, laminar, incompressible	$10^3 \leq$ Ra$\leq 10^5$, 0$\leq$ Ha$\leq$ 30, 0$\leq \chi \leq$ 0.03, 0$\leq \varphi \leq$ 90
Kumar and Gangawane [187]	LBM	Rectangular enclosure with blockage	2D, MHD, NC, laminar, incompressible, Newtonian, steady	2$\leq$ A$\leq$ 4, 2$\leq$ Le$\leq$ 10, $10^3 \leq$ Ra$\leq 10^5$,0$\leq$ Ha$\leq$ 100, -2$\leq$ N$\leq$ 2

Table 12
Research work on C-shaped enclosure.

References	Tools	Domain	Flow details	Constants
Chamkha et al. [8]	FVM, SIMPLE	C-shpaed enclosure	2D, steady, MHD, NC, CuO-H_2O nanofluid, Newtonain. laminar, incompressible	1000$\leq$ Ra$\leq$ 15000, 0$\leq$ Ha$\leq$ 45, 0%$\leq \chi \leq$ 6%, 0.1$\leq$ A$\leq$ 0.7
Mansour et al. [188]	FVM, SIMPLE	C-shpaed enclosure	2D, steady, MHD, MC, Cu-H_2O nanofluid, incompressible, Newtonian, laminar	0$\leq$ Ha$\leq$ 100, 0%$\leq \chi \leq$ 10%, Gr = 10^4

Table 13
Research work on channel flow type enclosure

References	Tools	Domain	Flow details	Constants
Mehrej et al. [189]	FVM, QUICK	Horizontal open channel enclosure	2D, MHD, Cu-H_2O nanofluid, laminar, Newtonian, unsteady, incompressible	0$\leq$ Ha$\leq$ 100, 0%$\leq \chi \leq$ 6%, 100$\leq$ Re$\leq$ 500, 0.001$\leq$ Ri$\leq$ 1, 0$\leq \varphi \leq$ 90
Mehrej et al. [190]	FVM, QUICK	Inclined open channel enclosure	2D, Cu-H_2O nanofluid, laminar, Newtonian, steady, incompressible	0$\leq \varphi \leq$ 360, 0%$\leq \chi \leq$ 6%, 100$\leq$ Re$\leq$ 500, Gr = 10^4
Hussain et al. [191]	FEM	Horizontal open channel enclosure with obstacle	2D, unsteady, MHD, MC, Al_2O_3-Cu-H_2O hybrid nanofluid	0.01$\leq$ Ri$\leq$ 20, 10$\leq$ Re$\leq$ 200, 0$\leq$ Ha$\leq$ 100, 0%$\leq \chi \leq$ 4%
Hussain et al. [192]	FEM	Inclined porous open channel enclosure	2D, steady, MC, laminar, Al_2O_3-H_2O nanofluid, incompressible, Newtonian	0.01$\leq$ Ri$\leq$ 20, 0$\leq \varphi \leq$ 360, 10$\leq$ Re$\leq$ 200,0%$\leq \chi \leq$ 4%, $10^{-6} \leq$ Da$\leq 10^{-3}$

cold wall was maintained at 306 K, while the hot wall was set at 346 K, and all other walls were insulated. The study considered three different scenarios, each involving a different shape of the hot block inside the enclosure: triangular, circular, and square. Furthermore, two different materials were utilized in the porous medium, namely sand and compact metallic powder. They observed that as the aspect ratio of the enclosure and χ increased, Egen decreased. Additionally, they found that the porous enclosure containing metallic powder exhibited higher Egen compared to the one containing sand. Ghasemiasl et al. [195] examined Egen in a double lid-driven I-shaped enclosure. They investigated six cases involving different hot object shapes (triangular, square, and circular) and two types of porous medium (sand and metallic powder). It was found that the sand porous medium had higher Egen compared to metallic powder for all hot block shapes. The triangular hot block had the highest Egen at 25.56%, followed by the square and circular geometries at 24.43% and 23.33%, respectively. In the case of metallic powder, the circular hot block had an Egen of 10.56%, the square geometry had 10.04%, and the triangular block had 9.76%. Tayebi et al. [196] examined Egen in an inclined I-shaped enclosure. To create different conditions, two hot cylinders were placed at varying positions within the enclosure. The findings of the study confirmed that an increase in the vortex viscosity parameter (K) resulted in a decrease in total Egen.

Table 14
Research work on I-shaped enclosure

References	Tools	Domain	Flow details	Constants
Armaghani et al. [193]	FDM, SUR	Inclined porous I-shaped enclosure	2D, steady, MHD, FC, Cu-H_2O nanofluid, incompressible, Newtonian, laminar	0$\leq$ Ha$\leq$ 20, $10^2 \leq$ Ra$\leq$ 10^3, $10^{-6} \leq$ Da$\leq 10^{-1}$
Asadi et al. [194]	FVM	lid-driven I-shaped porous enclosure with block	2D, steady, MC, two-phase, laminar, TiO_2-H_2O nanofluid, incompressible, Newtonian	0%$\leq \chi \leq$ 4%, 0.55$\leq$ A$\leq$ 0.85
Ghasemiasl et al. [195]	FVM, SIMPLE	Porous lid-driven I-shaped enclosure with blocks	2D, steady, MC, Al_2O_3-H_2O nanofluid	0%$\leq \chi \leq$ 4%
Tayebi et al. [196]	FEM	Inclined I-shaped enclosure with cylinders	2D, FC, steady, Al_2O_3-H_2O nanofluid	$10^4 \leq$ Ra$\leq$ 10^6, 0.2$\leq$ A$\leq$ 0.6, 2%$\leq \chi \leq$ 4%, 0$\leq \varphi \leq$ 90, 0.5$\leq$ K$\leq$ 2

Table 15 showcases various research studies focusing on L-shaped cavities. Some of the selected articles are described below:

Chamkha et al. [199] studied Egen in an L-shaped porous enclosure. They concluded that considering the Brownian diffusion and thermophoresis coefficients resulted in the highest rate of Egen. Furthermore, when the aspect ratio was increased from 0.3 to 0.7 for χ of 0.4, the average Egen increased by 2.3 times. Additionally, when χ was increased from 0.3 to 0.5 for an aspect ratio of 0.3, the average Egen rose by 106%. Seyyedi et al. [200] investigated Egen in an L-shaped enclosure. The findings revealed that the minimum Egen occurred when the magnetic field was inclined at 30^o, regardless of Ha values. Zhang et al. [201] studied Egen in an L-shaped enclosure. The findings revealed that the total Egen was particularly influenced by the magnetic field when dealing with the Oswald de Waele fluid. Additionally, it was observed that the total Egen decreased as the values of Ra and Ha increased. Furthermore, doubling the aspect ratio from 0.2 to 0.8 resulted in a twofold increase in the total Egen. Ghalambaz et al. [202] studied Egen in an L-shaped enclosure. It is seen that at low Ra, the dominant

Table 15
Research work on L-shaped enclosure

References	Tools	Domain	Flow details	Constants
Parvin and Chamkha [197]	FEM	L-shaped enclosure	2D, FC, Cu-H_2O nanofluid, steady, laminar, incompressible	$10^3 \leq$ Ra$\leq 10^6$, $0\leq \chi \leq 0.05$, Pr = 6.6
Rahimi et al. [198]	LBM	Hollow L-shaped enclosure	2D, steady, NC, laminar, SiO_2-TiO_2/H_2O-EG hybrid nanofluid	0.5%$\leq \chi \leq$ 3%, $10^3\leq$ Ra$\leq 10^6$, $0.1\leq$ A≤ 0.4
Chamkha et al. [199]	FVM, SIMPLE	Porous L-shaped enclosure	2D, steady, NC, laminar, CuO or TiO_2 or Al_2O_3-H_2O nanofluids, Newtonian, incompressible	$0.3\leq$ A≤ 0.7, 3%$\leq \chi \leq$ 5%, Ra = 1.424×10^6
Seyyedi et al. [200]	CV-FEM	Modified L-shaped enclosure	2D, MHD, Al_2O_3-H_2O nanofluid, NC, laminar	$10^5\leq$ Ra$\leq 10^5$, $0\leq \chi \leq 0.06$, m = 3, 4.8, 5.7, $0\leq \varphi \leq 90$, $0\leq$ Ha$\leq 10^2$, $0.25\leq$ A≤ 0.75
Zhang et al. [201]	FD-LBM	L-shaped enclosure	2D, MHD NC, laminar, steady, Newtonian, non-Newtonian	$10^5\leq$ Ra$\leq 10^5$, $0\leq$ Ha≤ 40, $0.2\leq$ A≤ 0.8, n = 0.8, 1.0, 1.4
Ghalambaz et al. [202]	FEM	L-shaped enclosure	2D, FC, laminar, steady, Cu-Al_2O_3-H_2O hybrid nanofluid, incompressible	$10^5\leq$ Ra$\leq 10^5$, $0\leq \chi \leq 0.05$, Pr = 6.2
Hussain et al. [203]	FEM	Elbow-shaped enclosure with cylinder	2D, MHD, MC, steady, non-Newtonian, Ag-MgO hybrid nanoparticles	$0.6\leq$ n≤ 1.8, $0.01\leq$ Ri≤ 10, $0\leq$ Ha≤ 100, $-75\leq \omega \leq 50$, Pr = 6.2, Re = 100, $0.3\leq$ A≤ 0.5, Ha = 25, $0.005\leq \chi \leq 0.02$

contributor to Egen was heat transfer. Conversely, at high Ra values, the opposite trend was observed, where heat transfer played a lesser role in Egen. Furthermore, the inclusion of nanoparticles in the system, especially at high Ra values, was found to enhance the overall Egen. Hussain et al. [203] examined Egen within an elbow-shaped enclosure. The enclosure had a wavy top wall and a hot quarter circle installed at the bottom left corner, while a rotating cylinder was positioned at the top of the left leg. The right internal horizontal wall remained cold, while the remaining boundaries were considered insulated. They observed that Egen resulting from fluid friction increased with the augmentation of Ha, but this effect was negligible for a power index of 1.4. They also noted that an increase in the magnetic field led to a rise in Egen due to the magnetic field. Based on their findings, they concluded that Egen would be minimal for non-Newtonian fluid and would increase with an increment in χ.

Table 16 presents a compilation of diverse research investigations centered around modified cavities. Some of the selected articles are described below:

Marzougui et al. [205] examined the behavior of Egen inside an enclosure with chamfered corners. It is observed that Egen decreased with the increase of Ha for constant χ. However, it is also observed that Egen increased with an increase in Ra. At very high Ra values, the impact of an increase in Ha was found to be negligible on thermal Egen. Additionally, the study revealed that Egen increased with an increase in χ, but this trend reversed after reaching a certain value of Ha. Beyond this threshold, Egen decreased with an increase in χ. Yıldız et al. [206] investigated Egen within an enclosure with a dome shape inclined at different angles. The study examined three dome angles, namely 15°, 30°, and 45°, corresponding to three different dome heights denoted as

Table 16
Research work on modified enclosure

References	Tools	Domain	Flow details	Constants
Mohammadtabar et al. [204]	FVM, SIMPLE	Modified rectangular enclosure	2D, steady, NC, laminar, Al_2O_3-H_2O nanofluid	$10^3\leq$ Ra$\leq 10^5$, $0\leq \chi \leq 0.1$, $1\leq \chi \leq 4$, $0.00005\leq Ec \leq 0.05$
Marzougui et al. [205]	FEM	Modified enclosure with chamfers	2D, MHD, Cu-H_2O nanofluid, laminar, Newtonian, unsteady	Pr = 7, $10^5\leq$ Ra$\leq 10^6$, $0\leq$ Ha$\leq 10^2$, $0.02\leq \chi \leq 0.08$
Yildiz et al. [206]	FVM, SIMPLE	Dome shaped modified square enclosure	2D, steady, NC, laminar	$10^4\leq$ Ra$\leq 10^6$, $0\leq \varphi \leq 90$, Pr = 0.71
Rehman et al. [207]	FEM	Fillet square enclosure with cylinder	2D, MHD, steady, ferric oxide–H_2O nanofluid, incompressible	$0\leq$ Ha$\leq 10^2$, $0\leq \omega \leq 4$, $0\leq \chi \leq 0.06$

R15, R30, and R45, respectively. It is seen that Egen reached its minimum value for the R45 dome enclosure compared to the other dome enclosure types. Additionally, the disparity in Egen between the R45 dome enclosure and the equivalent rectangular enclosure was more pronounced. On the other hand the Egen of the R15 dome enclosure was nearly identical to that of the rectangular enclosure. Interestingly, it was observed that enclosure inclinations of 30° and 60° resulted in the highest Egen. Rehman et al. [207] investigated Egen of a magnetized ferric oxide-water nanofluid surrounding a rotating heated cylinder inside a fillet square enclosure. The enclosure consisted of a hot bottom wall, while the remaining walls were cold, and a downward magnetic field was applied. It is found that an increase in Ha resulted in a reduction in Egen due to the viscous effect for constant χ. Furthermore, they observed a decrease in thermal Egen with Ha at a specific value of ϕ and the rotational speed of the cylinder.

Table 17 provides an assortment of research studies that focus on cavities with polygonal shapes. The following are succinct summaries of the selected articles included in the table:

Acharya [37] focused on laminar flow in an octagonal enclosure containing a circular cylinder equipped with four fins attached to its surface. It is seen that an increase in χ and Ra exhibited a positive correlation with Egen. Conversely, an increase in the strength of the magnetic field exhibited an inverse relationship with Egen. Higher magnetic field values were found to reduce the overall Egen. Additionally, the study investigated the impact of the fins' height on Egen. It was observed that increasing the height of the fins resulted in a decrease in Egen. This suggests that modifying the fins' dimensions can play a significant role in minimizing the overall Egen within the system. Majeed et al. [208] investigated the influence of magnetization on Egen and thermal flow within a hexagonal enclosure. The enclosure contained a cylinder object positioned at its center, while the upper, lower, and cylinder surface

Table 17
Research work on polygonal shaped enclosure

References	Tools	Domain	Flow details	Constants
Acharya [37]	FEM	Octagonal enclosure with cylinder	2D, MHD, steady, Ag-MgO-H_2O hybrid nanofluid, laminar, incompressible	$0\leq \chi \leq 0.015$, $10^3\leq$ Ra$\leq 10^5$, $0\leq$ Ha$\leq 10^2$
Majeed et al. [208]	FEM	Hexagonal enclosure with cylinder	2D, MHD, steady, incompressible, laminar, Ag-MgO-H_2O hybrid nanofluid	$0\leq$ Ha$\leq 10^2$, $5\leq$ Ri≤ 30, $0.02\leq \chi \leq 0.08$, $0.1\leq d_c\leq 0.3$, Pr = 6.2

walls were maintained at elevated temperatures. Conversely, the upper left boundary and lower right wall were kept cold, and the remaining boundaries were thermally insulated. They observed that as the values of Ri, Ha, and χ increased, the magnetic Egen also increased.

Table 18 presents a compilation of diverse research investigations centered around cavities with rhombic shapes. Some of the selected articles are described below:

Nayak et al. [210] investigated the Egen characteristics of a Cu-H_2O nanofluid within an inclined, skewed enclosure. The bottom boundary of the enclosure was aligned with the horizontal axis, while the side boundary formed an angle φ with the horizontal axis. They observed that, for a fixed inclination and skewed angle of the cavity, Egen increased with an increase in χ in the nanofluid. Additionally, they found that when the buoyancy effect was negligible, Egen became independent of the inclination angle. However, at a fixed Re, Egen increased with Ri. Moreover, an increase in χ led to an overall increase in Egen. Lastly, the enhancement in Egen diminished as the tilt angle of the cavity increased, particularly with a sharply skewed angle. Das and Basak [51] conducted a study on the Egen of Newtonian and incompressible fluids within a rhombic cavity. The cavity featured different angles of inclination for the side walls (45°, 60°, and 75°) and various area ratios (0.5, 1, and 1.5). Their findings indicated that higher Da values led to dominant Egen from fluid friction, while lower Da values resulted in dominant heat transfer Egen. By altering the area ratio to 0.5, 1, and 1.5, the total Egen witnessed a reduction of 46.37%, 39.43%, and 15.84%, respectively. The study also recommended an inclination angle of 45° and a Pr of 1000 for achieving moderate heat transfer and lower Egen, irrespective of the enclosure area. Furthermore, a lower Egen was observed with an area ratio of 0.5. Dutta et al. [212] explored the behavior of Egen in a rhombic enclosure. In their study, the bottom wall was heated, the top wall was cooled, and the remaining walls were thermally insulated. Their findings indicated that an increase in Ha led to a decrease in total Egen across different values of Ra and enclosure inclination angles.

Table 19 presents a compilation of diverse research investigations centered around semi-circular cavities. Some of the selected articles are described below:

Shafee et al. [215] explored Egen of a ferrofluid within a semi-annulus enclosure. The results demonstrated that increasing values of Da, Ra, and Ha corresponded to an elevation in magnetic Egen. Ghalambaz et al. [54] studied to examine Egen within an inclined semi-annular enclosure. The enclosure featured a hot internal cylinder surface and a cold outer shell surface. They observed that Egen due to fluid friction was higher in all investigated cases. They also observed that a higher volume fraction of NEPCM particles led to increased heat transfer Egen at low Ra values, while viscous Egen became dominant at higher Ra values. Furthermore, they found that both the total Egen and the enclosure inclination angle exhibited a positive correlation with Ra, indicating that higher Ra and steeper enclosure inclination angles resulted in greater Egen. Afshar et al. [216] investigated Egen characteristics of a hybrid fluid within a porous semi-circular enclosure featuring a wavy inner bottom surface. The findings of the study revealed that regardless of the specific profiles of the wavy bottom wall, an increase in amplitude led to an enhancement in Egen for all values of Ra.

Table 20 presents a compilation of diverse research investigations centered around U-shaped cavities. Some of the selected articles are described below:

Selimefendigil et al. [217] conducted an analysis of Egen in a U-shaped enclosure. The bottom boundary of the enclosure was hot and partially elastic, featuring an adiabatic rotating cylinder inserted at the left leg. The enclosure was vented through a cold inlet and an outlet located on the right leg, while all other boundaries remained insulated. The study revealed that the left domain exhibited a higher rate of Egen, which increased with higher Ha values. However, the right domain demonstrated a decrease in Egen for Ha values ranging from 40 to 75. In general, higher values of Ha are correlated with an increase in the rate of Egen. The influence of the modulus of elasticity on Egen was found to be weak. Furthermore, an increase in the rotational speed of the cylinder

Table 18
Research work on Rhombic enclosure

References	Tools	Domain	Flow details	Constants
Anandalakshmi and Basak [43]	FEM	Rhombic enclosure	2D, steady, NC, laminar, Newtonian, incompressible	$10^3\leq$ Ra$\leq 10^5$, $30\leq φ \leq 90$, $0.015\leq$ Pr$\leq 10^3$
Nayak et al. [209]	FVM, SIMPLEC	lid-driven Rhombic enclosure	2D, unsteady, MC, Cu–H_2O nanofluid, laminar, incompressible, Newtonian	$30\leq φ \leq 150$, $0\leq χ \leq 0.2$, $0.1\leq$ Ri≤ 5, Re = 200, 500, $10^3\leq$ Gr$\leq 5 \times 10^4$
Kavya et al. [61]	FEM	Rhombic enclosure	2D, steady, NC, laminar, Newtonian, incompressible	$45\leq φ \leq 75$, $0.5\leq$ A≤ 1.5, $0.015\leq$ Pr$\leq 10^3$, $10^3\leq$ Ra$\leq 10^5$
Nayak et al. [210]	CVM, SIMPLEC	lid-driven inclined Rhombic enclosure	2D, unsteady, MC, Cu–H_2O nanofluid, laminar, incompressible, Newtonian	$-30\leq φ \leq 30$, $0\leq χ \leq 0.2$, $10^2\leq$ Re$\leq 10^3$, $0.1\leq$ Ri≤ 5
Das and Basak [51]	FEM	Porous Rhombic enclosure	2D, steady, NC, laminar, Newtonian, incompressible	$45\leq φ \leq 75$, $0.5\leq$ A≤ 1.5, $0.015\leq$ Pr$\leq 10^3$, $10^{-5}\leq$ Da$\leq 10^{-2}$, Ra=10^6
Dutta et al. [211]	FEM	Rhombic enclosure	2D, MHD, NC, Cu–H_2O nanofluid, laminar, Newtonian, steady, incompressible	$10^3\leq$ Ra$\leq 10^6$, $0\leq$ Ha$\leq 10^2$, $30\leq φ \leq 60$, $0.01\leq χ \leq 0.05$

Table 19
Research work on semi-circular enclosure

References	Tools	Domain	Flow details	Constants
Mojumder et al. [213]	FEM	Half-moon shaped enclosure	2D, MHD, NC, steady, laminar, Newtonian, Fe_3O_4-H_2O, Co-Kerosene nanofluids, incompressible	$10^3\leq$ Ra$\leq 10^7$, $0\leq$ Ha≤ 100, $0\leq φ \leq 90$
Bezi et al. [214]	FVM, QUICK, RBSOR, AB	Semi-annular enclosure	2D, unsteady, NC, laminar, Au, Ag, Cu, CuO-H_2O nanofluids, Newtonian, incompressible	$10^3\leq$ Ra$\leq 10^5$, $0\leq φ \leq 180$, $0\leq χ \leq 0.08$
Shafee et al. [215]	CV-FEM	Porous semi-annulus enclosure	2D, MHD, Fe_3O_4-H_2O nanofluid, steady	$10^3\leq$ Ra$\leq 10^4$, $1\leq$ Ha≤ 40, $0.01\leq$ Da≤ 100
Ghalambaz et al. [54]	FEM	Semi-annular enclosure	2D, steady, NC, PCM, nanoparticles, laminar, Newtonian, incompressible	$10^4\leq$ Ra$\leq 10^6$, $0\leq$ Ste≤ 100, $0\leq χ \leq 0.04$, Pr = 6.2, $0\leq φ \leq 90$
Afshar et al. [216]	FEM	Porous wavy semi-circular enclosure	2D, FC, PCM, nanoparticles, steady, laminar, Newtonian, incompressible	$10^3\leq$ Ra$\leq 10^5$, $0\leq χ \leq 0.05$, $10^{-3}\leq$ Da$\leq 10^{-1}$

Table 20
Research work on U-shaped enclosure

References	Tools	Domain	Flow details	Constants
Cho et al. [2]	FVM, SIMPLE	U-shaped enclosure	2D, steady, NC, laminar, Al_2O_3-H_2O nanofluid, Newtonian, incompressible	$10^3 \leq$ Ra$\leq 10^6$, $0\leq \chi \leq 0.04$, Pr = 6.2
Selimefendigil et al. [217]	FEM, ALE	U-shaped vented enclosure with rotating cylinder	2D, MHD, FC, CNT-H_2O nanofluid, laminar, steady, Newtonian, incompressible	$100\leq$ Re≤ 500, $0\leq$ Ha≤ 75, $-300\leq \omega \leq 300$
Pasha et al. [218]	FEM	U-shaped enclosure with baffles & wavy walls	2D, steady, NC, PCM, nanoparticles	$10^4\leq$ Ra$\leq 10^5$, $0\leq \chi \leq 0.05$, $0\leq$ Ha≤ 20

resulted in an enhancement of Egen. Pasha et al. [218] conducted a study on Egen within a U-shaped enclosure featuring a wavy triangular bottom wall. They observed that when the baffles' length was equal to 0.1 times the values of Ra (10^4, 5×10^4, 10^5), there was only a slight change in the local Be. Additionally, for baffles with a length of 0.2L, an increase in Ra resulted in a reduction in the local Be under the influence of a magnetic field (Ha = 0, 20).

Table 21 presents a research on three dimensional cubical cavities. Below are the concise summaries of the selected articles featured in the table:

Abderrahmane et al. [17] conducted a study on Egen in a 3D triangular enclosure. The left vertical boundary had a zigzag geometry and was kept hot, while the base was insulated and the hypotenuse remained cold. They found that increasing Da enhanced fluid friction entropy and reduced Egen due to heat transfer. Higher Ha increased Egen due to heat transfer but minimized fluid friction entropy. The study concluded that a zigzag hot wall configuration improved heat transfer and reduced Egen. Al-Khazaal [231] conducted a study exploring the impact of hybrid nanofluid presence, along with a fin composed of composite materials, on Egen within a 3D cubic enclosure. They observed that the addition of nanoparticles led to an increase in Egen, irrespective of the fin conductivity ratio. Notably, the highest Egen occurred when the composite material conductivity ratio was Rc=1000, Ra=10^5, and χ=0.05. These findings highlight the potential of utilizing the fin to control the rate of Egen. Banik et al. [232] conducted a study on Egen of ferrofluid within a cubical enclosure featuring a central hot cylinder. They explored two setups. In the first setup, three magnets were placed on the vertical opposite walls of the enclosure. In the second setup, three configurations were considered, involving the individual placement of magnets on the enclosure walls and around the heat source. Adiabatic conditions were maintained near the magnets, while the walls at the ends of the cylinder remained adiabatic, and the remaining walls were cold. The findings indicated that the first setup resulted in a minimum Egen. Additionally, the study aimed to propose an effective technique for controlling Egen. Cherif et al. [233] conducted a study to investigate the Egen characteristics of hybrid nanoliquid inside a 3D triangular porous enclosure. The findings suggested that for Ha of 0 and a cylinder rotational speed of 1000, the heat transfer rate was higher, while Egen was lower. Furthermore, they observed that increasing Da and reducing Ha improved the heat transfer performance and minimized Egen. Conversely, higher Ha values had a detrimental effect on flow motion, resulting in increased Egen. Zisan et al. [234] conducted a study to investigate Egen within a cubic enclosure containing discrete heat sources positioned at the bottom. The widths of the heating surfaces were set at 0.2 times the length (L) of the enclosure. They examined three different configurations, each characterized by variations in the distance between the heat source (h) and the distance from the left surface (c). Configuration A had h = 0.4L and c = 0.5L, configuration B

Table 21
Research work on 3D enclosure

References	Tools	Domain	Flow details	Constants
Kolsi et al. [219]	CV-FDM, CDS	Cubical enclosure	3D, unsteady, NC, laminar, Al_2O_3-H_2O nanofluid, Newtonian, incompressible	$10^3\leq$ Ra$\leq 10^6$, $0\leq \chi \leq 0.20$, Pr = 6.2
Hussein et al. [1]	CV-FDM, CDS	Cubical Trapezoidal enclosure	3D, unsteady, NC, laminar, incompressible, Newtonian	$10^3\leq$ Ra$\leq 10^5$, $0\leq \varphi \leq 180$, Pr = 0.71
Kolsi et al. [220]	CV-FDM, CDS, SOR	Cubical enclosure with fin	3D, unsteady, NC	Pr = 0.7, $0.01\leq$ Rc≤ 100, $-60\leq \varphi \leq 60$, Ra=10^5
Kolsi et al. [221]	CV-FDM, CDS	Cubical enclosure with twin blocks	3D, unsteady, NC, laminar, Al_2O_3-H_2O nanofluid, incompressible	Pr = 6.2, $0\leq \chi \leq 0.15$, $10^4\leq$ Ra$\leq 10^6$
Kolsi et al. [222]	CV-FDM	Cubic enclosure with triangular body	3D, laminar, NC, unsteady	$10^4\leq$ Ra$\leq 10^6$, $0\leq \chi \leq 0.15$, $0.01\leq$ Rc≤ 100
Kolsi et al. [223]	CVM	Cubical enclosure	3D, Al_2O_3-H_2O nanofluid, unsteady, laminar, Newtonian, incompressible	Ra=10^5, $0\leq \chi \leq 0.2$, $10^{-3}\leq$ Ma$\leq 10^3$, Pr = 6.2
Al-Rashed et al. [224]	FDM CDS, SOR	Cubical enclosure with baffle	3D, CNT-H_2O nanofluid, MC, laminar, incompressible, Newtonian, unsteady	$10^3\leq$ Ra$\leq 10^5$, $0\leq \chi \leq 0.15$, Pr = 6.2, Re = 0, 100, $0\leq$ Ri≤ 10
Al-Rashed et al. [225]	FDM, SIMPLE, CDS	Cubical enclosure	3D, NC, laminar, incompressible, Newtonian, unsteady	$10^3\leq$ Ra$\leq 10^6$, Pr = 0.71
Oztop et al. [226]	FVM, CDS, SOR	Partially open cubic enclosure	3D, unsteady, NC	$10^3\leq$ Ra$\leq 10^5$, $0.25\leq$ h, d≤ 0.75
Salari et al. [227]	FVM, SIMPLE	Rectangular cubic enclosure	3D, unsteady, NC, laminar, MWCNTs-H_2O nanofluid & air, Newtonian, incompressible	$10^3\leq$ Ra$\leq 10^6$, $0\leq \varphi \leq 90$, $0.002\leq \chi \leq 0.01$
Al-Rashed et al. [228]	CVM, CDS, SOR	Cubical open enclosure with block	3D, unsteady, MC, laminar, Al_2O_3-H_2O nanofluid, incompressible	$0.01\leq$ Ri≤ 100, $0\leq \chi \leq 0.05$, Pr = 6.2, Re = 10
Hussein [229]	FVM, modified SIMPLE, ADI	Right angled triangular enclosure	3D, unsteady, MC, laminar	Pr = 0.71, $0.01\leq$ Ri≤ 10, Re = 100
Rahimi et al. [230]	LBM, MRT	Cuboid enclosure	3D, unsteady, MC, CuO-H_2O nanofluid	$10^3\leq$ Ra$\leq 10^6$, $0\leq \chi \leq 0.04$
Boulahia et al. [50]	FVM, two-phase mixture model, SIMPLE	Rectangular enclosure with internal blocage	3D, FC, TiO_2-Al_2O_3-Cu-H_2O hybrid nanofluid, laminar, Newtonian, incompressible	$10^3\leq$ Ra$\leq 10^6$, $0\leq \chi \leq 0.05$, $0\leq$ Am≤ 0.2
Abderrahmane et al. [17]	FEM	Triangular porous enclosure with cylinder	3D, steady, MHD, MC, laminar, Fe_3O_4- MWCNT-H_2O hybrid nanofluid	$10^{-5}\leq$ Da$\leq 10^{-2}$, $0\leq$ Ha$\leq 10^2$, $-500\leq \omega \leq 1000$
Al-Khazaal [231]	FEM	Cubic enclosure with fin	3D, unsteady, NC	$1\leq$ Rc$\leq 10^3$, $0\leq \chi \leq 0.05$,

(continued on next page)

Table 21 (*continued*)

References	Tools	Domain	Flow details	Constants
				$10^3 \leq$ Ra$\leq 10^5$
Banik et al. [232]	FVM, SIMPLE, QUICK	Cubical enclosure with cylinder	3D, MHD, ferrofluid, steady	Pr = 316, χ=0.1%
Cherif et al. [233]	FEM	Triangular porous enclosure with cylinders	3D, steady, MC, laminar, Fe_3O_4-MWCNT-H_2O hybrid nanoliquid	$10^{-5} \leq$ Da$\leq 10^{-2}$, $0 \leq$ Ha$\leq 10^2$, -500 $\leq \omega \leq$ 1000
Zisan et al. [234]	FEM	Cubic enclosure	3D, laminar, NC, unsteady, Newtonian, incompressible	$10^3 \leq$ Ra$\leq 10^6$, Pr = 0.71

had h = 0.4L and c = 0.7L, and configuration C had h = 0.8L and c = 0.5L. Their findings indicated that configuration A exhibited the maximum Egen, while configurations B and C demonstrated nearly equal levels of entropy formation.

Table 22 presents a research on cavities with concave/conves sides. Below are the concise summaries of the selected articles featured in the table:

Biswal and Basak [46] conducted a numerical analysis to investigate Egen within a 3D rectangular enclosure with curved side walls, which could be either concave or convex. The enclosure was differentially heated, and they considered three cases: case 1 with the smallest height of the curved surfaces, case 2 with a medium height, and case 3 with the maximum height. Their findings revealed that, irrespective of the values of Ra and Pr, the heat transfer Egen was consistently higher in the concave side cases due to the temperature gradient. Additionally, in case 3, where the enclosure had a narrow region in the middle position, the heat Egen was further increased. However, for the convex side cases (cases 1-3), regardless of the values of Ra and Pr, the heat Egen was higher near the top-right and bottom-left corners of the enclosure. Moreover, they observed that as the convexity of the wall increased, the heat Egen also increased. Furthermore, in concave cases 1 and 2, the maximum fluid friction Egen occurred at the middle position of the side walls. Biswal and Basak [236] examined Egen occurring in porous, three-dimensional triangular cavities with right angles. These cavities had either concave right walls (referred to as Case 1) or convex right walls (referred to as Case 2). They observed that an increase in Da and Pr resulted in a corresponding increase in the overall Egen, regardless of the curvature type of the wall. The maximum Egen was observed in Case 2, where the right wall had a highly convex shape, while the minimum Egen was observed in Case 1, where the right wall had a concave shape.

Table 22
Research work on the enclosure with concave/convex sides

References	Tools	Domain	Flow details	Constants
Kashani et al. [235]	FVM, SIMPLE	Enclosure with concave/convex sides	2D, steady, NC, laminar, Cu-H_2O nanofluid,	$0 \leq \chi \leq 5\%$, $10^5 \leq$ Ra$\leq 10^6$, $1 \leq$ A≤ 2
Biswal and Basak [46]	FEM	Enclosure with concave/convex sides	2D, NC, steady	$10^3 \leq$ Ra$\leq 10^5$, Pr = 0.015, 0.7, 1000
Biswal and Basak [236]	FEM	Right-angled triangular porous enclosure with concave/convex sides	2D, NC, steady	$10^{-5} \leq$ Da$\leq$ 10, Pr = 0.01, 7.2, 0.7, Ra = 10^6
Biswal and Basak [47]	FEM	Porous Enclosure with concave/ convex sides	2D, NC, steady	$10^{-5} \leq$ Da$\leq 10^{-2}$, Pr = 0.015, 7.2, Ra = 10^6

Biswal and Basak [47] investigated entropy generation within 3D rectangular porous cavities with concave and convex horizontal top and bottom walls. The study examined three cases, varying the height of the concave or convex surfaces. Case 1 represented the smallest height, case 2 the medium height, and case 3 the maximum height. They found that when the concave or convex surfaces were at their smallest height, the maximum heat transfer Egen occurred near the core region. For case 2 and case 3, with higher concave surfaces, the maximum heat transfer Egen was observed near the middle positions of the concave walls, at low Da, and for all Pr. However, for the convex cases, irrespective of the height, the maximum heat transfer Egen was found near the corner regions at low Da and for all Pr. At high Da, the maximum heat transfer Egen shifted towards the core of the enclosure for cases 1 and 2 (concave) and cases 1-3 (convex).

Table 23 presents research on cavities with different shapes that are not discussed above. Below are the concise summaries of the selected articles featured in the table:

Dogonchi et al. [245] examined the entropy generation characteristics of oxide nanoparticles within a cylindrical enclosure featuring a wavy crown and a flat bottom wall, both of which were adiabatic. It was found that as the curvature increased, Egen also increased. The highest Egen was observed in the vicinity of the cylinder and the wavy wall. Dogonchi et al. [246] explored the natural convection behavior of iron nanoliquid within a porous enclosure with a star-shaped geometry. The enclosure contained two cylinders, with the left cylinder being heated and the right cylinder being cooled. The outer surface of the enclosure was adiabatic. The study findings indicated that Egen decreased with an increase in Ha and decreased with an increase in Da. Moreover, regardless of the value of Ra, an increase in porosity resulted in reduced Egen. Dogonchi et al. [247] employed numerical analysis to investigate the effect of hybrid nanoliquid within a star-shaped porous enclosure. The enclosure contained three cylinders, with two of them being cold and one being hot. The outer surface of the enclosure was thermally insulated. It is observed that the maximum Egen occurred at the center of the enclosure, where energy was lost among the active cylinders. Tayebi et al. [248] studied entropy generation behavior inside a circular enclosure containing a cylindrical object with four extended fins on its surface. The fins on the cylinder surface were maintained at a high temperature, while the outer surface of the enclosure remained cold. They observed that at low Ra, the dominant contribution to Egen stemmed from heat transfer. Conversely, at high Ra, fluid friction Egen became the dominant factor.

Table 24 presents a research on mixed type cavities. Below are the concise summaries of the selected articles featured in the table:

Das et al. [53] conducted numerical analysis to investigate the impact of different heater element positions on the thermal and hydraulic behavior, as well as Egen, in square and triangular cavities. The study considered three types of cavities: regular isosceles triangular, inverted isosceles triangular, and square. Three cases were examined based on the placement of heaters: case 1 featured a larger heater in the lower half and a smaller heater in the center; case 2 had a larger heater in the center and a smaller one in the lower half; and case 3 involved two heaters of similar length placed in the center and lower halves. They found that the maximum heat Egen occurred along the interaction line between the hot and cold sides of the enclosure walls, while this value was lower on the walls due to reduced temperature gradients at low Ra values across all cases. Khan et al. [249] examined the natural convection and Egen of a hybrid nanofluid inside square and rectangular enclosures. It is observed that decreasing the aspect ratio of the enclosure resulted in a reduction in Egen. Notably, the minimum value of Egen occurred when the aspect ratio reached 0.5. Additionally, the study revealed that Egen increased with χ at a constant Ra. The maximum Egen was observed at a χ = 0.001.

Additional Literature Review:

The investigation of Egen within various geometric configurations of porous cavities has provided insights into the interplay of Egen due to

Table 23
Research work on other types of cavities

References	Tools	Domain	Flow details	Constants
Rahimi et al. [237]	LBM	H-shaped enclosure	2D, laminar, NC, steady, SiO_2-TiO_2/H_2O-EG hybrid nanofluid, Newtonian, incompressible	0.5%≤ χ ≤ 3%, 10^3≤ Ra≤ 10^6
Li et al. [238]	CV-FEM	Wavy porous tank	2D, Fe_3O_4-H_2O nanoliquid, MHD, laminar, steady	10^3≤ Ra≤ 10^5, Ha=1, 40, Da=0.01, 100, χ=0.04
Seyyedi et al. [239]	CV-FEM, FVM, SIMPLE	Quarter-annulus enclosure	2D, MHD, NC, steady, laminar	10^3≤ Ra≤ 10^5, 0≤ φ ≤ 90, 0≤ Ha≤ 20
Sachica et al. [240]	CVM	Plus-shaped enclosure	MHD, MC, 2D, Al_2O_3-H_2O nanofluid, unsteady, Newtonian, incompressible	0≤ Ha≤ 10, -1≤ Ri≤ 5, 0≤ χ ≤ 0.2, 300≤ Re≤ 700, Pr=7.0
Seyyedi [241]	CV-FEM	Cardioid shaped enclosure inside cylinder	2D, NC, Cu-H_2O nanofluid, steady	10^3≤ Ra≤ 10^5, 0≤ Ha≤ 15, m=3, 0.01≤ Da≤ 100, χ=0.04, Pr = 6.2
Tayebi et al. [242]	FVM	Annular elliptical enclosure	2D, NC, steady, Cu-Al_2O_3-H_2O hybrid nanoliquid	Pr = 6.2, 10^3≤ Ra≤ 2 × 10^5, -5≤ q≤ 5, 0%≤ χ ≤ 9%
Zhang et al. [243]	FVM, SIMPLE	Inclined enclosure	2D, steady, NC, laminar, Al_2O_3-H_2O nanofluid, incompressible, Newtonian	0%≤ χ ≤ 6%,0≤ Rd≤ 2, 10^3≤ Ra≤ 10^5, 0≤ Ha≤ 40, 0.3≤ A≤ 0.7
Ahmed et al. [38]	FEM	Porous prismatic enclosures	2D, PCM, unsteady	0≤ Rd≤ 5, 0≤ φ ≤ 90, 0%≤ χ ≤ 5%, Da=10^{-3}
Chammam et al. [244]	FEM	Complex shaped enclosure	2D, MHD, NC, Fe_3O_4-H_2O nanoliquid, steady	0.1≤ A≤ 0.3,10^3≤ Ra≤ 10^5, Ha = 0, 20, χ = 0.02, 0≤ Rd≤ 0.3
Dogonchi et al. [245]	FEM	Crown wavy enclosure	2D, NC, steady, Al_2O_3-H_2O nanoliquid	10^3≤ Ra≤ 10^5, 0≤ Ha≤ 20, 10^{-3}≤ Da≤ 10^{-1}, 0.1≤ Rd≤ 0.3, 0≤ φ ≤ 90, 0.01≤ χ ≤ 0.04
Dogonchi et al. [246]	FEM	Porous enclosure with two square cylinders	2D, Fe_3O_4-H_2O nanoliquid, MHD, NC, steady	10^3≤ Ra≤ 10^5, 0≤ Ha≤ 40, 0.3≤ A≤ 0.5, 0.01≤ Da≤ 100, χ=0.02, m=3, 4.8, 5.7
Dogonchi et al. [247]	FEM	Wavy porous enclosure with three circular cylinders	2D, MHD, NC, steady, Cu-Al_2O_3-H_2O hybrid nanoliquid	10^3≤ Ra≤ 10^5, 0≤ Ha≤ 40, m=5.7, 0.01≤ Da≤ 10^2, χ = 0.02
Tayebi et al. [248]	FEM	Annular enclosure with fins	2D, MHD, NC, Al_2O_3-H_2O nanoliquid, steady	10^3≤ Ra≤ 10^5, 0≤ Ha≤ 40, 1%≤ χ ≤ 4%, 0.05≤ A≤ 0.15

HT and fluid friction under different conditions. Bhardwaj and Dalal's study [250] on a right-angled triangular cavity identified Egen due to HT as the primary irreversibility source at low Da and Ra values, with a notable convergence of Egen values between Egen due to HT and fluid friction at high Ra. Meshram et al. [251] extended this exploration to a square cavity, highlighting that at low Da, Egen due to HT dominates across cavity inclinations, while at higher Da, fluid friction becomes the dominant factor, revealing a sensitivity to cavity inclination at elevated Da values. Chandra Pal et al. [252] introduced hot circular objects in a porous square cavity, emphasizing the impact of Da on Egen, with a shift from HT dominance at lower Da to variability with Ra at higher Da. Dutta et al. [212] expanded the investigation to a quadrantal porous cavity, revealing a transition in dominant factors from HT to frictional Egen with increasing Da. Bhowmick et al. [253] explored NC and Egen in a square cavity with a hot object, observing wavelength-dependent variations in Egen due to HT and friction, demonstrating the nuanced influence of geometry and Ra. Finally, Dutta et al.'s [254] study on a deviated rhombic porous cavity contributed insights into the insensitivity of HT Egen to Da and the nuanced effect of phase shift angle on total Egen, thereby establishing a cohesive narrative on the intricate relationship between cavity geometry, Egen due to HT, and Egen due to fluid friction in porous media.

Table 24
Research work on mixed-type cavities

References	Tools	Domain	Flow details	Constants
Das and Basak [52]	FEM	Square & triangular cavities	2D, steady, NC, Newtonian, laminar, incompressible	Pr = 0.015, 7.2, 10^3≤ Ra≤ 10^5
Das et al. [53]	FEM	Square & triangular cavities	2D, steady, NC, Newtonian, laminar, incompressible	Pr = 0.015, 7.2, 10^3≤ Ra≤ 10^5
Khan et al. [249]	LBM	Square & rectangular cavities	2D, FC, MWCNT-Fe_3O_4-H_2O hybrid nanofluid, incompressible, steady	0.5≤ A≤ 2, 10^3≤ Ra≤ 10^5, 0≤ χ ≤ 0.01

Ahn et al.'s [255] examination of an annular cylindrical cavity establishes the foundation by emphasizing the dominance of friction-induced Egen for specific Be values, particularly at low Ma values, a finding resonated by Nayak et al. [256] in their study of a hexagonal cavity with a periodic magnetic field. Al-Amir et al.'s [257] exploration in a Z-staggered cavity filled with a nanofluid introduces the influence of corrugated walls on Egen, adding complexity to the relationship between Ra and Egen observed by Arshad Siddiqui et al. [258] in an I-shaped cavity with a magnetic ferrofluid, highlighting the significance of Ha. Hashemi-Tilehnoee et al.'s [259] examination of a cubic cavity with conductive spherical blocks further contributes by linking Egen variations to the combined effects of thermal radiation and a magnetic field, complementing Hamza et al.'s [260] study on Egen within a porous square cavity, where the imposition of a magnetic force highlighted Egen. Collectively, these studies underscore the intricate interplay between parameters such as Be, Ha, Ma, and Ra in determining Egen, providing a holistic understanding of engineering applications seeking to enhance efficiency and performance in complex systems.

6. Conclusions

In conclusion, it can be said that analyzing Egen inside an enclosure and its correlation to various factors such as system geometry, orientation, flow setups, fluid properties, augmentation and alteration of fluid properties through the introduction of nanoparticles, external factors such as magnetic fields, etc. has been done extensively from the perspective of thermal system optimization. From the present review, it is very evident that there is a positive correlation between thermal augmentation and the enhancement of Egen. This is very fundamental as well as intuitive since the augmentation of heat transfer basically represents the greater rate of thermal transport from the thermal source to the heat sink. Since such transfer is unidirectional and governed by the temperature gradient, a greater degree of irreversibility is associated with a higher rate of thermal transport. Therefore, it can be seen that Egen increases as Ra, Pr, Re, and Ri increase. The most fundamental way to look at this topic is to analyze the increment of Egen in light of Nu augmentation. All the factors that contribute to the increase in Nu also contribute to the enhancement of local and overall Egen. Therefore, with the increase in nanofluid concentration at the initial stage, Egen also increases. The same thing is observed in the case of porous media. As Da increases, Nu decreases, and therefore, Egen decreases.

Other than the thermal gradient, there are many other factors that also contribute to Egen in varying ways. One of the most important factors among them is the frictional characteristic, which is the mechanical equivalent of thermal irreversibility. Therefore, any complicated geometry that contributes to the formation of eddies, an adverse pressure gradient, a sudden change in flow direction, or an obstacle to normal flow behavior experiences greater local and average Egen, which is very evident from the present review. Thus, in this review article, it is observed that the rate of Egen is higher when there is a rotating cylinder inside the enclosure since the rotating cylinder experiences greater flow drag as it rotates. As a result, the higher the rotational speed, the greater the Egen. The same conclusion can be drawn for other types of moving boundaries as well. Due to similar reasoning, fluids with higher viscosity also experience greater Egen. This is because, as the viscosity increases, the drag force and fluid friction will also increase. Therefore, the system undergoes greater Egen. As presented in the non-dimensional form, Pr is higher for higher viscosity fluids, and therefore, fluids with a higher Pr have higher Egen.

The thermal gradient and frictional behavior are the internal characteristics of any thermal system. One of the most crucial external factors is the external magnetic field. With the application of the external magnetic field, the charged particles, nanoparticles, and dipoles present in the fluid try to align themselves with the magnetic field line. Therefore, the convection current is suppressed, which reduces the irreversibility associated with the flow. Thus, Egen decreases. Since Ha represents the magnetic field strength in its non-dimensional form, the higher Ha, the lower the Egen. Through the analysis of such internal and external factors, the present article lays the foundation for future research directions. To make it more comprehensive, the present article discusses the spatial and temporal orientation of the flow system, different dimensional and non-dimensional parameters, different methods and algorithms to solve the problems numerically, and the type of meshing to reach an optimum solution with reasonable accuracy. Such a comprehensive review and its meticulous categorization contribute to its novelty and possess great potential for future research endeavors.

7. Limitations and Future Research

In this review, more than 200 peer-reviewed articles on entropy generation and its analysis in various enclosures with diverse geometries, fluids, and boundary conditions are summarized. The field of entropy generation in enclosures has been extensively studied from the perspectives of thermodynamics, fluid mechanics, and heat transfer. While these studies have provided a thorough understanding of the latest advancements and findings in this area of study, some limitations remain. Here are some potential limitations.

- A primary limitation of these studies is their reliance on the square enclosure as a representative model for practical thermofluid systems in mathematical modeling. The walls of these enclosures are assumed to be smooth and made of homogeneous material, with completely rigid surfaces. However, these assumptions neglect various physical and geometric factors, such as surface roughness, non-homogeneous surface materials, and surface compressibility, which can compromise the model's accuracy. These factors can contribute to irreversibility in the system and significantly impact entropy generation characteristics.
- The simple mathematical model may not capture all the complex features of the system. Hence, both the qualitative and quantitative analyses may be questioned concerning their generalizability and the applicability of their findings to practical purposes.
- Conventionally, the fluid in the enclosure is assumed to have uniform thermophysical properties, and in most cases, it is also assumed to be incompressible. Furthermore, boundary conditions are often assumed to be ideal, such as perfectly insulated walls and uniform thermal diffusivity of the wall. These assumptions may introduce uncertainties in the quantification of entropy generation.
- Simulating a thermofluid system for entropy generation analysis involves a complex interplay between multiple independent variables. Uncertainty in each variable may not have the same effect on the final outcome, with some having a negligible impact and others significantly influencing the final quantification of entropy generation. To enhance confidence in the numerical analysis results, it is crucial to quantify the uncertainties. This involves evaluating the thermal system while considering uncertainties in each independent variable, including initial conditions, thermophysical properties of the system, etc., and observing how the outcome changes accordingly. However, this aspect of numerical analysis has been widely neglected in existing research.
- Most of the reviewed articles assume a single boundary condition on each wall. However, in practical cases, a boundary may have multiple conditions, including convection and radiation. Although accurately specifying such boundary conditions is challenging, most existing literature assumes that a single boundary assumes only one type of boundary condition. However, experimental and computational analyses have shown that this assumption is not always verified. This is significant since both analyses demonstrate that in such cases, radiation plays a crucial role in the thermal stratification of the system, which can affect entropy generation.
- Entropy generation is typically quantified using formulas derived for a system in thermodynamic equilibrium. However, for transient analysis, this assumption does not hold true. Hence, idealistic formulas may not capture the non-equilibrium characteristics of the system, leading to inaccuracies in the results.
- Entropy generation is the combined result of various thermophysical mechanisms, including heat transfer, fluid friction, turbulence, etc. Some studies neglect certain entropy generation mechanisms, assuming that the neglected mechanism will not significantly affect the final results. However, little to no effort is made in these articles to justify their reasoning for such simplifications. Consequently, these simplifications can lead to an incomplete assessment of overall entropy generation, resulting in a flawed understanding of the physical processes governing entropy generation in cavities.

Although significant progress has been made in characterizing entropy generation in closed conduits, future studies must consider certain limitations. These limitations include the use of inappropriate and simplistic geometries and assumptions, a lack of experimental validation, a sensitivity to uncertainty in independent variables, and the complexity of entropy generation analysis. Overcoming these limitations can improve the accuracy of the analysis and the dependability of the results, leading to a deeper understanding of entropy generation in enclosure research.

Ethical approval

It is not required for this study.

CRediT authorship contribution statement

Goutam Saha: Conceptualization, Data curation, Formal analysis, Investigation, Methodology, Resources, Supervision, Validation, Visualization, Writing – original draft, Writing – review & editing. **Ahmed A. Y. Al-Waaly:** Data curation, Formal analysis, Investigation, Methodology, Visualization, Writing – original draft, Writing – review & editing.

Maruf Md Ikram: Writing – original draft, Writing – review & editing.
Raghav Bihani: Writing – original draft, Writing – review & editing.
Suvash C. Saha: Writing – original draft, Writing – review & editing.

Declaration of competing interest

The authors declare that they have no known competing financial interests or personal relationships that could have appeared to influence the work reported in this paper.

Data availability

No data was used for the research described in the article.

Acknowledgment

We would like to acknowledge the English Language Writing Service at Michigan State University for their invaluable assistance in reviewing and refining the linguistic and syntactical aspects of our manuscript, contributing to the overall enhancement of the scholarly quality of our work.

Funding

This study is a self-funded research.

Appendix

Non-dimensional Parameters and their Physical Significance

Stefan number (*Ste*):

The Stefan number quantifies the relationship between the transfer rates of sensible heat and latent heat. In practical terms, it finds significance in characterizing phase change phenomena, notably during processes like melting and freezing [261].

$$Ste = \frac{Sensible\ Heat}{Latent\ Heat} = \frac{C_p \Delta T}{H_{fs}}$$

where C_p is the specific heat, ΔT is the temperature difference between phases, and H_{fs} is the latent heat of fusion.

Schmidt number (*Sc*):

The Schmidt number expresses the relationship between kinematic viscosity (momentum diffusivity) and mass diffusivity. In a broader context, Sc provides insight into the comparative importance of momentum and mass transport within a system. This parameter holds particular relevance when dealing with processes involving both mass and momentum transfer simultaneously, such as convection and boundary layer flows [262].

$$\mathrm{Sc} = \frac{Viscous\ Diffusion\ Rate}{Mass\ Diffusion\ Rate} = \frac{\nu}{D}$$

where, ν is the kinematic viscosity, and D is the mass diffusivity.

Sherwood number (*Sh*):

The Sherwood number represents the relationship between the rate of convective mass transfer and the rate of diffusive mass transfer. Its significance lies in measuring how effectively mass is transferred through convection compared to pure diffusion. This parameter serves as an indicator of the efficiency of convective mass transfer processes in a range of applications, such as heat exchangers, reactors, and biological systems [263].

$$Sh = \frac{Convective\ Mass\ Transfer}{Mass\ Diffusion\ rate} = \frac{K_m L_c}{D}$$

where K_m is convective mass transfer rate, D is the mass diffusivity, and L_c is characteristic length.

Reynolds number (*Re*):

Reynolds number is the ratio of inertial forces to viscous forces within a fluid. Its practical importance lies in its ability to determine whether a fluid flow exhibits laminar or turbulent behavior. In various engineering and scientific applications, Reynolds number emerges as a critical parameter, providing valuable insights into the dynamics of fluid behavior [262].

$$Re = \frac{Intertia\ Force}{Viscous\ Force} = \frac{\rho u L_c}{\mu}$$

where, u,ρ, *and*μ is respectively the velocity, density, and dynamic viscosity of the fluid, L_c is characteristic length.

Peclet number (*Pe*):

The Peclet number, characterized as the ratio between the rate of advection (convective transport) and the rate of diffusion, holds importance in discerning the relative influence of convection and diffusion in a given process. Its utility extends to predicting the prevailing mode of heat or mass transfer within a system [262].

$$Pe = \frac{Advective\ Transport\ Rate}{Mass\ Diffusion\ Rate} = \frac{u L_c}{D}$$

where u is the characteristic velocity of the fluid, L_c is a characteristic length scale, and D is the diffusion coefficient of the substance being transported.

Marangoni number (*Ma*):

The Marangoni number (*Ma*) is the dimensionless ratio of interfacial tension gradients to viscous forces. Its physical significance lies in delineating the driving force behind Marangoni convection-a phenomenon where fluid movement is triggered by fluctuations in surface tension. This parameter plays a crucial role in numerous applications, including thin-film coating, crystal growth, and microfluidics [262].

$$Ma = \frac{Surface\ Tension\ Force}{Viscous\ Force} = \frac{\Delta\sigma L_c}{\sigma\mu}$$

where Δσ represents the gradient of interfacial tension, L_c is a characteristic length scale, μ is the dynamic viscosity of the fluid, and σ is the surface tension.

Knudsen number (*Kn*):

The Knudsen number (*Kn*) is the dimensionless ratio of a gas molecule's mean free path to a characteristic length scale. Its practical importance lies in gauging the impact of rarefaction effects in gas flow, helping to discern whether the flow is situated in the continuum regime or the rarefied regime [262].

$$Kn = \frac{Molecular\ Mean\ Free\ Path}{Representative\ Physical\ Length} = \frac{\lambda}{L}$$

where λ is the molecular mean free path, and L is a characteristic length scale.

Hartmann number (*Ha*):

The Hartmann number, represented by *Ha*, gauges the interplay between electromagnetic and viscous forces within a moving electrically conductive fluid. This dimensionless parameter holds notable importance in magnetohydrodynamics (MHD) applications like liquid metal cooling and magnetic levitation, delineating the effects of an external magnetic field on fluid behavior [264].

$$Ha = \frac{Electromagnetic\ Force}{Viscous\ Force\ in\ Magneto - Hydrodyamics} = B\sqrt{\frac{\sigma\mu}{\rho\nu}}$$

where, B is the strength of the applied magnetic field, σ is the electrical conductivity of the fluid, μ is the magnetic permeability of the fluid, ρ is the density of the fluid, ν is the kinematic viscosity of the fluid.

Rayleigh number (*Ra*):

The Rayleigh number (*Ra*) assesses the balance between buoyancy and viscous forces within a fluid. Its practical importance lies in predicting the occurrence of natural convection driven by density fluctuations in the fluid. Ra is a crucial parameter for understanding heat transfer processes in a range of systems, including thermal plumes, natural convection in enclosures, and the design of heat exchangers [265].

$$Ra = \frac{Buyoancy\ Force}{Viscous\ Force} = \frac{g\beta\Delta TL^3}{\nu\alpha}$$

where g is the acceleration due to gravity, β is the coefficient of volume expansion, ΔT is the temperature difference across the fluid, L is a characteristic length scale, ν is the kinematic viscosity of the fluid, and α is the thermal diffusivity of the fluid.

Prandtl number (*Pr*):

The Prandtl number signifies the ratio of momentum diffusivity to thermal diffusivity within a fluid. In practical terms, *Pr* elucidates how momentum and thermal diffusion rates compare in a fluid [262].

$$Pr = \frac{\text{Momentum Diffusivity}}{\text{Thermal Diffusivity}} = \frac{\nu}{\alpha}$$

where ν is the kinematic viscosity of the fluid, α is the thermal diffusivity of the fluid.

Darcy number (*Da*):

The Darcy number (*Da*) represents the relationship between the permeability of a porous medium and the square of the characteristic length scale. In a practical context, *Da* serves as a measure of the resistance encountered by fluid flow in a porous medium. Its utility extends to the examination of fluid flow in various porous media scenarios, including applications such as filtration, groundwater flow, and petroleum reservoir engineering [266].

$$Da = \frac{K}{L^2}$$

where K is the permeability of the medium, L is the length.

Lewis number (*Le*):

The Lewis number (*Le*) denotes the relationship between thermal diffusivity and mass diffusivity. In a practical context, *Le* provides a measure of the relative rates at which heat and mass are transported within a system. This parameter holds significance across various applications, such as combustion, evaporation, and drying processes [262].

$$Le = \frac{\alpha}{D}$$

where α is the thermal diffusivity of the fluid, and D is the mass diffusivity of the fluid.

Eckert number (*Ec*):

The Eckert number (*Ec*) represents the ratio of a fluid's kinetic energy to the enthalpy difference. In a practical context, *Ec* serves as a measure of the importance of viscous dissipation in a flow. Its relevance is particularly pronounced in high-speed flows, where it plays a crucial role in determining the temperature increase due to friction [262].

$$Ec = \frac{Kinetic\ energy}{Enthalpy\ Difference} = \frac{\kappa_E}{(C_p\ \Delta T)}$$

where κ_E is the kinetic energy, C_p is the specific heat at constant pressure, ΔT is the temperature difference.

Soret number (*Sr*):

The Soret number, denoted as *Sr*, expresses the proportion of the thermos-diffusion coefficient to the mass diffusivity. The Soret number specifically refers to the phenomenon of thermophoresis, where a component in a mixture migrates due to a temperature gradient [267].

$$Sr = \frac{Thermal\ Diffusivity}{Mass\ Diffusivity} = \frac{\alpha}{D}$$

where α is the thermal diffusivity, and *D* is the mass diffusivity.

Dufour number (*Du*):

The Dufour number (*Du*) is defined as the ratio of thermal diffusion flux to mass diffusion flux. *Du* characterizes the heat diffusion arising from concentration gradients, playing a crucial role in diverse applications such as combustion, drying, and gas separation processes [267].

$$Du = \frac{D_T}{D}$$

where D_T is the thermal diffusion coefficient, *D* is the mass diffusion coefficient.

Bingham number (*Bn*):

The Bingham number quantifies the ratio between a fluid's yield stress and its viscous stress. Its physical significance lies in describing the non-Newtonian behavior exhibited by Bingham plastic fluids. Essentially, it serves as a determinant to ascertain whether the fluid will undergo flow or maintain a stationary state in the presence of a given shear stress [268].

$$Bn = \frac{\tau_o L_c}{\mu u}$$

where, τ_0 is the yield stress, L_c is the characteristic length, μ is the dynamic viscosity, and $u$is the velocity of the fluid.

References

[1] A.K. Hussein, K. Lioua, R. Chand, S. Sivasankaran, R. Nikbakhti, D. Li, B. M. Naceur, B.A. Habib, Three-dimensional unsteady natural convection and entropy generation in an inclined cubical trapezoidal cavity with an isothermal bottom wall, Alexandria Engineering Journal 55 (2) (2016) 741–755, https://doi.org/10.1016/j.aej.2016.01.004.

[2] C.-C. Cho, H.-T. Yau, C.-H. Chiu, K.-C. Chiu, Numerical investigation into natural convection and entropy generation in a nanofluid-filled U-shaped cavity, Entropy 17 (9) (2015) 5980–5994, https://doi.org/10.3390/e17095980.

[3] K. Chang, G. Constantinescu, S.-O. Park, Analysis of the flow and mass transfer processes for the incompressible flow past an open cavity with a laminar and a fully turbulent incoming boundary layer, Journal of Fluid Mechanics 561 (2006) 113–145, https://doi.org/10.1017/S0022112006000735.

[4] R. Ellahi, S.M. Sait, N. Shehzad, Z. Ayaz, A hybrid investigation on numerical and analytical solutions of electro-magnetohydrodynamics flow of nanofluid through porous media with entropy generation, International Journal of Numerical Methods for Heat & Fluid Flow 30 (2) (2020) 834–854, https://doi.org/10.1108/HFF-06-2019-0506.

[5] M. Salari, E.H. Malekshah, M.H. Malekshah, Three-dimensional numerical analysis of the natural convection and entropy generation of MWCNTs-H_2O and air as two immiscible fluids in a rectangular cuboid with fillet corners, Numerical Heat Transfer. Part A, Applications 71 (8) (2017) 881–894, https://doi.org/10.1080/10407782.2017.1309213.

[6] M.A. Sheremet, H.F. Oztop, I. Pop, N. Abu-Hamdeh, Analysis of entropy generation in natural convection of nanofluid inside a square cavity having hot solid block: Tiwari and das' model, Entropy 18 (1) (2016) 9, https://doi.org/10.3390/e18010009. –9.

[7] F. Selimefendigil, H.F. Öztop, Natural convection and entropy generation of nanofluid filled cavity having different shaped obstacles under the influence of magnetic field and internal heat generation, Journal of the Taiwan Institute of Chemical Engineers 56 (2015) 42–56, https://doi.org/10.1016/j.jtice.2015.04.018.

[8] A. Chamkha, M. Ismael, A. Kasaeipoor, T. Armaghani, Entropy generation and natural convection of CuO-water nanofluid in C-shaped cavity under magnetic field, Entropy 18 (2) (2016) 50, https://doi.org/10.3390/e18020050.

[9] R. Parveen, T.R. Mahapatra, Numerical simulation of MHD double diffusive natural convection and entropy generation in a wavy enclosure filled with nanofluid with discrete heating, Heliyon 5 (9) (2019) e02496, https://doi.org/10.1016/j.heliyon.2019.e02496. –e02496.

[10] A. Rahimi, A. Kasaeipoor, E.H. Malekshah, L. Kolsi, Natural convection analysis by entropy generation and heatline visualization using lattice Boltzmann method in nanofluid filled cavity included with internal heaters- Empirical thermo-physical properties, International Journal of Mechanical Sciences 133 (2017) 199–216, https://doi.org/10.1016/j.ijmecsci.2017.08.044.

[11] A. Ahlawat, M.K. Sharma, Effects of heated block comprised porous stratum and micropolar hybrid nanofluid on convective heat transfer and entropy generation in a square enclosure, Heat Transfer 51 (6) (2022) 5320–5347, https://doi.org/10.1002/htj.22549.

[12] M. Alipanah, A.A. Ranjbar, E. Farnad, F. Alipanah, Entropy Generation of Natural Convection Heat Transfer in a Square Cavity Using Al_2O_3-Water Nanofluid, Heat Transfer, Asian Research 44 (7) (2015) 641–656, https://doi.org/10.1002/htj.21141.

[13] T.V. Morosuk, Entropy generation in conduits filled with porous medium totally and partially, International Journal of Heat and Mass Transfer 48 (12) (2005) 2548–2560, https://doi.org/10.1016/j.ijheatmasstransfer.2005.01.018.

[14] O. Çiçek, A.F. Baytaş, A.C. Baytaş, Entropy generation of mixed convection of SWCNT–water nanofluid filled an annulus with a rotating cylinder and porous lining under LTNE, International Journal of Numerical Methods for Heat & Fluid Flow 31 (5) (2021) 1588–1617, https://doi.org/10.1108/HFF-04-2020-0229.

[15] L. El Moutaouakil, M. Boukendil, Z. Zrikem, A. Abdelbaki, Natural convection and thermal radiation influence on nanofluids in a cubical cavity, Heat and Technology 38 (1) (2020) 59–68, https://doi.org/10.18280/ijht.380107.

[16] M.S. Ishak, A.I. Alsabery, A. Chamkha, I. Hashim, Effect of finite wall thickness on entropy generation and natural convection in a nanofluid-filled partially heated square cavity, International Journal of Numerical Methods for Heat & Fluid Flow 30 (3) (2020) 1518–1546, https://doi.org/10.1108/HFF-06-2019-0505.

[17] A. Abderrahmane, N.A.A. Qasem, O. Younis, R. Marzouki, A. Mourad, N.A. Shah, J.D. Chung, MHD hybrid nanofluid mixed convection heat transfer and entropy generation in a 3-d triangular porous cavity with zigzag wall and rotating cylinder, Mathematics 10 (5) (2022) 769, https://doi.org/10.3390/math10050769.

[18] S. Marzougui, F. Mebarek-Oudina, M. Magherbi, A. Mchirgui, Entropy generation and heat transport of Cu–water nanoliquid in porous lid-driven cavity through magnetic field, International Journal of Numerical Methods for Heat & Fluid Flow 32 (6) (2022) 2047–2069, https://doi.org/10.1108/HFF-04-2021-0288.

[19] O.D. Makinde, Second law analysis for variable viscosity hydromagnetic boundary layer flow with thermal radiation and Newtonian heating, Entropy 13 (8) (2011) 1446–1464, https://doi.org/10.3390/e13081446.

[20] A.K. Hussein, M.A. Mahdi, O. Younis, Numerical Simulation of Entropy Generation of Conjugate Heat Transfer in A Porous Cavity with Finite Walls and Localized Heat Source, Journal of Advanced Research in Fluid Mechanics and Thermal Sciences 84 (2) (2021) 116–151, https://doi.org/10.37934/arfmts.84.2.116151.

[21] A. Zaib, M.M. Rashidi, A.J. Chamkha, K. Bhattacharyya, Numerical solution of second law analysis for MHD Casson nanofluid past a wedge with activation energy and binary chemical reaction, International Journal of Numerical Methods for Heat & Fluid Flow 27 (12) (2017) 2816–2834, https://doi.org/10.1108/HFF-02-2017-0063.

[22] P. Sreedevi, P.S. Reddy, Entropy generation and heat transfer analysis of alumina and carbon nanotubes based hybrid nanofluid inside a cavity, Physica Scripta 96 (8) (2021) 85210, https://doi.org/10.1088/1402-4896/ac0077. –.
[23] A.H. Mahmoudi, I. Pop, M. Shahi, Effect of magnetic field on natural convection in a triangular enclosure filled with nanofluid, International Journal of Thermal Sciences 59 (2012) 126–140, https://doi.org/10.1016/j.ijthermalsci.2012.04.006.
[24] M.A. Mansour, S.E. Ahmed, A.J. Chamkha, Entropy generation optimization for MHD natural convection of a nanofluid in porous media-filled enclosure with active parts and viscous dissipation, International Journal of Numerical Methods for Heat & Fluid Flow 27 (2) (2017) 379–399, https://doi.org/10.1108/HFF-10-2015-0408.
[25] E. Belahmadi, R. Bessaïh, MHD heat transfer and entropy production of an Al_2O_3-water nanofluid in a horizontal cylinder, Heat Transfer 50 (5) (2021) 4892–4907, https://doi.org/10.1002/htj.22108.
[26] S. Hussain, K. Mehmood, M. Sagheer, MHD mixed convection and entropy generation of water–alumina nanofluid flow in a double lid-driven cavity with discrete heating, Journal of Magnetism and Magnetic Materials 419 (2016) 140–155, https://doi.org/10.1016/j.jmmm.2016.06.006.
[27] S. Mahmud, R.A. Fraser, Magnetohydrodynamic free convection and entropy generation in a square porous cavity, International Journal of Heat and Mass Transfer 47 (14) (2004) 3245–3256, https://doi.org/10.1016/j.ijheatmasstransfer.2004.02.005.
[28] C. Sivaraj, M.A. Sheremet, MHD natural convection and entropy generation of ferrofluids in a cavity with a non-uniformly heated horizontal plate, International Journal of Mechanical Sciences 149 (2018) 326–337, https://doi.org/10.1016/j.ijmecsci.2018.10.017.
[29] A. Kumar, R. Kothari, S.K. Sahu, S.I. Kundalwal, M.P. Paulraj, Numerical investigation of cross plate fin heat sink integrated with phase change material for cooling application of portable electronic devices, International Journal of Energy Research 45 (6) (2021) 8666–8683, https://doi.org/10.1002/er.6404.
[30] E. Macdonald, R. Salas, D. Espalin, M. Perez, E. Aguilera, D. Muse, R.B. Wicker, 3D Printing for the Rapid Prototyping of Structural Electronics, IEEE Access 2 (2014) 234–242, https://doi.org/10.1109/ACCESS.2014.2311810.
[31] M. Lin, K. Sumathy, Y.J. Dai, X.K. Zhao, Performance investigation on a linear Fresnel lens solar collector using cavity receiver, Solar Energy 107 (2014) 50–62, https://doi.org/10.1016/j.solener.2014.05.026.
[32] S. Taller, G. VanCoevering, B.D. Wirth, G.S. Was, Predicting structural material degradation in advanced nuclear reactors with ion irradiation, Scientific Reports 11 (1) (2021) 2949, https://doi.org/10.1038/s41598-021-82512-w. –2949.
[33] H. Li, Y. Li, B. Huang, T. Xu, Numerical investigation on the optimum thermal design of the shape and geometric parameters of microchannel heat exchangers with cavities, Micromachines 11 (8) (2020) 721, https://doi.org/10.3390/MI11080721.
[34] D. Rauch, M. Dietrich, T. Simons, U. Simon, A. Porch, R. Moos, Microwave Cavity Perturbation Studies on H-form and Cu Ion-Exchanged SCR Catalyst Materials: Correlation of Ammonia Storage and Dielectric Properties, Topics in Catalysis 60 (3-5) (2017) 243–249, https://doi.org/10.1007/s11244-016-0605-z.
[35] M.S. Hossain, J.A. Gonzalez, R.M. Hernandez, M.A.I. Shuvo, J. Mireles, A. Choudhuri, Y. Lin, R.B. Wicker, Fabrication of smart parts using powder bed fusion additive manufacturing technology, Additive Manufacturing 10 (2016) 58–66, https://doi.org/10.1016/j.addma.2016.01.001.
[36] G. Saha, A.A.Y. Al-Waaly, M.C. Paul, S.C. Saha, Heat Transfer in Cavities: Configurative Systematic Review, Energies 16 (5) (2023) 2338, https://doi.org/10.3390/en16052338.
[37] N. Acharya, On the hydrothermal behavior and entropy analysis of buoyancy driven magnetohydrodynamic hybrid nanofluid flow within an octagonal enclosure fitted with fins: Application to thermal energy storage, Journal of Energy Storage 53 (2022) 105198, https://doi.org/10.1016/j.est.2022.105198.
[38] S.E. Ahmed, Z.A.S. Raizah, Analysis of the entropy due to radiative flow of nano–encapsulated phase change materials within inclined porous prismatic enclosures: Finite element simulation, Journal of Energy Storage 40 (2021) 102719, https://doi.org/10.1016/j.est.2021.102719.
[39] S.E. Ahmed, M.A. Mansour, A. Mahdy, Analysis of Natural Convection–Radiation Interaction Flow in a Porous Cavity with Al2O3–Cu Water Hybrid Nanofluid: Entropy Generation, Arabian Journal for Science and Engineering 47 (12) (2022) 15245–15259, https://doi.org/10.1007/s13369-021-06495-6.
[40] A.I. Alsabery, A.I. Alsabery, I. Hashim, A. Hajjar, M.S. Pour, Entropy generation and natural convection flow of hybrid nanofluids in a partially divided wavy cavity including solid blocks, Energies 13 (11) (2020) 2942, https://doi.org/10.3390/en13112942.
[41] A.I. Alsabery, M.A. Ismael, A.J. Chamkha, I. Hashim, Numerical investigation of mixed convection and entropy generation in a wavy-walled cavity filled with nanofluid and involving a rotating cylinder, Entropy 20 (9) (2018) 664, https://doi.org/10.3390/e20090664.
[42] A.I. Alsabery, T. Tayebi, R. Roslan, A.J. Chamkha, I. Hashim, Entropy generation and mixed convection flow inside a wavy-walled enclosure containing a rotating solid cylinder and a heat source, Entropy 22 (6) (2020) 606, https://doi.org/10.3390/E22060606.
[43] R. Anandalakshmi, T. Basak, Natural convection in rhombic enclosures with isothermally heated side or bottom wall: Entropy generation analysis, European Journal of Mechanics, B, Fluids 54 (2015) 27–44, https://doi.org/10.1016/j.euromechflu.2015.05.004.
[44] S. Arun, A. Satheesh, Mesoscopic analysis of MHD double diffusive natural convection and entropy generation in an enclosure filled with liquid metal, Journal of the Taiwan Institute of Chemical Engineers 95 (2019) 155–173, https://doi.org/10.1016/j.jtice.2018.10.015.
[45] S. Bhardwaj, A. Dalal, S. Pati, Influence of wavy wall and non-uniform heating on natural convection heat transfer and entropy generation inside porous complex enclosure, Energy 79 (2015) 467–481, https://doi.org/10.1016/j.energy.2014.11.036. C.
[46] P. Biswal, T. Basak, Entropy generation based approach on natural convection in enclosures with concave/convex side walls, International Journal of Heat and Mass Transfer 82 (2015) 213–235, https://doi.org/10.1016/j.ijheatmasstransfer.2014.10.036.
[47] P. Biswal, T. Basak, Role of thermal and flow characteristics on entropy generation during natural convection in porous enclosures with curved walls subjected to Rayleigh-Bénard heating, International Journal of Heat and Mass Transfer 109 (2017) 1261–1280, https://doi.org/10.1016/j.ijheatmasstransfer.2017.01.118.
[48] P. Biswal, A. Nag, T. Basak, Analysis of thermal management during natural convection within porous tilted square cavities via heatline and entropy generation, International Journal of Mechanical Sciences 115-116 (2016) 596–615, https://doi.org/10.1016/j.ijmecsci.2016.07.011.
[49] Z. Boulahia, A Detailed Numerical Investigation for Various Types of Entropy Generation and Magnetohydrodynamic (MHD) Free Convection within a Corrugated Cavity Comprising Nanofluid and a Hot Object Positioned in the Middle, International Journal of Applied and Computational Mathematics 7 (6) (2021), https://doi.org/10.1007/s40819-021-01146-8.
[50] Z. Boulahia, C. Boulahia, R. Sehaqui, Two-phase computation of free convection and entropy generation inside an enclosure filled by a hybrid Al_2O_3-TiO_2-Cu water nanofluid having a corrugated heat source using the generalized Buongiorno's mathematical model: Employment of finite volume method, Materials Today : Proceedings 30 (2020) 1056–1067, https://doi.org/10.1016/j.matpr.2020.05.523.
[51] D. Das, T. Basak, Thermal management investigation on fluid processing within porous rhombic cavities: Heatlines versus entropy generation, Canadian Journal of Chemical Engineering 95 (7) (2017) 1399–1416, https://doi.org/10.1002/cjce.22771.
[52] D. Das, T. Basak, Role of distributed/discrete solar heaters for the entropy generation studies in the square and triangular cavities during natural convection, Applied Thermal Engineering 113 (2017) 1514–1535, https://doi.org/10.1016/j.applthermaleng.2016.11.042.
[53] D. Das, L. Lukose, T. Basak, Role of multiple discrete heaters to minimize entropy generation during natural convection in fluid filled square and triangular enclosures, International Journal of Heat and Mass Transfer 127 (2018) 1290–1312, https://doi.org/10.1016/j.ijheatmasstransfer.2018.05.163.
[54] M. Ghalambaz, S.A.M. Mehryan, M. Mozaffari, A. Hajjar, M. El Kadri, N. Rachedi, M. Sheremet, O. Younis, S. Nadeem, Entropy generation and natural convection flow of a suspension containing nano-encapsulated phase change particles in a semi-annular cavity, Journal of Energy Storage 32 (2020) 101834, https://doi.org/10.1016/j.est.2020.101834.
[55] K. Ghasemi, M. Siavashi, Lattice Boltzmann numerical simulation and entropy generation analysis of natural convection of nanofluid in a porous cavity with different linear temperature distributions on side walls, Journal of Molecular Liquids 233 (2017) 415–430, https://doi.org/10.1016/j.molliq.2017.03.016.
[56] N.S. Gibanov, M.A. Sheremet, H.F. Oztop, K Al-Salem, MHD natural convection and entropy generation in an open cavity having different horizontal porous blocks saturated with a ferrofluid, Journal of Magnetism and Magnetic Materials 452 (2018) 193–204, https://doi.org/10.1016/j.jmmm.2017.12.075.
[57] H. Hamzah, C. Canpolat, L.M. Jasim, B. Sahin, Hydrothermal index and entropy generation of a heated cylinder placed between two oppositely rotating cylinders in a vented cavity, International Journal of Mechanical Sciences 201 (2021) 106465, https://doi.org/10.1016/j.ijmecsci.2021.106465. –.
[58] S.H. Hussain, Analysis of heatlines and entropy generation during double-diffusive MHD natural convection within a tilted sinusoidal corrugated porous enclosure, Engineering Science and Technology, an International Journal 19 (2) (2016) 926–945, https://doi.org/10.1016/j.jestch.2015.12.001.
[59] G.G. Ilis, M. Mobedi, B. Sunden, Effect of aspect ratio on entropy generation in a rectangular cavity with differentially heated vertical walls, International Communications in Heat and Mass Transfer 35 (6) (2008) 696–703, https://doi.org/10.1016/j.icheatmasstransfer.2008.02.002.
[60] M.S. Ishak, A.I. Alsabery, I. Hashim, A.J. Chamkha, Entropy production and mixed convection within trapezoidal cavity having nanofluids and localised solid cylinder, Scientific Reports 11 (1) (2021) 14700, https://doi.org/10.1038/s41598-021-94238-w. –14700.
[61] D. Kavya, D. Das, T. Basak, Analysis of thermal management on processing of fluids within rhombic cavities: Heatlines vs. entropy generation, Journal of the Taiwan Institute of Chemical Engineers 68 (2016) 301–322, https://doi.org/10.1016/j.jtice.2016.09.014.
[62] G.H.R. Kefayati, Heat transfer and entropy generation of natural convection on non-Newtonian nanofluids in a porous cavity, Powder Technology 299 (2016) 127–149, https://doi.org/10.1016/j.powtec.2016.05.032.
[63] G.H.R. Kefayati, Simulation of natural convection and entropy generation of non-Newtonian nanofluid in a porous cavity using Buongiorno's mathematical model, International Journal of Heat and Mass Transfer 112 (2017) 709–744, https://doi.org/10.1016/j.ijheatmasstransfer.2017.04.121.
[64] G.H.R. Kefayati, Double-diffusive natural convection and entropy generation of Bingham fluid in an inclined cavity, International Journal of Heat and Mass Transfer 116 (2018) 762–812, https://doi.org/10.1016/j.ijheatmasstransfer.2017.09.065.

[65] G.H.R. Kefayati, H. Tang, Simulation of natural convection and entropy generation of MHD non-Newtonian nanofluid in a cavity using Buongiorno's mathematical model, International Journal of Hydrogen Energy 42 (27) (2017) 17284–17327, https://doi.org/10.1016/j.ijhydene.2017.05.093.
[66] G.R. Kefayati, FDLBM simulation of entropy generation due to natural convection in an enclosure filled with non-Newtonian nanofluid, Powder Technology 273 (2015) 176–190, https://doi.org/10.1016/j.powtec.2014.12.042.
[67] G.R. Kefayati, FDLBM simulation of entropy generation in double diffusive natural convection of power-law fluids in an enclosure with Soret and Dufour effects, International Journal of Heat and Mass Transfer 89 (2015) 267–290, https://doi.org/10.1016/j.ijheatmasstransfer.2015.05.058.
[68] G.R. Kefayati, Simulation of heat transfer and entropy generation of MHD natural convection of non-Newtonian nanofluid in an enclosure, International Journal of Heat and Mass Transfer 92 (2016) 1066–1089, https://doi.org/10.1016/j.ijheatmasstransfer.2015.09.078.
[69] G.R. Kefayati, H. Tang, Mesoscopic simulation of double-diffusive natural convection and entropy generation of Bingham fluid in an open cavity, European Journal of Mechanics, B, Fluids 69 (2018) 1–45, https://doi.org/10.1016/j.euromechflu.2018.01.002.
[70] P.A.K. Lam, K. Arul Prakash, A numerical study on natural convection and entropy generation in a porous enclosure with heat sources, International Journal of Heat and Mass Transfer 69 (2014) 390–407, https://doi.org/10.1016/j.ijheatmasstransfer.2013.10.009.
[71] S.A.M. Mehryan, M. Izadi, A.J. Chamkha, M.A. Sheremet, Natural convection and entropy generation of a ferrofluid in a square enclosure under the effect of a horizontal periodic magnetic field, Journal of Molecular Liquids 263 (2018) 510–525, https://doi.org/10.1016/j.molliq.2018.04.119.
[72] D. Ramakrishna, T. Basak, S. Roy, E. Momoniat, Analysis of thermal efficiency via analysis of heat flow and entropy generation during natural convection within porous trapezoidal cavities, International Journal of Heat and Mass Transfer 77 (2014) 98–113, https://doi.org/10.1016/j.ijheatmasstransfer.2014.04.002.
[73] B. Sahin, Effects of the center of linear heating position on natural convection and entropy generation in a linearly heated square cavity, International Communications in Heat and Mass Transfer 117 (2020) 104675, https://doi.org/10.1016/j.icheatmasstransfer.2020.104675.
[74] B. Şahin, Numerical analysis of entropy generation in a square cavity filled with boron-water nanofluid, Journal of the Brazilian Society of Mechanical Sciences and Engineering 42 (3) (2020), https://doi.org/10.1007/s40430-020-2214-9.
[75] A. Shahriari, H.R. Ashorynejad, I. Pop, Entropy generation of MHD nanofluid inside an inclined wavy cavity by lattice Boltzmann method, Journal of Thermal Analysis and Calorimetry 135 (1) (2019) 283–303, https://doi.org/10.1007/s10973-018-7061-x.
[76] A.K. Singh, T. Basak, A. Nag, S. Roy, Role of entropy generation on thermal management during natural convection in tilted porous square cavities, Journal of the Taiwan Institute of Chemical Engineers 50 (2015) 153–172, https://doi.org/10.1016/j.jtice.2014.12.026.
[77] A.K. Singh, S. Roy, T. Basak, E. Momoniat, Role of Entropy Generation On Thermal Management During Natural Convection in a Tilted Square Cavity with Isothermal and Non-Isothermal Hot Walls, Numerical Heat Transfer. Part A, Applications 66 (11) (2014) 1243–1267, https://doi.org/10.1080/10407782.2014.892402.
[78] S. Taghizadeh, A. Asaditaheri, Heat transfer and entropy generation of laminar mixed convection in an inclined lid driven enclosure with a circular porous cylinder, International Journal of Thermal Sciences 134 (2018) 242–257, https://doi.org/10.1016/j.ijthermalsci.2018.08.018.
[79] D. Zhang, H. Peng, X. Ling, Lattice Boltzmann method for thermomagnetic convection and entropy generation of paramagnetic fluid in porous enclosure under magnetic quadrupole field, International Journal of Heat and Mass Transfer 127 (2018) 224–236, https://doi.org/10.1016/j.ijheatmasstransfer.2018.07.004.
[80] T. Basak, A.K. Singh, T.P.A. Sruthi, S. Roy, Finite element simulations on heat flow visualization and entropy generation during natural convection in inclined square cavities, International Communications in Heat and Mass Transfer 51 (2014) 1–8, https://doi.org/10.1016/j.icheatmasstransfer.2013.11.009.
[81] W.M. El-Maghlany, K.M. Saqr, M.A. Teamah, Numerical simulations of the effect of an isotropic heat field on the entropy generation due to natural convection in a square cavity, Energy Conversion and Management 85 (2014) 333–342, https://doi.org/10.1016/j.enconman.2014.05.093.
[82] M.A. Ismael, T. Armaghani, A.J. Chamkha, Conjugate heat transfer and entropy generation in a cavity filled with a nanofluid-saturated porous media and heated by a triangular solid, Journal of the Taiwan Institute of Chemical Engineers 59 (2016) 138–151, https://doi.org/10.1016/j.jtice.2015.09.012.
[83] H.R. Ashorynejad, B. Hoseinpour, Investigation of different nanofluids effect on entropy generation on natural convection in a porous cavity, European Journal of Mechanics, B, Fluids 62 (2017) 86–93, https://doi.org/10.1016/j.euromechflu.2016.11.016.
[84] A.el malik Bouchoucha, R. Bessaïh, H.F. Oztop, K. Al-Salem, F Bayrak, Natural convection and entropy generation in a nanofluid filled cavity with thick bottom wall: Effects of non-isothermal heating, International Journal of Mechanical Sciences 126 (2017) 95–105, https://doi.org/10.1016/j.ijmecsci.2017.03.025.
[85] M. Siavashi, V. Bordbar, P. Rahnama, Heat transfer and entropy generation study of non-Darcy double-diffusive natural convection in inclined porous enclosures with different source configurations, Applied Thermal Engineering 110 (2017) 1462–1475, https://doi.org/10.1016/j.applthermaleng.2016.09.060.
[86] M.A. Sheremet, T. Grosan, I. Pop, Natural convection and entropy generation in a square cavity with variable temperature side walls filled with a nanofluid: Buongiorno's mathematical model, Entropy 19 (7) (2017) 337, https://doi.org/10.3390/e19070337.
[87] A.I. Alsabery, M.S. Ishak, A.J. Chamkha, I. Hashim, Entropy generation analysis and natural convection in a nanofluid-filled square cavity with a concentric solid insert and different temperature distributions, Entropy 20 (5) (2018) 336, https://doi.org/10.3390/e20050336.
[88] D. Kashyap, A.K. Dass, Two-phase lattice Boltzmann simulation of natural convection in a Cu-water nanofluid-filled porous cavity: Effects of thermal boundary conditions on heat transfer and entropy generation, Advanced Powder Technology : the International Journal of the Society of Powder Technology, Japan 29 (11) (2018) 2707–2724, https://doi.org/10.1016/j.apt.2018.07.020.
[89] A. Rahimi, A. Kasaeipoor, E.H. Malekshah, M. Palizian, L. Kolsi, Lattice Boltzmann numerical method for natural convection and entropy generation in cavity with refrigerant rigid body filled with DWCNTs-water nanofluid-experimental thermo-physical properties, Thermal Science and Engineering Progress 5 (2018) 372–387, https://doi.org/10.1016/j.tsep.2018.01.005.
[90] M. Siavashi, R. Yousofvand, S. Rezanejad, Nanofluid and porous fins effect on natural convection and entropy generation of flow inside a cavity, Advanced Powder Technology: the International Journal of the Society of Powder Technology, Japan 29 (1) (2018) 142–156, https://doi.org/10.1016/j.apt.2017.10.021.
[91] W. Al-Kouz, A. Al-Muhtady, W. Owhaib, S. Al-Dahidi, M. Hader, R. Abu-Alghanam, Entropy generation optimization for rarified nanofluid flows in a square cavity with two fins at the hot wall, Entropy 21 (2) (2019) 103, https://doi.org/10.3390/e21020103.
[92] S. Baghsaz, S. Rezanejad, M. Moghimi, Numerical investigation of transient natural convection and entropy generation analysis in a porous cavity filled with nanofluid considering nanoparticles sedimentation, Journal of Molecular Liquids 279 (2019) 327–341, https://doi.org/10.1016/j.molliq.2019.01.117.
[93] X. Zhou, Y. Jiang, X. Li, K. Cheng, X. Huai, X. Zhang, H. Huang, Numerical investigation of heat transfer enhancement and entropy generation of natural convection in a cavity containing nano liquid-metal fluid, International Communications in Heat and Mass Transfer 106 (2019) 46–54, https://doi.org/10.1016/j.icheatmasstransfer.2019.05.003.
[94] P. Gokulavani, M. Muthtamilselvan, B. Abdalla, Impact of injection/suction and entropy generation of the porous open cavity with the hybrid nanofluid, Journal of Thermal Analysis and Calorimetry 147 (4) (2022) 3299–3312, https://doi.org/10.1007/s10973-021-10636-2.
[95] A. Mahmoudi, I. Mejri, M.A. Abbassi, A. Omri, Analysis of the entropy generation in a nanofluid-filled cavity in the presence of magnetic field and uniform heat generation/absorption, Journal of Molecular Liquids 198 (2014) 63–77, https://doi.org/10.1016/j.molliq.2014.07.010.
[96] I. Mejri, A. Mahmoudi, M.A. Abbassi, A. Omri, Magnetic field effect on entropy generation in a nanofluid-filled enclosure with sinusoidal heating on both side walls, Powder Technology 266 (2014) 340–353, https://doi.org/10.1016/j.powtec.2014.06.054.
[97] M. Mamourian, K. Milani Shirvan, I. Pop, Sensitivity analysis for MHD effects and inclination angles on natural convection heat transfer and entropy generation of Al2O3-water nanofluid in square cavity by Response Surface Methodology, International Communications in Heat and Mass Transfer 79 (2016) 46–57, https://doi.org/10.1016/j.icheatmasstransfer.2016.10.001.
[98] A.J. Ahrar, M.H. Djavareshkian, Novel hybrid lattice Boltzmann technique with TVD characteristics for simulation of heat transfer and entropy generations of MHD and natural convection in a cavity, Numerical Heat Transfer. Part B, Fundamentals 72 (6) (2017) 431–449, https://doi.org/10.1080/10407790.2017.1409528.
[99] N.S. Gibanov, M.A. Sheremet, H.F. Oztop, K Al-Salem, Effect of uniform inclined magnetic field on natural convection and entropy generation in an open cavity having a horizontal porous layer saturated with a ferrofluid, Numerical Heat Transfer. Part A, Applications 72 (6) (2017) 479–494, https://doi.org/10.1080/10407782.2017.1386515.
[100] K. Ghasemi, M. Siavashi, MHD nanofluid free convection and entropy generation in porous enclosures with different conductivity ratios, Journal of Magnetism and Magnetic Materials 442 (2017) 474–490, https://doi.org/10.1016/j.jmmm.2017.07.028.
[101] S. Malik, A.K. Nayak, MHD convection and entropy generation of nanofluid in a porous enclosure with sinusoidal heating, International Journal of Heat and Mass Transfer 111 (2017) 329–345, https://doi.org/10.1016/j.ijheatmasstransfer.2017.03.123.
[102] M. Mohammadpourfard, H. Aminfar, S. Ahangar Zonouzi, Numerical Investigation of the Magnetic Field Effects on the Entropy Generation and Heat Transfer in a Nanofluid Filled Cavity with Natural Convection, Heat Transfer, Asian Research 46 (5) (2017) 409–433, https://doi.org/10.1002/htj.21222.
[103] N.S. Gibanov, M.A. Sheremet, H.F. Oztop, N. Abu-Hamdeh, Mixed convection with entropy generation of nanofluid in a lid-driven cavity under the effects of a heat-conducting solid wall and vertical temperature gradient, European Journal of Mechanics, B, Fluids 70 (2018) 148–159, https://doi.org/10.1016/j.euromechflu.2018.03.002.
[104] M.A. Mansour, S. Siddiqa, R.S.R. Gorla, A.M. Rashad, Effects of heat source and sink on entropy generation and MHD natural convection of Al_2O_3-Cu/water hybrid nanofluid filled with square porous cavity, Thermal Science and Engineering Progress 6 (2018) 57–71, https://doi.org/10.1016/j.tsep.2017.10.014.
[105] A.M. Rashad, T. Armaghani, A.J. Chamkha, M.A. Mansour, Entropy generation and MHD natural convection of a nanofluid in an inclined square porous cavity:

Effects of a heat sink and source size and location, Chinese Journal of Physics 56 (1) (2018) 193–211, https://doi.org/10.1016/j.cjph.2017.11.026.
[106] A.J. Ahrar, M.H. Djavareshkian, A.R. Ahrar, Numerical simulation of Al2O3-water nanofluid heat transfer and entropy generation in a cavity using a novel TVD hybrid LB method under the influence of an external magnetic field source, Thermal Science and Engineering Progress 14 (2019) 100416, https://doi.org/10.1016/j.tsep.2019.100416.
[107] A.A.A.A. Al-Rashed, Investigating the effect of alumina nanoparticles on heat transfer and entropy generation inside a square enclosure equipped with two inclined blades under magnetic field, International Journal of Mechanical Sciences 152 (2019) 312–328, https://doi.org/10.1016/j.ijmecsci.2019.01.008.
[108] A.A. Alnaqi, S. Aghakhani, A.H. Pordanjani, R. Bakhtiari, A. Asadi, M.-D. Tran, Effects of magnetic field on the convective heat transfer rate and entropy generation of a nanofluid in an inclined square cavity equipped with a conductor fin: Considering the radiation effect, International Journal of Heat and Mass Transfer 133 (2019) 256–267, https://doi.org/10.1016/j.ijheatmasstransfer.2018.12.110.
[109] A.I. Alsabery, R. Mohebbi, A.J. Chamkha, I. Hashim, Impacts of magnetic field and non-homogeneous nanofluid model on convective heat transfer and entropy generation in a cavity with heated trapezoidal body, Journal of Thermal Analysis and Calorimetry 138 (2) (2019) 1371–1394, https://doi.org/10.1007/s10973-019-08249-x.
[110] S.P. Goqo, H. Mondal, P. Sibanda, S.S. Motsa, A multivariate spectral quasilinearisation method for entropy generation in a square cavity filled with porous medium saturated by nanofluid, Case Studies in Thermal Engineering 14 (2019) 100415, https://doi.org/10.1016/j.csite.2019.100415.
[111] A. Hajatzadeh Pordanjani, S. Aghakhani, A.A. Alnaqi, M. Afrand, Effect of alumina nano-powder on the convection and the entropy generation of water inside an inclined square cavity subjected to a magnetic field: Uniform and non-uniform temperature boundary conditions, International Journal of Mechanical Sciences 152 (2019) 99–117, https://doi.org/10.1016/j.ijmecsci.2018.12.030.
[112] K.S. Al Kalbani, M.M. Rahman, M. Ziad Saghir, Entropy generation in hydromagnetic nanofluids flow inside a tilted square enclosure under local thermal nonequilibrium condition, International Journal of Thermofluids 5-6 (2020) 100031, https://doi.org/10.1016/j.ijft.2020.100031.
[113] Y. Li, M. Firouzi, A. Karimipour, M. Afrand, Effect of an inclined partition with constant thermal conductivity on natural convection and entropy generation of a nanofluid under magnetic field inside an inclined enclosure: Applicable for electronic cooling, Advanced Powder Technology : the International Journal of the Society of Powder Technology, Japan 31 (2) (2020) 645–657, https://doi.org/10.1016/j.apt.2019.11.020.
[114] Z. Li, A.K. Hussein, O. Younis, M. Afrand, S. Feng, Natural convection and entropy generation of a nanofluid around a circular baffle inside an inclined square cavity under thermal radiation and magnetic field effects, International Communications in Heat and Mass Transfer 116 (2020) 104650, https://doi.org/10.1016/j.icheatmasstransfer.2020.104650. –.
[115] K.M. Rabbi, M. Sheikholeslami, A. Karim, A. Shafee, Z. Li, I. Tlili, Prediction of MHD flow and entropy generation by Artificial Neural Network in square cavity with heater-sink for nanomaterial, Physica A 541 (2020) 123520, https://doi.org/10.1016/j.physa.2019.123520.
[116] F. Selimefendigil, H.F. Öztop, Effects of conductive curved partition and magnetic field on natural convection and entropy generation in an inclined cavity filled with nanofluid, Physica A 540 (2020) 123004, https://doi.org/10.1016/j.physa.2019.123004.
[117] S.M. Seyyedi, A.S. Dogonchi, M. Hashemi-Tilehnoee, M. Waqas, D.D. Ganji, Investigation of entropy generation in a square inclined cavity using control volume finite element method with aided quadratic Lagrange interpolation functions, International Communications in Heat and Mass Transfer 110 (2020) 104398, https://doi.org/10.1016/j.icheatmasstransfer.2019.104398.
[118] T. Tayebi, A.J. Chamkha, Entropy generation analysis due to MHD natural convection flow in a cavity occupied with hybrid nanofluid and equipped with a conducting hollow cylinder, Journal of Thermal Analysis and Calorimetry 139 (3) (2020) 2165–2179, https://doi.org/10.1007/s10973-019-08651-5.
[119] Y. Khetib, A.A. Alahmadi, A. Alzaed, H. Azimy, M. Sharifpur, G. Cheraghian, Effect of straight, inclined and curved fins on natural convection and entropy generation of a nanofluid in a square cavity influenced by a magnetic field, Processes 9 (8) (2021) 1339, https://doi.org/10.3390/pr9081339.
[120] S.P. Reddy, P. Sreedevi, Entropy generation and heat transfer analysis of magnetic hybrid nanofluid inside a square cavity with thermal radiation, European Physical Journal Plus 136 (1) (2021), https://doi.org/10.1140/epjp/s13360-020-01025-z.
[121] Z. Tian, A. Shahsavar, A.A.A.A. Al-Rashed, S. Rostami, Numerical simulation of nanofluid convective heat transfer in an oblique cavity with conductive edges equipped with a constant temperature heat source: Entropy production analysis, Computers & Mathematics with Applications 81 (1) (2021) 725–736, https://doi.org/10.1016/j.camwa.2019.12.007.
[122] P.S. Reddy, P. Sreedevi, Effect of thermal radiation on heat transfer and entropy generation analysis of MHD hybrid nanofluid inside a square cavity, Waves in Random and Complex Media (2022) 1–33, https://doi.org/10.1080/17455030.2021.2023780.
[123] P.B.A. Reddy, T. Salah, S. Jakeer, M.A. Mansour, A.M. Rashad, Entropy generation due to magneto-natural convection in a square enclosure with heated corners saturated porous medium using Cu/water nanofluid, Chinese Journal of Physics 77 (2022) 1863–1884, https://doi.org/10.1016/j.cjph.2022.01.012.
[124] P.S. Reddy, P. Sreedevi, V.N. Reddy, Entropy generation and heat transfer analysis of magnetic nanofluid flow inside a square cavity filled with carbon nanotubes, Chemical Thermodynamics and Thermal Analysis 6 (2022) 100045, https://doi.org/10.1016/j.ctta.2022.100045.
[125] M.A. Shah, K. Pan, M. Ibrahim, T. Saeed, Use of neural network and machine learning in optimizing heat transfer and entropy generated in a cavity filled with nanofluid under the influence of magnetic field: A numerical study, Engineering Analysis with Boundary Elements 139 (2022) 113–131, https://doi.org/10.1016/j.enganabound.2022.03.012.
[126] R. Akhter, M. Mokaddes Ali, M.A. Alim, Entropy generation due to hydromagnetic buoyancy-driven hybrid-nanofluid flow in partially heated porous cavity containing heat conductive obstacle, Alexandria Engineering Journal 62 (2023) 17–45, https://doi.org/10.1016/j.aej.2022.07.005.
[127] S. Bilal, I.A. Ali Shah, S. Marzougui, F Ali, Entropy analysis in single phase nanofluid in square enclosure under effectiveness of inclined magnetic field by executing finite element simulations, Geoenergy Science and Engineering (2023) 211483, https://doi.org/10.1016/j.geoen.2023.211483.
[128] V. Kumar, S.V.S.S.N.V.G.K. Murthy, B.V.R. Kumar, Multi-force effect on fluid flow, heat and mass transfer, and entropy generation in a stratified fluid-saturated porous enclosure, Mathematics and Computers in Simulation 203 (2023) 328–367, https://doi.org/10.1016/j.matcom.2022.06.025.
[129] A.I. Alsabery, F. Selimefendigil, I. Hashim, A.J. Chamkha, M. Ghalambaz, Fluid-structure interaction analysis of entropy generation and mixed convection inside a cavity with flexible right wall and heated rotating cylinder, International Journal of Heat and Mass Transfer 140 (2019) 331–345, https://doi.org/10.1016/j.ijheatmasstransfer.2019.06.003.
[130] A. Hajatzadeh Pordanjani, S. Aghakhani, A. Karimipour, M. Afrand, M. Goodarzi, Investigation of free convection heat transfer and entropy generation of nanofluid flow inside a cavity affected by magnetic field and thermal radiation, Journal of Thermal Analysis and Calorimetry 137 (3) (2019) 997–1019, https://doi.org/10.1007/s10973-018-7982-4.
[131] F. Selimefendigil, H.F. Oztop, Mixed convection and entropy generation of nanofluid flow in a vented cavity under the influence of inclined magnetic field. Microsystem Technologies : Sensors, Actuators, Systems Integration 25 (12) (2019) 4427–4438, https://doi.org/10.1007/s00542-019-04350-1.
[132] A.I. Alsabery, E. Gedik, A.J. Chamkha, I. Hashim, Impacts of heated rotating inner cylinder and two-phase nanofluid model on entropy generation and mixed convection in a square cavity, Heat and Mass Transfer 56 (1) (2020) 321–338, https://doi.org/10.1007/s00231-019-02698-8.
[133] D. Kashyap, A.K. Dass, H.F. Oztop, N. Abu-Hamdeh, Multiple-relaxation-time lattice Boltzmann analysis of entropy generation in a hot-block-inserted square cavity for different Prandtl numbers, International Journal of Thermal Sciences 165 (2021) 106948, https://doi.org/10.1016/j.ijthermalsci.2021.106948. –.
[134] O. Çiçek, A.C. Baytaş, A numerical investigation of the particle behaviors and entropy generation in mixed convection inside a vented enclosure, International Journal of Thermal Sciences 185 (2023) 108058, https://doi.org/10.1016/j.ijthermalsci.2022.108058.
[135] F. Selimefendigil, H.F. Öztop, MHD mixed convection and entropy generation of power law fluids in a cavity with a partial heater under the effect of a rotating cylinder, International Journal of Heat and Mass Transfer 98 (2016) 40–51, https://doi.org/10.1016/j.ijheatmasstransfer.2016.02.092.
[136] T. Wang, Z. Huang, G. Xi, Entropy generation for mixed convection in a square cavity containing a rotating circular cylinder using a local radial basis function method, International Journal of Heat and Mass Transfer 106 (2017) 1063–1073, https://doi.org/10.1016/j.ijheatmasstransfer.2016.10.082.
[137] G.R. Kefayati, H. Tang, MHD thermosolutal natural convection and entropy generation of Carreau fluid in a heated enclosure with two inner circular cold cylinders, using LBM, International Journal of Heat and Mass Transfer 126 (2018) 508–530, https://doi.org/10.1016/j.ijheatmasstransfer.2018.06.026.
[138] G.R. Kefayati, H. Tang, Double-diffusive laminar natural convection and entropy generation of Carreau fluid in a heated enclosure with an inner circular cold cylinder (Part II: Entropy generation), International Journal of Heat and Mass Transfer 120 (2018) 683–713, https://doi.org/10.1016/j.ijheatmasstransfer.2017.12.081.
[139] M. Vahabzadeh Bozorg, M. Siavashi, Two-phase mixed convection heat transfer and entropy generation analysis of a non-Newtonian nanofluid inside a cavity with internal rotating heater and cooler, International Journal of Mechanical Sciences 151 (2019) 842–857, https://doi.org/10.1016/j.ijmecsci.2018.12.036.
[140] B. Iftikhar, T. Javed, M.A. Siddiqu, Entropy generation analysis during MHD mixed convection flow of non-Newtonian fluid saturated inside the square cavity, Journal of Computational Science 66 (2023) 101907, https://doi.org/10.1016/j.jocs.2022.101907.
[141] K.M. Shirvan, S. Mirzakhanlari, A.J. Chamkha, M. Mamourian, Numerical simulation and sensitivity analysis of effective parameters on natural convection and entropy generation in a wavy surface cavity filled with a nanofluid using RSM, Numerical Heat Transfer. Part A, Applications 70 (10) (2016) 1157–1177, https://doi.org/10.1080/10407782.2016.1230396.
[142] A.J. Chamkha, F. Selimefendigil, MHD free convection and entropy generation in a corrugated cavity filled with a porous medium saturated with nanofluids, Entropy 20 (11) (2018) 846, https://doi.org/10.3390/e20110846.
[143] S.K. Pal, S. Bhattacharyya, I. Pop, Effect of solid-to-fluid conductivity ratio on mixed convection and entropy generation of a nanofluid in a lid-driven enclosure with a thick wavy wall, International Journal of Heat and Mass Transfer 127 (2018) 885–900, https://doi.org/10.1016/j.ijheatmasstransfer.2018.06.078.
[144] A.I. Alsabery, M.A. Ismael, A.J. Chamkha, I. Hashim, Impact of finite wavy wall thickness on entropy generation and natural convection of nanofluid in cavity partially filled with non-Darcy porous layer, Neural Computing & Applications 32 (17) (2020) 13679–13699, https://doi.org/10.1007/s00521-020-04776-z.

[145] B.P. Geridonmez, H.F. Oztop, Entropy generation due to magneto-convection of a hybrid nanofluid in the presence of a wavy conducting wall, Mathematics 10 (24) (2022) 4663, https://doi.org/10.3390/math10244663.

[146] A.I. Alsabery, T. Tayebi, A.J. Chamkha, I. Hashim, Effect of rotating solid cylinder on entropy generation and convective heat transfer in a wavy porous cavity heated from below, International Communications in Heat and Mass Transfer 95 (2018) 197–209, https://doi.org/10.1016/j.icheatmasstransfer.2018.05.003.

[147] C.-C. Cho, Heat transfer and entropy generation of mixed convection flow in Cu-water nanofluid-filled lid-driven cavity with wavy surface, International Journal of Heat and Mass Transfer 119 (2018) 163–174, https://doi.org/10.1016/j.ijheatmasstransfer.2017.11.090.

[148] A. Chattopadhyay, S.K. Pandit, H.F. Oztop, An analysis of thermal performance and entropy generation in a wavy enclosure with moving walls, European Journal of Mechanics, B, Fluids 79 (2020) 12–26, https://doi.org/10.1016/j.euromechflu.2019.08.006.

[149] S. Afsana, M.M. Molla, P. Nag, L.K. Saha, S. Siddiqa, MHD natural convection and entropy generation of non-Newtonian ferrofluid in a wavy enclosure, International Journal of Mechanical Sciences 198 (2021) 106350, https://doi.org/10.1016/j.ijmecsci.2021.106350.

[150] A. Abderrahmane, O. Younis, H. Sh. Majdi, K. Guedri, W. Jamshed, S.S.P.M. Isa, R. Marzouki, S Baghaei, Exploration of Ostwald-de Waele non-Newtonian nanofluid subject to Lorentz force, and entropy optimization in a corrugated porous medium enclosure: Galerkin finite element analysis, Journal of Magnetism and Magnetic Materials 562 (2022) 169834, https://doi.org/10.1016/j.jmmm.2022.169834. –.

[151] S. Hussain, S. Shoeibi, T. Armaghani, Impact of magnetic field and entropy generation of Casson fluid on double diffusive natural convection in staggered cavity, International Communications in Heat and Mass Transfer 127 (2021) 105520, https://doi.org/10.1016/j.icheatmasstransfer.2021.105520.

[152] G. Rasool, A.M. Saeed, A.I. Lare, A. Abderrahmane, K. Guedri, H. Vaidya, R. Marzouki, Darcy-Forchheimer flow of water conveying multi-walled carbon nanoparticles through a vertical cleveland Z-staggered cavity subject to entropy generation, Micromachines 13 (5) (2022) 744, https://doi.org/10.3390/mi13050744.

[153] V.M. Rathnam, P. Biswal, T. Basak, Analysis of entropy generation during natural convection within entrapped porous triangular cavities during hot or cold fluid disposal, Numerical Heat Transfer. Part A, Applications 69 (9) (2016) 931–956, https://doi.org/10.1080/10407782.2015.1109362.

[154] F. Selimefendigil, H.F. Öztop, A.J. Chamkha, MHD mixed convection and entropy generation of nanofluid filled lid driven cavity under the influence of inclined magnetic fields imposed to its upper and lower diagonal triangular domains, Journal of Magnetism and Magnetic Materials 406 (2016) 266–281, https://doi.org/10.1016/j.jmmm.2016.01.039.

[155] N.S. Bondareva, M.A. Sheremet, H.F. Oztop, N. Abu-Hamdeh, Entropy generation due to natural convection of a nanofluid in a partially open triangular cavity, Advanced Powder Technology : the International Journal of the Society of Powder Technology, Japan 28 (1) (2017) 244–255, https://doi.org/10.1016/j.apt.2016.09.030.

[156] M. Roy, S. Roy, T. Basak, Role of moving horizontal walls on entropy generation during mixed convection within entrapped triangular cavities, International Communications in Heat and Mass Transfer 85 (2017) 92–99, https://doi.org/10.1016/j.icheatmasstransfer.2017.04.011.

[157] M. Roy, P. Biswal, S. Roy, T. Basak, Role of various moving walls on entropy generation during mixed convection within entrapped porous triangular cavities, Numerical Heat Transfer. Part A, Applications 71 (4) (2017) 423–447, https://doi.org/10.1080/10407782.2016.1277927.

[158] A.J. Chamkha, F. Selimefendigil, H.F. Oztop, MHD mixed convection and entropy generation in a lid-driven triangular cavity for various electrical conductivity models, Entropy 20 (12) (2018) 903, https://doi.org/10.3390/e20120903.

[159] W. Liu, A. Shahsavar, A.A. Barzinjy, A.A.A.A. Al-Rashed, M. Afrand, Natural convection and entropy generation of a nanofluid in two connected inclined triangular enclosures under magnetic field effects, International Communications in Heat and Mass Transfer 108 (2019) 104309, https://doi.org/10.1016/j.icheatmasstransfer.2019.104309.

[160] F. Selimefendigil, H.F. Oztop, A.J. Chamkha, Analysis of mixed convection and entropy generation of nanofluid filled triangular enclosure with a flexible sidewall under the influence of a rotating cylinder, Journal of Thermal Analysis and Calorimetry 135 (2) (2019) 911–923, https://doi.org/10.1007/s10973-018-7317-5.

[161] M. Afrand, A.H. Pordanjani, S. Aghakhani, H.F. Oztop, N. Abu-Hamdeh, Free convection and entropy generation of a nanofluid in a tilted triangular cavity exposed to a magnetic field with sinusoidal wall temperature distribution considering radiation effects, International Communications in Heat and Mass Transfer 112 (2020) 104507, https://doi.org/10.1016/j.icheatmasstransfer.2020.104507.

[162] Z. Li, A. Shahsavar, K. Niazi, A.A.A.A. Al-Rashed, P. Talebizadehsardari, The effects of vertical and horizontal sources on heat transfer and entropy generation in an inclined triangular enclosure filled with non-Newtonian fluid and subjected to magnetic field, Powder Technology 364 (2020) 924–942, https://doi.org/10.1016/j.powtec.2019.10.076.

[163] A. Aghaei, H. Khorasanizadeh, G. Sheikhzadeh, M. Abbaszadeh, Numerical study of magnetic field on mixed convection and entropy generation of nanofluid in a trapezoidal enclosure, Journal of Magnetism and Magnetic Materials 403 (2016) 133–145, https://doi.org/10.1016/j.jmmm.2015.11.067.

[164] F. Selimefendigil, H.F. Öztop, N. Abu-Hamdeh, Natural convection and entropy generation in nanofluid filled entrapped trapezoidal cavities under the influence of magnetic field, Entropy 18 (2) (2016) 43, https://doi.org/10.3390/e18020043.

[165] M.S. Astanina, M.A. Sheremet, H.F. Oztop, N. Abu-Hamdeh, MHD natural convection and entropy generation of ferrofluid in an open trapezoidal cavity partially filled with a porous medium, International Journal of Mechanical Sciences 136 (2018) 493–502, https://doi.org/10.1016/j.ijmecsci.2018.01.001.

[166] H. F. Mebarek-Oudina, R. Fares, A. Aissa, R.W. Lewis, N. Abu-Hamdeh, Entropy and convection effect on magnetized hybrid nano-liquid flow inside a trapezoidal cavity with zigzagged wall International Communications in Heat and Mass Transfer 125 (2021) 105279 https://doi.org/10.1016/j.icheatmasstransfer.2021.105279.

[167] P. Mondal, T.R. Mahapatra, MHD double-diffusive mixed convection and entropy generation of nanofluid in a trapezoidal cavity, International Journal of Mechanical Sciences 208 (2021) 106665, https://doi.org/10.1016/j.ijmecsci.2021.106665. –.

[168] P. Mondal, T.R. Mahapatra, R. Parveen, Entropy generation in nanofluid flow due to double diffusive MHD mixed convection, Heliyon 7 (3) (2021) e06143, https://doi.org/10.1016/j.heliyon.2021.e06143. –e06143.

[169] T. Mahapatra, B.C. Saha, D. Pal, S.K. Pandit, Analysis of Heatline and Entropy Generation during Magnetohydrodynamic Natural Convection in a Trapezoidal Enclosure, International Journal of Applied and Computational Mathematics 8 (6) (2022), https://doi.org/10.1007/s40819-022-01473-4.

[170] M.S. Shuvo, M.H. Hasib, S. Saha, Entropy generation and characteristics of mixed convection in lid-driven trapezoidal tilted enclosure filled with nanofluid, Heliyon 8 (12) (2022), https://doi.org/10.1016/j.heliyon.2022.e12079 e12079–e12079.

[171] A.M. Zidan, T. Tayebi, A. Sattar Dogonchi, A.J. Chamkha, M.B. Ben Hamida, A. M. Galal, Entropy-based analysis and economic scrutiny of magneto thermal natural convection enhancement in a nanofluid-filled porous trapezium-shaped cavity having localized baffles, Waves in Random and Complex Media (2022) 1–21, https://doi.org/10.1080/17455030.2022.2084651.

[172] A.S.M. Aljaloud, Hybrid nanofluid mixed convection in a cavity under the impact of the magnetic field by lattice Boltzmann method: Effects of barrier temperature on heat transfer and entropy, Engineering Analysis with Boundary Elements 147 (2023) 276–291, https://doi.org/10.1016/j.enganabound.2022.12.007.

[173] M. Roy, S. Roy, T. Basak, Analysis of entropy generation on mixed convection in square enclosures for various horizontal or vertical moving wall(s), International Communications in Heat and Mass Transfer 68 (2015) 258–266, https://doi.org/10.1016/j.icheatmasstransfer.2015.08.023.

[174] M. Roy, T. Basak, S. Roy, Analysis of entropy generation during mixed convection in porous square cavities: Effect of thermal boundary conditions, Numerical Heat Transfer. Part A, Applications 68 (9) (2015) 925–957, https://doi.org/10.1080/10407782.2015.1023134.

[175] M. Roy, T. Basak, S. Roy, I. Pop, Analysis of entropy generation for mixed convection in a square cavity for various thermal boundary conditions, Numerical Heat Transfer. Part A, Applications 68 (1) (2015) 44–74, https://doi.org/10.1080/10407782.2014.955352.

[176] R. Bouabda, M. Bouabid, A.B. Brahim, M. Magherbi, Numerical study of entropy generation in mixed MHD convection in a square lid-driven cavity filled with Darcy-Brinkman-Forchheimer porous medium, Entropy 18 (12) (2016) 436, https://doi.org/10.3390/e18120436. –436.

[177] M. Roy, S. Roy, T. Basak, Analysis of entropy generation for mixed convection within porous square cavities: Effects of various moving walls, Numerical Heat Transfer. Part A 70 (7) (2016) 738–762, https://doi.org/10.1080/10407782.2016.1193354.

[178] S. Hussain, K. Mehmood, M. Sagheer, M. Yamin, Numerical simulation of double diffusive mixed convective nanofluid flow and entropy generation in a square porous enclosure, International Journal of Heat and Mass Transfer 122 (2018) 1283–1297, https://doi.org/10.1016/j.ijheatmasstransfer.2018.02.082.

[179] P. Barnoon, D. Toghraie, R.B. Dehkordi, H. Abed, MHD mixed convection and entropy generation in a lid-driven cavity with rotating cylinders filled by a nanofluid using two phase mixture model, Journal of Magnetism and Magnetic Materials 483 (2019) 224–248, https://doi.org/10.1016/j.jmmm.2019.03.108.

[180] D. Kashyap, A.K. Dass, Effect of boundary conditions on heat transfer and entropy generation during two-phase mixed convection hybrid Al.sub.2O.sub.3-Cu/water nanofluid flow in a cavity, International Journal of Mechanical Sciences 157 (2019) 45, https://doi.org/10.1016/j.ijmecsci.2019.04.014.

[181] A. Alshare, A. Abderrahmane, K. Guedri, O. Younis, M. Fayz-Al-Asad, H.M. Ali, W. Al-Kouz, Hydrothermal and entropy investigation of nanofluid natural convection in a lid-driven cavity concentric with an elliptical cavity with a wavy boundary heated from below, Nanomaterials 12 (9) (2022) 1392, https://doi.org/10.3390/nano12091392.

[182] M. Salari, A. Rezvani, A. Mohammadtabar, M. Mohammadtabar, Numerical Study of Entropy Generation for Natural Convection in Rectangular Cavity with Circular Corners, Heat Transfer Engineering 36 (2) (2015) 186–199, https://doi.org/10.1080/01457632.2014.909221.

[183] B. Fersadou, H. Kahalerras, W. Nessab, D. Hammoudi, Effect of magnetohydrodynamics on heat transfer intensification and entropy generation of nanofluid flow inside two interacting open rectangular cavities, Journal of Thermal Analysis and Calorimetry 138 (5) (2019) 3089–3108, https://doi.org/10.1007/s10973-019-08343-0.

[184] W.M. El-Maghlany, A.A. Minea, Ionanofluids natural convection heat transfer and entropy generation in a rectangular cavity: Viscosity influence, Journal of Molecular Liquids 338 (2021) 116651, https://doi.org/10.1016/j.molliq.2021.116651. –.

[185] J.-T. Hu, S.-J. Mei, Combined thermal and moisture convection and entropy generation in an inclined rectangular enclosure partially saturated with porous

wall: Nonlinear effects with Soret and Dufour numbers, International Journal of Mechanical Sciences 199 (2021) 106412, https://doi.org/10.1016/j.ijmecsci.2021.106412.

[186] S. Alqaed, J. Mustafa, M. Sharifpur, Numerical investigation and optimization of natural convection and entropy generation of alumina/H_2O nanofluid in a rectangular cavity in the presence of a magnetic field with artificial neural networks, Engineering Analysis with Boundary Elements 140 (2022) 507–518, https://doi.org/10.1016/j.enganabound.2022.04.034.

[187] S. Kumar, K.M. Gangawane, Entropy generation study due to MHD double-diffusive convection in the rectangular cavity with built-in rectangular blockage, Numerical Heat Transfer. Part A, Applications (2023) 1–21, https://doi.org/10.1080/10407782.2022.2155738.

[188] M.A. Mansour, T. Armaghani, A.J. Chamkha, A.M. Rashad, Entropy generation and nanofluid mixed convection in a C-shaped cavity with heat corner and inclined magnetic field, The European Physical Journal 228 (12) (2019) 2619–2645, https://doi.org/10.1140/epjst/e2019-900050-3.

[189] Z. Mehrez, A. El Cafsi, A. Belghith, P. Le Quéré, MHD effects on heat transfer and entropy generation of nanofluid flow in an open cavity, Journal of Magnetism and Magnetic Materials 374 (2015) 214–224, https://doi.org/10.1016/j.jmmm.2014.08.010.

[190] Z. Mehrez, A. El Cafsi, A. Belghith, P. Le Quéré, The entropy generation analysis in the mixed convective assisting flow of Cu–water nanofluid in an inclined open cavity, Advanced Powder Technology : the International Journal of the Society of Powder Technology, Japan 26 (5) (2015) 1442–1451, https://doi.org/10.1016/j.apt.2015.07.020.

[191] S. Hussain, S.E. Ahmed, T. Akbar, Entropy generation analysis in MHD mixed convection of hybrid nanofluid in an open cavity with a horizontal channel containing an adiabatic obstacle, International Journal of Heat and Mass Transfer 114 (2017) 1054–1066, https://doi.org/10.1016/j.ijheatmasstransfer.2017.06.135.

[192] S. Hussain, K. Mehmood, M. Sagheer, A. Farooq, Entropy generation analysis of mixed convective flow in an inclined channel with cavity with Al_2O_3-water nanofluid in porous medium, International Communications in Heat and Mass Transfer 89 (2017) 198–210, https://doi.org/10.1016/j.icheatmasstransfer.2017.10.009.

[193] T. Armaghani, A. Chamkha, A.M. Rashad, M.A. Mansour, Inclined magneto: convection, internal heat, and entropy generation of nanofluid in an I-shaped cavity saturated with porous media, Journal of Thermal Analysis and Calorimetry 142 (6) (2020) 2273–2285, https://doi.org/10.1007/s10973-020-09449-6.

[194] A. Asadi, S. Rafizadeh, M. Molana, R. Ghasemiasl, T. Armaghani, Two-phase study of nanofluids mixed convection and entropy generation in an I-shaped porous cavity with triangular hot block and different aspect ratios, Mathematical Methods in the Applied Sciences (2020), https://doi.org/10.1002/mma.7006.

[195] R. Ghasemiasl, M. Molana, T. Armaghani, M.S. Pour, The effects of hot blocks geometry and particle migration on heat transfer and entropy generation of a novel I-shaped porous enclosure, Sustainability 13 (13) (2021) 7190, https://doi.org/10.3390/su13137190.

[196] T. Tayebi, A.S. Dogonchi, A.J. Chamkha, M.B. Ben Hamida, S. El-Sapa, A. M. Galal, Micropolar nanofluid thermal free convection and entropy generation through an inclined I-shaped enclosure with two hot cylinders, Case Studies in Thermal Engineering 31 (2022) 101813, https://doi.org/10.1016/j.csite.2022.101813.

[197] S. Parvin, A.J. Chamkha, An analysis on free convection flow, heat transfer and entropy generation in an odd-shaped cavity filled with nanofluid, International Communications in Heat and Mass Transfer 54 (2014) 8–17, https://doi.org/10.1016/j.icheatmasstransfer.2014.02.031.

[198] A. Rahimi, A. Kasaeipoor, E.H. Malekshah, A. Amiri, Natural convection analysis employing entropy generation and heatline visualization in a hollow L-shaped cavity filled with nanofluid using lattice Boltzmann method- experimental thermo-physical properties, Physica. E, Low-Dimensional Systems & Nanostructures 97 (2018) 82–97, https://doi.org/10.1016/j.physe.2017.10.004.

[199] A.J. Chamkha, G. Jomardiani, M.A. Ismael, R. Ghasemiasl, T. Armaghani, Thermal and entropy analysis in L-shaped non-Darcian porous cavity saturated with nanofluids using Buongiorno model: Comparative study, Mathematical Methods in the Applied Sciences (2020), https://doi.org/10.1002/mma.6797.

[200] S.M. Seyyedi, A.S. Dogonchi, M. Hashemi-Tilehnoee, M. Waqas, D.D. Ganji, Entropy generation and economic analyses in a nanofluid filled L-shaped enclosure subjected to an oriented magnetic field, Applied Thermal Engineering 168 (2020) 114789, https://doi.org/10.1016/j.applthermaleng.2019.114789.

[201] R. Zhang, S. Aghakhani, A. Hajatzadeh Pordanjani, S.M. Vahedi, A. Shahsavar, M. Afrand, Investigation of the entropy generation during natural convection of Newtonian and non-Newtonian fluids inside the L-shaped cavity subjected to magnetic field: application of lattice Boltzmann method, European Physical Journal Plus 135 (2) (2020), https://doi.org/10.1140/epjp/s13360-020-00169-2.

[202] M. Ghalambaz, S.M.H. Zadeh, A. Veismoradi, M.A. Sheremet, I. Pop, Free convection heat transfer and entropy generation in an odd-shaped cavity filled with a Cu-Al_2O_3 hybrid nanofluid, Symmetry 13 (1) (2021) 1–17, https://doi.org/10.3390/sym13010122.

[203] S. Hussain, M.S. Pour, M. Jamal, T. Armaghani, MHD Mixed Convection and Entropy Analysis of Non-Newtonian Hybrid Nanofluid in a Novel Wavy Elbow-Shaped Cavity with a Quarter Circle Hot Block and a Rotating Cylinder, Experimental Techniques 47 (1) (2023) 17–36, https://doi.org/10.1007/s40799-022-00549-6.

[204] M. Mohammadtabar, F. Mohammadtabar, R. Shokri, M. Sadrzadeh, Numerical Investigation of the Entropy Generation Due to Natural Convection in a Partially Heated Square Cavity Filled With Nanofluids, Heat Transfer Engineering 38 (17) (2017) 1506–1521, https://doi.org/10.1080/01457632.2016.1255092.

[205] S. Marzougui, F. Mebarek-Oudina, A. Assia, M. Magherbi, Z. Shah, K. Ramesh, Entropy generation on magneto-convective flow of copper–water nanofluid in a cavity with chamfers, Journal of Thermal Analysis and Calorimetry 143 (3) (2021) 2203–2214, https://doi.org/10.1007/s10973-020-09662-3.

[206] Ç. Yıldız, A.E. Yıldız, M. Arıcı, N.A. Azmi, A. Shahsavar, Influence of dome shape on flow structure, natural convection and entropy generation in enclosures at different inclinations: A comparative study, International Journal of Mechanical Sciences 197 (2021) 106321, https://doi.org/10.1016/j.ijmecsci.2021.106321.

[207] N. Rehman, R. Mahmood, A. Hussain Majeed, K. Ur Rehman, W. Shatanawi, Finite element analysis on entropy generation in MHD Iron(III) Oxide-Water NanoFluid equipped in partially heated fillet cavity, Journal of Magnetism and Magnetic Materials 565 (2023) 170269, https://doi.org/10.1016/j.jmmm.2022.170269.

[208] A.H. Majeed, R. Mahmood, H. Shahzad, A.A. Pasha, N. Islam, M.M. Rahman, Numerical simulation of thermal flows and entropy generation of magnetized hybrid nanomaterials filled in a hexagonal cavity, Case Studies in Thermal Engineering 39 (2022) 102293, https://doi.org/10.1016/j.csite.2022.102293.

[209] R.K. Nayak, S. Bhattacharyya, I. Pop, Numerical study on mixed convection and entropy generation of Cu–water nanofluid in a differentially heated skewed enclosure, International Journal of Heat and Mass Transfer 85 (2015) 620–634, https://doi.org/10.1016/j.ijheatmasstransfer.2015.01.116.

[210] R.K. Nayak, S. Bhattacharyya, I. Pop, Heat transfer and entropy generation in mixed convection of a nanofluid within an inclined skewed cavity, International Journal of Heat and Mass Transfer 102 (2016) 596–609, https://doi.org/10.1016/j.ijheatmasstransfer.2016.06.049.

[211] S. Dutta, A.K. Biswas, S. Pati, Numerical analysis of natural convection heat transfer and entropy generation in a porous quadrantal cavity, International Journal of Numerical Methods for Heat & Fluid Flow 29 (12) (2019) 4826–4849, https://doi.org/10.1108/HFF-11-2018-0678.

[212] S. Dutta, N. Goswami, A.K. Biswas, S. Pati, Numerical investigation of magnetohydrodynamic natural convection heat transfer and entropy generation in a rhombic enclosure filled with Cu-water nanofluid, International Journal of Heat and Mass Transfer 136 (2019) 777–798, https://doi.org/10.1016/j.ijheatmasstransfer.2019.03.024.

[213] S. Mojumder, K.M. Rabbi, S. Saha, M. Hasan, S.C. Saha, Magnetic field effect on natural convection and entropy generation in a half-moon shaped cavity with semi-circular bottom heater having different ferrofluid inside, Journal of Magnetism and Magnetic Materials 407 (2016) 412–424, https://doi.org/10.1016/j.jmmm.2016.01.046.

[214] S. Bezi, B. Souayeh, N. Ben-Cheikh, B. Ben-Beya, Numerical simulation of entropy generation due to unsteady natural convection in a semi-annular enclosure filled with nanofluid, International Journal of Heat and Mass Transfer 124 (2018) 841–859, https://doi.org/10.1016/j.ijheatmasstransfer.2018.03.109.

[215] A. Shafee, R.U. Haq, M. Sheikholeslami, J.A. Ali Herki, T.K. Nguyen, An entropy generation analysis for MHD water based Fe3O4 ferrofluid through a porous semi annulus cavity via CVFEM, International Communications in Heat and Mass Transfer 108 (2019) 104295, https://doi.org/10.1016/j.icheatmasstransfer.2019.104295.

[216] S.R. Afshar, S.R. Mishra, A.S. Dogonchi, N. Karimi, A.J. Chamkha, H. Abulkhair, Dissection of entropy production for the free convection of NEPCMs-filled porous wavy enclosure subject to volumetric heat source/sink, Journal of the Taiwan Institute of Chemical Engineers 128 (2021) 98–113, https://doi.org/10.1016/j.jtice.2021.09.006.

[217] F. Selimefendigil, H.F. Öztop, M. Sheikholeslami, Impact of local elasticity and inner rotating circular cylinder on the magneto-hydrodynamics forced convection and entropy generation of nanofluid in a U-shaped vented cavity, Mathematical Methods in the Applied Sciences (2020), https://doi.org/10.1002/mma.6930.

[218] A.A. Pasha, M.K. Nayak, K. Irshad, M.M. Alam, A.S. Dogonchi, A.J. Chamkha, A. M. Galal, Entropy and hydrothermal analyses of nano-encapsulated phase change materials within a U-shaped enclosure: Impact of diverse structures of baffles and corrugated wall, Journal of Energy Storage 59 (2023) 106532, https://doi.org/10.1016/j.est.2022.106532.

[219] L. Kolsi, A.K. Hussein, M.N. Borjini, H.A. Mohammed, H.B. Aïssia, Computational Analysis of Three-Dimensional Unsteady Natural Convection and Entropy Generation in a Cubical Enclosure Filled with Water-Al2O3 Nanofluid, Arabian Journal for Science and Engineering 39 (11) (2014) 7483–7493, https://doi.org/10.1007/s13369-014-1341-y.

[220] L. Kolsi, H.F. Oztop, N. Abu-Hamdeh, A. Alghamdi, M. Naceur Borjini, Three dimensional analysis of natural convection and entropy generation in a sharp edged finned cavity, Alexandria Engineering Journal 55 (2) (2016) 991–1004, https://doi.org/10.1016/j.aej.2016.02.030.

[221] L. Kolsi, K. Kalidasan, A. Alghamdi, M.N. Borjini, P.R. Kanna, Natural convection and entropy generation in a cubical cavity with twin adiabatic blocks filled by aluminum oxide-water nanofluid, Numerical Heat Transfer. Part A, Applications 70 (3) (2016) 242–259, https://doi.org/10.1080/10407782.2016.1173478.

[222] L. Kolsi, H.F. Oztop, A. Alghamdi, N. Abu-Hamdeh, M.N. Borjini, H.B. Aissia, A computational work on a three dimensional analysis of natural convection and entropy generation in nanofluid filled enclosures with triangular solid insert at the corners, Journal of Molecular Liquids 218 (2016) 260–274, https://doi.org/10.1016/j.molliq.2016.02.083.

[223] L. Kolsi, E. Lajnef, W. Aich, A. Alghamdi, M. Ahmed Aichouni, M.N. Borjini, H. Ben Aissia, Numerical investigation of combined buoyancy-thermocapillary convection and entropy generation in 3D cavity filled with Al2O3 nanofluid,

Alexandria Engineering Journal 56 (1) (2017) 71–79, https://doi.org/10.1016/j.aej.2016.09.005.

[224] A.A.A.A. Al-Rashed, W. Aich, L. Kolsi, O. Mahian, A.K. Hussein, M.N. Borjini, Effects of movable-baffle on heat transfer and entropy generation in a cavity saturated by CNT suspensions: Three-dimensional modeling, Entropy 19 (5) (2017) 200, https://doi.org/10.3390/e19050200.

[225] A.A.A.A. Al-Rashed, L. Kolsi, A.K. Hussein, W. Hassen, M. Aichouni, M.N. Borjini, Numerical study of three-dimensional natural convection and entropy generation in a cubical cavity with partially active vertical walls, Case Studies in Thermal Engineering 10 (C) (2017) 100–110, https://doi.org/10.1016/j.csite.2017.05.003.

[226] H.F. Oztop, L. Kolsi, A. Alghamdi, N. Abu-Hamdeh, M.N. Borjini, H. Ben Aissia, Numerical analysis of entropy generation due to natural convection in three-dimensional partially open enclosures, Journal of the Taiwan Institute of Chemical Engineers 75 (2017) 131–140, https://doi.org/10.1016/j.jtice.2017.03.014.

[227] M. Salari, E. Hasani Malekshah, M. Hasani Malekshah, M. Alavi, R. Hajihashemi, 3D numerical analysis of natural convection and entropy generation within tilted rectangular enclosures filled with stratified fluids of MWCNTs/water nanofluid and air, Journal of the Taiwan Institute of Chemical Engineers 80 (2017) 624–638, https://doi.org/10.1016/j.jtice.2017.08.041.

[228] A.A.A.A. Al-Rashed, K. Kalidasan, L. Kolsi, R. Velkennedy, A. Aydi, A.K. Hussein, E.H. Malekshah, Mixed convection and entropy generation in a nanofluid filled cubical open cavity with a central isothermal block, International Journal of Mechanical Sciences 135 (2018) 362–375, https://doi.org/10.1016/j.ijmecsci.2017.11.033.

[229] A.K. Hussein, Entropy generation due to the transient mixed convection in a three- dimensional right-angle triangular cavity, International Journal of Mechanical Sciences 146-147 (2018) 141–151, https://doi.org/10.1016/j.ijmecsci.2018.07.012.

[230] A. Rahimi, A. Kasaeipoor, A. Amiri, M.H. Doranehgard, E.H. Malekshah, L. Kolsi, Lattice Boltzmann method based on Dual-MRT model for three-dimensional natural convection and entropy generation in CuO–water nanofluid filled cuboid enclosure included with discrete active walls, Computers & Mathematics with Applications 75 (5) (2018) 1795–1813, https://doi.org/10.1016/j.camwa.2017.11.037.

[231] A.Z. Al-Khazaal, Effects of composite material fin conductivity on natural convection heat transfer and entropy generation inside 3D cavity filled with hybrid nanofluid, Journal of Thermal Analysis and Calorimetry 147 (5) (2022) 3709–3720, https://doi.org/10.1007/s10973-021-10737-y.

[232] S. Banik, A.S. Mirja, N. Biswas, R. Ganguly, Entropy analysis during heat dissipation via thermomagnetic convection in a ferrofluid-filled enclosure, International Communications in Heat and Mass Transfer 138 (2022) 106323, https://doi.org/10.1016/j.icheatmasstransfer.2022.106323.

[233] B.M. Cherif, A. Abderrahmane, A.M. Saeed, N.A.A. Qasem, O. Younis, R. Marzouki, J.D. Chung, N.A. Shah, Hydrothermal and entropy investigation of nanofluid mixed convection in triangular cavity with wavy boundary heated from below and rotating cylinders, Nanomaterials 12 (9) (2022) 1469, https://doi.org/10.3390/nano12091469.

[234] H.T.A. Zisan, T.H. Ruvo, S. Saha, Entropy generation and natural convection on a cubic cavity with a pair of heat source at different configurations, International Communications in Heat and Mass Transfer 134 (2022) 106033, https://doi.org/10.1016/j.icheatmasstransfer.2022.106033.

[235] S. Kashani, A.A. Ranjbar, M. Mastiani, H. Mirzaei, Entropy generation and natural convection of nanoparticle-water mixture (nanofluid) near water density inversion in an enclosure with various patterns of vertical wavy walls, Applied Mathematics and Computation 226 (2014) 180–193, https://doi.org/10.1016/j.amc.2013.10.054.

[236] P. Biswal, T. Basak, Role of various concave/convex walls exposed to solar heating on entropy generation during natural convection within porous right angled triangular enclosures, Solar Energy 137 (2016) 101–121, https://doi.org/10.1016/j.solener.2016.07.008.

[237] A. Rahimi, M. Sepehr, M.J. Lariche, M. Mesbah, A. Kasaeipoor, E.H. Malekshah, Analysis of natural convection in nanofluid-filled H-shaped cavity by entropy generation and heatline visualization using lattice Boltzmann method, Physica. E, Low-Dimensional Systems & Nanostructures 97 (2018) 347–362, https://doi.org/10.1016/j.physe.2017.12.003.

[238] Z. Li, M. Hedayat, M. Sheikholeslami, A. Shafee, H. Zrelli, I. Tlili, T.K. Nguyen, Numerical simulation for entropy generation and hydrothermal performance of nanomaterial inside a porous cavity using Fe_3O_4 nanoparticles, Physica A 524 (2019) 272–288, https://doi.org/10.1016/j.physa.2019.04.146.

[239] S.M. Seyyedi, A.S. Dogonchi, M. Hashemi-Tilehnoee, Z. Asghar, M. Waqas, D. D. Ganji, A computational framework for natural convective hydromagnetic flow via inclined cavity: An analysis subjected to entropy generation, Journal of Molecular Liquids 287 (2019) 110863, https://doi.org/10.1016/j.molliq.2019.04.140.

[240] D. Sáchica, C. Treviño, L. Martínez-Suástegui, Numerical study of magnetohydrodynamic mixed convection and entropy generation of Al_2O_3-water nanofluid in a channel with two facing cavities with discrete heating, The International Journal of Heat and Fluid Flow 86 (2020), https://doi.org/10.1016/j.ijheatfluidflow.2020.108713.

[241] S.M. Seyyedi, On the entropy generation for a porous enclosure subject to a magnetic field: Different orientations of cardioid geometry, International Communications in Heat and Mass Transfer 116 (2020) 104712, https://doi.org/10.1016/j.icheatmasstransfer.2020.104712.

[242] T. Tayebi, H.F. Öztop, A.J. Chamkha, Natural convection and entropy production in hybrid nanofluid filled-annular elliptical cavity with internal heat generation or absorption, Thermal Science and Engineering Progress 19 (2020) 100605, https://doi.org/10.1016/j.tsep.2020.100605.

[243] R. Zhang, A. Ghasemi, A.A. Barzinjy, M. Zareei, S.M. Hamad, M. Afrand, Simulating natural convection and entropy generation of a nanofluid in an inclined enclosure under an angled magnetic field with a circular fin and radiation effect, Journal of Thermal Analysis and Calorimetry 139 (6) (2020) 3803–3816, https://doi.org/10.1007/s10973-019-08729-0.

[244] W. Chammam, S. Nazari, S.Z. Abbas, Numerical scrutiny of entropy generation and ferro-nanoliquid magnetic natural convection inside a complex enclosure subjected to thermal radiation, International Communications in Heat and Mass Transfer 125 (2021) 105319, https://doi.org/10.1016/j.icheatmasstransfer.2021.105319.

[245] A.S. Dogonchi, M.S. Sadeghi, M. Ghodrat, A.J. Chamkha, Y. Elmasry, R. Alsulami, Natural convection and entropy generation of a nanoliquid in a crown wavy cavity: Effect of thermo-physical parameters and cavity shape, Case Studies in Thermal Engineering 27 (2021) 101208, https://doi.org/10.1016/j.csite.2021.10120.

[246] A.S. Dogonchi, S.R. Mishra, A.J. Chamkha, M. Ghodrat, Y. Elmasry, H. Alhumade, Thermal and entropy analyses on buoyancy-driven flow of nanofluid inside a porous enclosure with two square cylinders: Finite element method, Case Studies in Thermal Engineering 27 (2021) 101298, https://doi.org/10.1016/j.csite.2021.101298.

[247] A.S. Dogonchi, T. Tayebi, N. Karimi, A.J. Chamkha, H. Alhumade, Thermal-natural convection and entropy production behavior of hybrid nanoliquid flow under the effects of magnetic field through a porous wavy cavity embodies three circular cylinders, Journal of the Taiwan Institute of Chemical Engineers 124 (2021) 162–173, https://doi.org/10.1016/j.jtice.2021.04.033.

[248] T. Tayebi, A. Sattar Dogonchi, N. Karimi, H. Ge-JiLe, A.J. Chamkha, Y. Elmasry, Thermo-economic and entropy generation analyses of magnetic natural convective flow in a nanofluid-filled annular enclosure fitted with fins, Sustainable Energy Technologies and Assessments 46 (2021) 101274, https://doi.org/10.1016/j.seta.2021.101274.

[249] N.H. Khan, M.K. Paswan, M.A. Hassan, Natural convection of hybrid nanofluid heat transport and entropy generation in cavity by using Lattice Boltzmann Method, Journal of the Indian Chemical Society 99 (3) (2022) 100344, https://doi.org/10.1016/j.jics.2022.100344.

[250] S. Bhardwaj, A. Dalal, Analysis of natural convection heat transfer and entropy generation inside porous right-angled triangular enclosure, International Journal of Heat and Mass Transfer 65 (2013) 500–513, https://doi.org/10.1016/j.ijheatmasstransfer.2013.06.020.

[251] P. Meshram, S. Bhardwaj, A. Dalal, S. Pati, Effects of the inclination angle on natural convection heat transfer and entropy generation in a square porous enclosure, Numerical Heat Transfer, Part A: Applications 70 (11) (2016) 1271–1296, https://doi.org/10.1080/10407782.2016.1230433.

[252] G. Chandra Pal, N. Goswami, S Pati, Numerical investigation of unsteady natural convection heat transfer and entropy generation from a pair of cylinders in a porous enclosure, Numerical Heat Transfer, Part A: Applications 74 (6) (2018) 1323–1341, https://doi.org/10.1080/10407782.2018.1507887.

[253] D. Bhowmick, P.R. Randive, S. Pati, H. Agrawal, A. Kumar, P. Kumar, Natural convection heat transfer and entropy generation from a heated cylinder of different geometry in an enclosure with non-uniform temperature distribution on the walls, Journal of Thermal Analysis and Calorimetry 141 (2) (2020) 839–857, https://doi.org/10.1007/s10973-019-09054-2.

[254] S. Dutta, N. Goswami, S. Pati, A.K. Biswas, Natural convection heat transfer and entropy generation in a porous rhombic enclosure: Influence of non-uniform heating, Journal of Thermal Analysis and Calorimetry 144 (4) (2021) 1493–1515, https://doi.org/10.1007/s10973-020-09634-7.

[255] K. Ahn, B. Kanimozhi, M. Muthtamilselvan, Q. Al-Mdallal, T. Abdeljawad, Production of entropy due to combined buoyancy and Marangoni convection in a cylindrical annular enclosure, Case Studies in Thermal Engineering 49 (2023) 103340, https://doi.org/10.1016/j.csite.2023.103340.

[256] M.K. Nayak, A.S. Dogonchi, A. Rahbari, Free convection of Al2O3-water nanofluid inside a hexagonal-shaped enclosure with cold diamond-shaped obstacles and periodic magnetic field, Case Studies in Thermal Engineering 50 (2023) 103429, https://doi.org/10.1016/j.csite.2023.103429.

[257] Q.R. Al-Amir, H.K. Hamzah, F.H. Ali, M. Hatami, W. Al-Kouz, A. Al-Manea, R. Al-Rbaihat, A. Alahmer, Investigation of Natural Convection and Entropy Generation in a Porous Titled Z-Staggered Cavity Saturated by TiO_2-Water Nanofluid, International Journal of Thermofluids 19 (2023) 100395, https://doi.org/10.1016/j.ijft.2023.100395.

[258] M. Arshad Siddiqui, B. Iftikhar, T Javed, Convective heat transfer enhancement and entropy generation analysis for radiative flow of ferrofluid inside the enclosure with non-uniform magnetic field, Journal of Magnetism and Magnetic Materials 584 (2023) 171101, https://doi.org/10.1016/j.jmmm.2023.171101.

[259] M. Hashemi-Tilehnoee, S.M. Seyyedi, E. Palomo Del Barrio, M. Sharifpur, Analysis of natural convection and the generation of entropy within an enclosure filled with nanofluid-packed structured pebble beds subjected to an external magnetic field and thermal radiation, Journal of Energy Storage 73 (2023) 109223, https://doi.org/10.1016/j.est.2023.109223.

[260] N.H. Hamza, N.M. Abdulrazzaq, M.A. Theeb, M. Sheremet, A. Abdulkadhim, The influence of magnetic field on entropy generation in a wavy cavity equipped with internal heated plate using Darcy–Brinkman–Forchheimer model, International Journal of Thermofluids 20 (2023) 100463, https://doi.org/10.1016/j.ijft.2023.100463.

[261] A.A. Hussien, W. Al-Kouz, M.E. Hassan, A.A. Janvekar, A.J. Chamkha, A review of flow and heat transfer in cavities and their applications, European Physical Journal Plus 136 (4) (2021), https://doi.org/10.1140/epjp/s13360-021-01320-3.
[262] B.E. Rapp, Microfluidics: Modeling, Mechanics and Mathematics, First edition, Elsevier Science, 2016.
[263] P. Albrand, B. Lalanne, Mass transfer rate in gas-liquid Taylor flow: Sherwood numbers from numerical simulations, Chemical Engineering Science 280 (2023) 119011, https://doi.org/10.1016/j.ces.2023.119011. -.
[264] D. Krasnov, O. Zikanov, T. Boeck, Numerical study of magnetohydrodynamic duct flow at high Reynolds and Hartmann numbers, Journal of Fluid Mechanics 704 (2012) 421–446, https://doi.org/10.1017/jfm.2012.256.
[265] D. Saury, N. Rouger, F. Djanna, F. Penot, Natural convection in an air-filled cavity: Experimental results at large Rayleigh numbers, International Communications in Heat and Mass Transfer 38 (6) (2011) 679–687, https://doi.org/10.1016/j.icheatmasstransfer.2011.03.019.
[266] M.J.S. de Lemos, Turbulence in Porous Media: Modeling and Applications, 2nd ed., Elsevier Science, 2012.
[267] T. Hayat, S.A. Shehzad, A. Alsaedi, Soret and Dufour effects on magnetohydrodynamic (MHD) flow of Casson fluid, Applied Mathematics and Mechanics 33 (10) (2012) 1301–1312, https://doi.org/10.1007/s10483-012-1623-6.
[268] G.H.R. Kefayati, R.R. Huilgol, Lattice Boltzmann Method for simulation of mixed convection of a Bingham fluid in a lid-driven cavity, International Journal of Heat and Mass Transfer 103 (2016) 725–743, https://doi.org/10.1016/j.ijheatmasstransfer.2016.07.102.